Preparation of and functionalization of supramolecular materials with ionic liquids based on host-guest interactions

A Doctoral Thesis

by

Garry Sinawang

Submitted to

The Graduate School of Science, Osaka University

August, 2019

Acknowledgement

First of all, the author want to thank God because without Him, the author is nothing. This research work was carried out from 2016 to 2019 under the direction of Professor Dr. Yoshinori Takashima, Professor Dr. Hiroyasu Yamaguchi, and Professor Dr. Akira Harada at the department of Macromolecular Science, Graduate School of Science, Osaka University. The author would like to express his great gratitude to all Professors for their guidance and assistance throughout this study.

The author is also grateful to Assistant Professor Dr. Yuichiro Kobayashi, Lecturer Dr. Motofumi Osaki, and Assistant Professor Dr. Yongtai Zheng for helpful suggestion and all members of Takashima Laboratory and Yamaguchi Laboratory for their cooperation and friendship.

Grateful acknowledgements are also made to Professor Dr. Hiroshi Uyama for kindly supply of cellulose nanofibers. Professor Dr. Tadashi Inoue and Associate Professor Dr. Osamu Urakawa for access to conductivity measurement, Dr. Naoya Inazumi for NMR measurement, and also Dr. Akihiro Ito for SEM experiments.

Last but not least, the author want to thank all of family members who always supporting and giving guidance during hard time. Without their guidance maybe the author cannot finish this doctoral program at Osaka University.

August, 2019

GARRY SINAWANG

Garry Sinawang

Contents

Chapter 1
General introduction

1.1. Supramolecular chemistry

Supramolecular chemistry was first defined by Jean –M. Lehn in his findings regarding cryptands.[1] The idea of supramolecular chemistry was inspired by the "lock and key"[2] model of Emil Fischer, who was awarded the Nobel Prize in Chemistry in 1902. Supramolecular chemistry has become an increasingly popular topic since Jean –M. Lehn,[3] Donald J. Cram[4] and Charles J. Pedersen[5] were awarded the Nobel Prize in Chemistry in 1987 for their work in this field. Since then, various interesting methods through supramolecular approach have been reported (Figure 1-1).

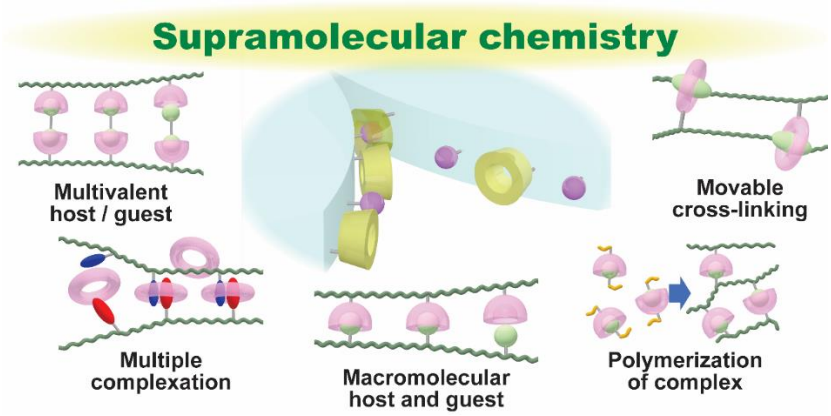

Figure 1-1. Supramolecular chemistry

Self-healing materials using supramolecular chemistry can be designed by two major principal approaches: "physical" and "chemical" approaches. Physical approaches are based on utilizing healing agents[6] or stress-relaxation mechanisms. Chemical approaches are based on the formation of multiple non-covalent bonds, such as Diels-Alder (DA) reactions,[7] hydrogen bonds (H-bond),[8] π-π stacking,[9-10] metal-ligand interactions,[11-12] electrostatic interactions,[13] hydrophobic interactions,[14] and host-guest interactions. The mechanical properties of these non-covalent bonds are derived from the supramolecular polymer network in the presence of secondary interactions that bind liquid-like building blocks into plastic or rubbery polymers in hydrated and non-hydrated

states. The self-healing of supramolecular polymers with non-covalent bonds has been summarized in several review articles.[15-18] Among those non-covalent bonds, host-guest interactions have played an important role in supramolecular chemistry because of their dynamic nature.[19]

1.2. Host-guest interactions

Host-guest interactions are formed by inclusion complexes between macrocyclic compounds serving as host molecules and guest molecules locked inside the cavity. The inclusion complexes form because the host molecules have external features that enable them to interact with solvent and internal features that bind the guest molecules through either a specific shape or a favorable environment. This condition mostly occurs when hydrophobic guest molecules are sequestered into the hydrophobic inner cavity of host molecules because of solvophobic interactions with water. The complex stability constant, *K*, expressed the formation of host-guest inclusion complexes which is determined by the equilibrium:

$$n\mathrm{H} + m\mathrm{G} \rightleftarrows n\mathrm{H} \cdot m\mathrm{G}$$

$$K = \frac{[n\mathrm{H} \cdot m\mathrm{G}]}{[\mathrm{H}]^n[G]^m}$$

where H is the host molecule, G is the guest molecule, and *n* and *m* represent the number of host and guest molecules, respectively.[20-22] In most cases, *n*=1 and *m*=1 or 2. This equilibrium in host-guest interactions is mainly driven by H-bonds, π-π stacking, van der Waals forces, or hydrophobic interactions. Self-healing properties are mostly tested by cutting the materials into pieces and reattaching them again to reform host-guest inclusion complexes between the host and guest molecules on the cut surface. Additional tests were performed by adding competitive molecules to inhibit the formation of interactions in the polymer materials.

1.3. Macrocyclic compound

Over the past three decades, a wide variety of macrocyclic compounds, such as crown ethers,[23-24] cucurbit[*n*]urils,[25-27] calix[*n*]arenes,[28-29] pillar[*n*]arenes,[30-33] and cyclodextrins (CDs),[34-37] have been used as host molecules for host-guest interactions. The author only employs CDs to be used as host molecules for preparing supramolecular materials. CDs are a family of macrocyclic oligosaccharides, which composed of 6 (α), 7 (β), or 8 (γ) α-1,4-linked D-glucopyranose. Table 1-1 shows the physical properties of CDs.

Table 1-1. Chemical structure and physical properties of α, β, and γ-CD

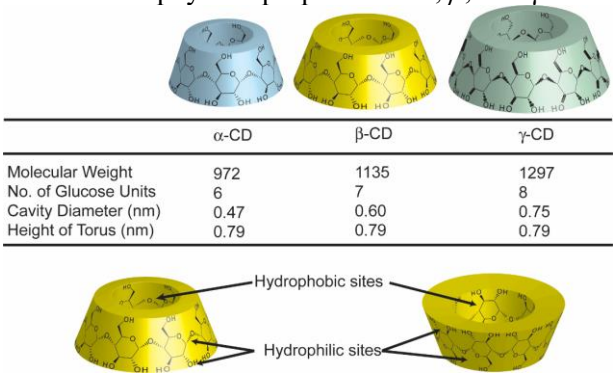

	α-CD	β-CD	γ-CD
Molecular Weight	972	1135	1297
No. of Glucose Units	6	7	8
Cavity Diameter (nm)	0.47	0.60	0.75
Height of Torus (nm)	0.79	0.79	0.79

Molecular recognitions from CDs are realized from hydrophobic and *van der Waals* interaction between CD cavity with suitable hydrophobic guests. There are three types known molecular recognition interactions such as into main chain, side chain, and sequential complex (Figure 1-2).[38-43]

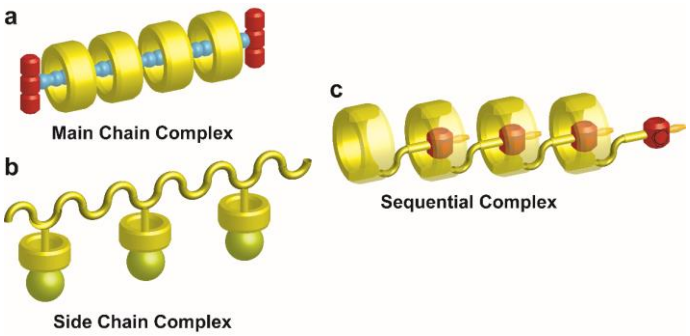

Figure 1-2. Molecular recognition interactions.

Supramolecular materials prepared mostly using molecular recognition at side chain with two kind of approaches: (1) from attaching host polymer and guest polymer or (2) polymerization of inclusion complex from host and guest monomers (Figure 1-3).

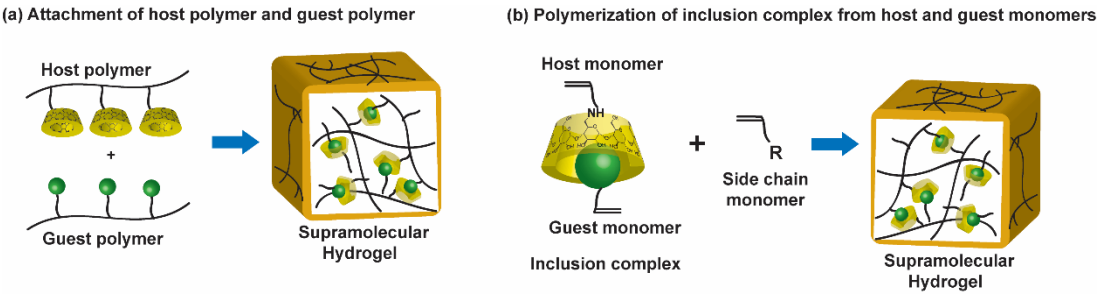

Figure 1-3. Illustrations of two approaches to prepare supramolecular materials from molecular recognition at side chain: (**a**) attaching host polymer and guest polymer or (**b**) polymerization of inclusion complex from host and guest monomers.

1.4. Sol-gel transition through side chain molecular recognition

Molecular recognition of polymeric hydrogel from mixture of host polymer and guest polymer has been reported.[44] Gels are divided into two main categories: physical[45-47] and chemical[48-50] interactions. Physical interactions gels based on non-covalently cross-linkers are easier to be tuned than those with covalently cross-linked bonds. Several method to control the physical properties like preparing low-molecular weight physical gels[51-56] or forming hydrogels through host-guest interactions[57-60] have been studied and it found that using host-guest interactions prone to be more sensitive to the external stimuli.

1.4.1. Photoresponsive sol-gel transition through side chain molecular recognition

First published work regarding polymerization of host-guest inclusion between CDs as host molecules and guest molecules was through investigation of sol-gel transition between CDs and azobenzene (Azo) under ultraviolet (UV) or visible light irradiation. It was reported mixture of CDs and Azo showed viscosity change after photoirradiation but the mixture did not form hydrogel.[61] To obtain hydrogel by inclusion complex, curdlan modified α-CD (CD-CUR) and guest polymer with Azo ($pAC_{12}AZO$) were mixed in DMSO.[62] This was the first light-responsive hydrogel formed by inclusion complex.

Figure 1-4 shows irradiation of hydrogel by UV (λ=365 nm) made the gel converted into sol (*trans*-Azo turned into *cis*-Azo). However, irradiating the hydrogel with visible light (λ=430 nm) or heating to 60 ºC, it turned back to gel (*cis*-Azo turned back to *trans*-Azo). This sol-gel transition from irradiation was also characterized from its viscosity change by using steady-shear viscosity measurement.

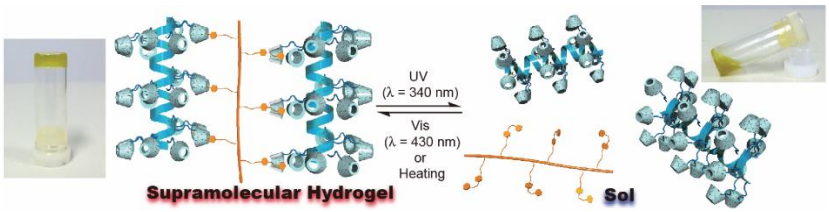

Figure 1-4. Schematic illustration of a photoresponsive sol-gel transition material with CD-CUR and $pAC_{12}Azo$ upon irradiating with UV light (λ = 365 nm) and visible light (λ = 430 nm) or heating at 60º C. Reproduced with permission from ref. 62. Copyright 2010 WILEY-VCH Verlag GmbH & Co. KGaA.

1.4.2. Redox-responsive sol-gel transition through side chain molecular recognition

The sol-gel transition also occurs in hydrogel formed by inclusion complex between β-CD with acrylic acid (pAA-β-CD) with ferrocene with acrylic acid (pAA-Fc).[63] The hydrogels showed redox responsive by treating the hydrogel with sodium hypochlorite (NaClO) as oxidizing agent turned the gel into sol due to oxidation of ferrocenium cation (Fc^+). Then treating the sol with reducing agent [glutathione (GSH)] restored the gel.

1.5. Self-healing materials

The persistence of man-made polymers has become an environmental concern because the degradation of waste is a threat to human health, wildlife, the oceans, and landfills. This warning has prompted researchers to devise the idea of sustainable materials. One of the efforts in this field is to develop materials that can heal themselves after damage. Therefore, synthetic methods to design and construct self-healing materials[64-66] have attracted attention over the years.[67-73] Lehn et al. pioneered self-healing materials using dynamic covalent polymers.[74-78]

Recently, supramolecular chemistry have been popular to be used as self-healing materials because it offered fast reversibility under ambient conditions and have become a popular research topic in materials design.[8, 79-81] An ideal self-healing material not only could be rapidly healed but also could restore its mechanical properties.[82-83]

1.5.1. Redox-responsive self-healing materials

Supramolecular self-healing materials based on macrocyclic compounds are inspired by macroscopic self-assembly[84] and sol-gel transitions[62] in hydrogels. Supramolecular self-healing materials containing macrocyclic compounds were pioneered using *β*-cyclodextrin (*β*-CD) as a host molecule and ferrocene (Fc) as a guest molecule.[63, 85] The resulting hydrogel was constructed by formation of an inclusion complex of *β*-CD and acrylic acid (pAA-*β*-CD) with Fc and acrylic acid (pAA-Fc). As the hydrogel was redox responsive, treating the hydrogel with an oxidizing agent [sodium hypochlorite (NaClO)] turned the gel into a sol due to the change of Fc into the ferrocenium cation (Fc^+) upon oxidation. Subsequently, treating the sol with a reducing agent [glutathione (GSH)] restored the gel.

The self-healing properties of this hydrogel were observed from a mixture of the inclusion complex between pAA-*β*-CD and pAA-Fc in boric acid/KCl/NaOH buffer solution at pH 9, which afforded pAA-*β*-CD/pAA-Fc gel. The contact surface disappeared after 24 hours of reattachment, and the gel recovered 84% of its initial strength (Figure 1-5). Improving self-healing speed also can be done by treating cut surface with a reducing agent also whereas adding an oxidizing agent prevented the adhesion process.

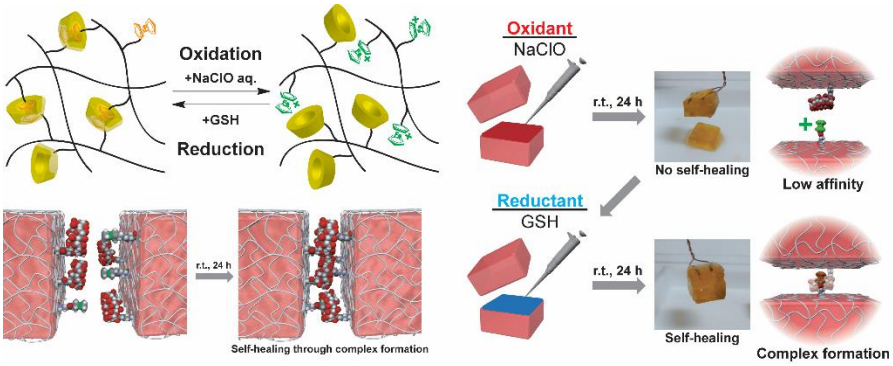

Figure 1-5. Self-healing by redox responsiveness: treating the hydrogels with an oxidizing agent (NaClO) inhibits the self-healing, but treating with a reducing agent (GSH) restores their self-healing ability. Reproduced from ref. 85. This work is licensed under the Creative Commons Attribution-NonCommercial-ShareAlike 3.0 Unported License.

1.5.2. Self-healing hydrogel formed by host-guest interactions inclusion complexes

Mixing a host polymer and guest polymer showed the disadvantage that the host units and guest units did not form perfect inclusion complexes. This phenomenon caused restrictions on the molecular mobility during the formation of self-healing materials. Therefore, another approach for preparing self-healing materials was introduced by polymerizing an inclusion complex between host and guest monomers.

The journey towards investigating the self-healing of supramolecular materials via the polymerization of host-guest inclusion complexes began with the β-CD and Ad host-guest pair (Figure 1-6).[86-87] Prior to polymerization, the adamantane (Ad) monomer and β-CD monomer were mixed together in water at room temperature to form the inclusion complex. The hydrogel was prepared by radical copolymerization of the inclusion complex mixture between the Ad monomer and β-CD monomer with acrylamide (AAm) as the side chain using tetramethylethylenediamine (TEMED) and ammonium persulfate (APS) as the initiator system.

The [β-CD-Ad gel(7,6)] self-healing properties of the hydrogel were investigated by cutting and adhering freshly cut pieces at the cut surface in water to form a single piece of gel. The adhesive strength was measured using a creep meter at a tensile speed of 1 mm/s, and the gel showed an 84% recovery ratio within 24 hours; however, a longer adhesion time resulted in a higher recovery ratio. Fabricating supramolecular materials with both self-healing properties and mechanical performance remains a challenge.

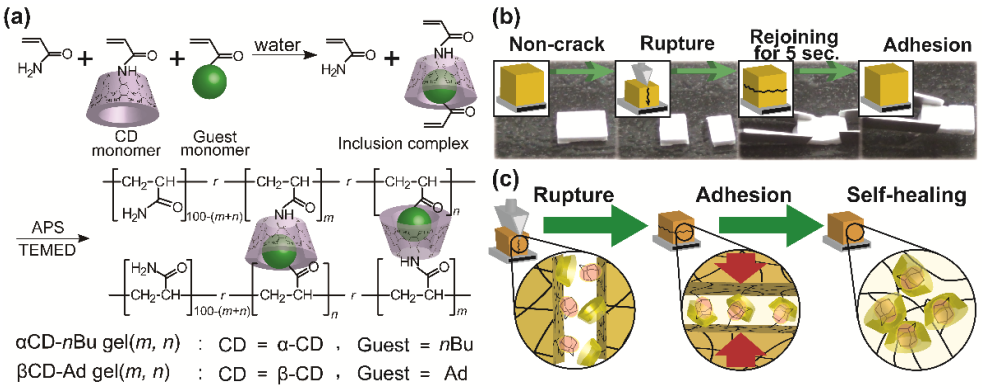

Figure 1-6. (**a**) Chemical structures of hydrogels formed by host-guest interactions inclusion complexes (**b**) Schematic illustration of self-healing hydrogels [*β*-CD-Ad gel(7,6)] between cut surface. Reproduced with permission from ref. 86. Copyright 2013 WILEY-VCH Verlag GmbH & Co. KGaA.

1.5.3. Self-healing xerogel formed by host-guest interactions

Soft materials are not favorable for applications, so dried hydrogels (xerogels) were prepared based on the same host-guest interaction structure as the hydrogel to prepare a hard material.[88] The preparation method was the same as that of the *β*-CD-Ad hydrogels, except that the gel was dried at room temperature for 2 days and in a vacuum oven (27 ºC) for one day to obtain the corresponding xerogel. To test its self-healing properties, the xerogel was cut, and then 2 μL of water was added to the cut surface before re-adhering the pieces instead of placing the gel in the water (Figure 1-7). The adhesion surface was observed by microscope to observe the self-healing behavior, and the xerogel showed a recovery ratio of approximately 40% within 24 hours. After 48 hours, the recovery ratio increased to 88%.

Although the self-healing rate of the xerogel was slower than that of the hydrogel, the preparation of a self-healing hard material was a breakthrough in supramolecular materials.

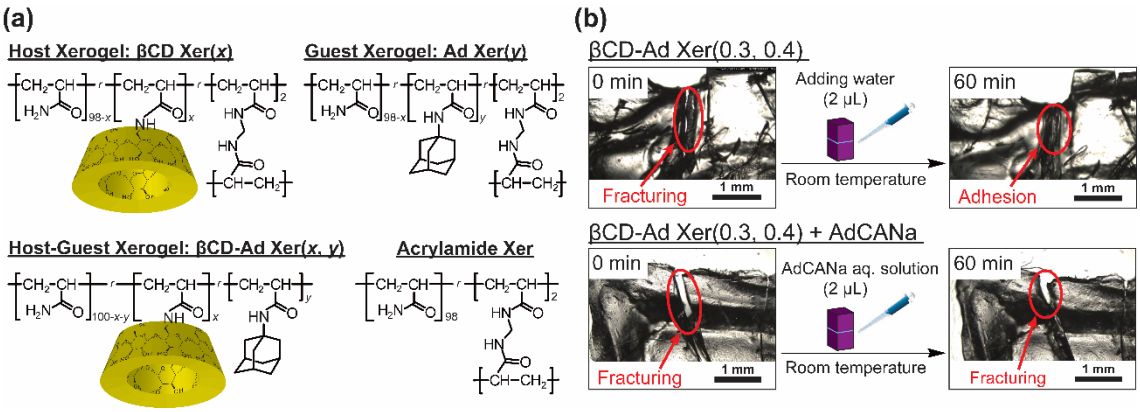

Figure 1-7. (**a**) Chemical structures of xerogels. (**b**) Self-healing of *β*-CD-Ad Xer(0.3,0.4). Reprinted with permission from ref. 88. Copyright 2015 American Chemical Society.

1.5.4. Tough self-healing hydrogel formed by host-guest interactions

Self-healing materials from polymerization of host-guest inclusion complex already successfully prepared however the hydrogel showed a white turbid appearance and was not transparent. When the concentration of the host-guest inclusion complex was decreased to 2 mol%, the gel turned into a transparent gel.[89] The gel was prepared with the same method as the xerogel, but for a more in-depth investigation, the side-chain polymer was changed to *N,N*-dimethylacrylamide (DMAAm), *N*-isopropylacrylamide (NIPAAm), hydroxymethacrylamide (HMAAm), and hydroxyethylacrylate (HEA).

The results for the variation in the side-chain polymer showed that the gel with HEA had the best mechanical and self-healing properties. Compared to the gels in previous work, this gel showed good flexibility with better mechanical properties and resisted being stabbed with a cutter (Figure 1-8). To investigate its self-healing properties, the gel was cut and reattached under humid conditions. After 24 hours of adhesion time, the gel showed a 45% recovery ratio. The transparent gel healed faster than the turbid gel because lower host-guest contents mean higher mobility in the gel, which led to a shorter time needed to self-heal. Additionally, compared to the gels in previous studies, such as tough polymeric gels,[90-91] multiple network gels,[92-94] nanocomposite gels,[95] slide-ring gel,[96-97] four-armed macromolecules,[98-99] and dually cross-linked gels,[100] tough hydrogels did not need “sacrificial bonds”[101] to dissipate deformation force because the host-guest interactions already acted as the “recoverable sacrificial bonds”.

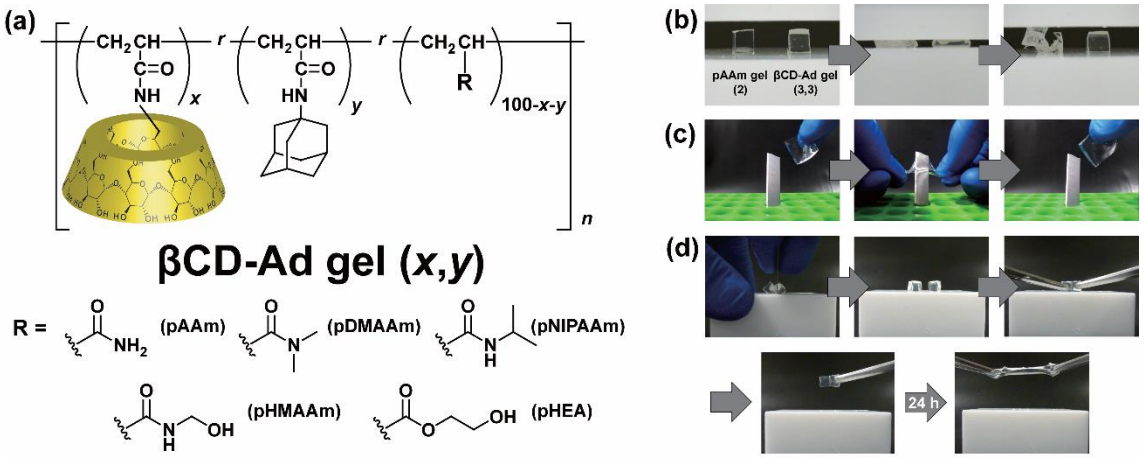

Figure 1-8. (**a**) Chemical structures of tough hydrogels. (**b-c**) Resistant test of *β*-CD-Ad gel. (**d**) Self-healing experiment *β*-CD-Ad gel. Reproduced from ref. 89. Copyright 2016 WILEY-VCH Verlag GmbH & Co. KGaA.

At this point, hydrogels possessing high flexibility, toughness, and self-healing properties were successfully prepared. However, the self-healing ratio result still was not satisfactory, and humid conditions were still needed to achieve self-healing properties; thus, another composition that had different types of CD and guest groups while maintaining a transparent appearance was needed.[102] CD molecules that had distance (*β*-CDAAmMe) and no distance (*β*-CDAAm) from the side chain while using the same guest molecules was also one of the aspects tested. Surprisingly, *β*-CDAAmMe has better mechanical properties than *β*-CDAAm, so *β*-CDAAmMe is preferable for use in conjunction with the guest molecules. Three linear alkyl guest molecules [n-butyl acrylate (BuA), hexyl acrylate (HexA), and dodecyl acrylate (DodA)] and four spherical guest molecules [isobornyl acrylate (Ibr), adamantyl acrylamide (AdAAm), hydroxyadamantyl acrylate (HAdA), and ethyladamantyl acrylate (EtAdA)] were chosen. Compared to other guest groups, the combination of *β*-CDAAmMe and AdAAm was found to provide better self-healing in the dry state. For this combination, self-healing was achieved without any influence of water. The self-healing ratio after 24 hours of reattachment was 60% at 100 ºC, and when the self-healing was investigated as a function of time, it remained relatively constant over 24 hours. This xerogel demonstrated a higher self-healing recovery ratio than the gel in previous work, also could be self-healed in a completely dry state.

1.6. Multi-stimuli responsive materials

Multi-stimuli-responsiveness has also become an emerging area in polymeric materials.[103-104] Thus, to fabricate polymeric materials with multi-stimuli-responsiveness, complicated molecular design is necessary. Recently, mechanochromic functional materials have been utilizing dynamic covalent bonds as detector to various stimuli such as stress, heat, and light[105-109] while also have self-healing properties. Introducing host-guest interactions such as non-covalent bonds might provide an effective approach to prepare multifunctional supramolecular materials. Several supramolecular materials with stimuli-responsive properties have been reported previously.[110-111]

1.6.1. Multifunctional stimuli responsive self-healing materials

Color changes of supramolecular materials are the easiest way to investigate multi-stimuli-responsive materials because they can be visibly observed.[112] Phenolphthalein (PP) was chosen as the guest molecule, and β-CD was chosen as the host molecule.[113] The inclusion complex between β-CD and PP did not exhibit a purple color at pH 10, but when PP was ejected from the β-CD cavity, the color of the gel became purple. In addition to pH stimuli, PP can also respond to thermal stimuli in the presence of β-CD.[114-115] Multifunctional stimuli-responsive supramolecular materials were prepared by radical copolymerization of an inclusion complex mixture with AAm using APS as an initiator and TEMED as a co-catalyst, and the resulting gel was dried in ambient temperature for 3 days to obtain a β-CD-PP-AAm gel (Figure 1-9).[116]

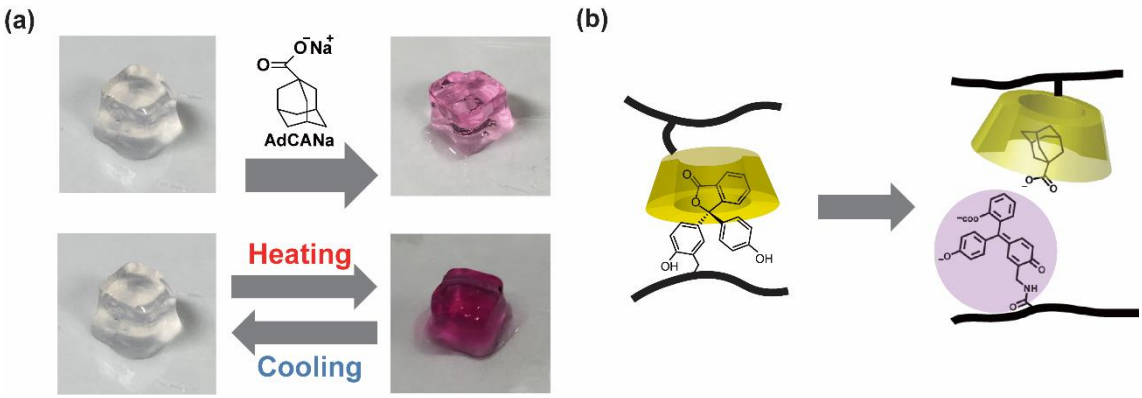

Figure 1-9. (**a**) Color reaction of a β-CD-PP-AAm hydrogel(2,2) triggered by the addition of AdCANa and controlled by heating and cooling. (**b**) Mechanism of color change. Reprinted with permission from ref. 116. Copyright 2017 American Chemical Society.

This hydrogel showed pH- and thermoresponsive properties. The pH-responsiveness was investigated by immersing the *β*-CD-PP-AAm gel in KH_2PO_4/NaOH buffer solution (pH=8) in the presence of adamantane carboxylic acid sodium salt (AdCANa). Because the association constant of *β*-CD with AdCANA is larger than that with PP, the included PP unit dissociated from the *β*-CD cavity, which changed the color of gel to purple. The inclusion complex between *β*-CD and PP did not exhibit a purple color at pH 10, but when competitive guest molecules were added, the color of the solution changed. Regarding its thermoresponsiveness, the colorless gel turned purple upon heating to 87 ºC in KH_2PO_4/NaOH buffer solution (pH=8), but the gel returned to the colorless state when the temperature decreased. The thermoresponsiveness results indicated that the condition was reversible and that this gel may also show self-healing properties.

With regard to self-healing properties, the gel was prepared using HEA as a side-chain polymer instead of AAm because HEA is softer than AAm, which allowed self-healing properties to easily be obtained. The gel was cut and then re-adhered under dry conditions within 24 hours of adhesion time, resulting in a 65% recovery ratio.

1.6.2. Cationic alkyl guest

The functionality of supramolecular host-guest interactions can be affected by formation and dissociation of the cross-links. However, *pseudo*[2]rotaxane structure or stopper functional unit was used to investigate this condition as in the inclusion complex. Assuming that the introduction of second-guest units would affected the hydrogels then supramolecular hydrogels should be designed with two chemical guest units. Viologen derivatives are great option as a second unit in the guest molecules.[117] Due to electric repulsion, viologen derivatives with cationic properties were not included in the CD cavity.[118] The viologen units at the terminal functionality acted not as a bulky stoppers but as electric stoppers which prevent dissociation. When stress was applied, the CD still slid through the viologen-alkyl chain unit, and there was an electric barrier between the CD and the viologen unit before complete dissociation.

The hydrogel was obtained by radical copolymerization of a mixture of inclusion complexes of viologen monomer and CD monomer with acrylamide (AAm) using ammonium persulfate (APS) as an initiator and tetramethylethylenediamine (TEMED) as

a co-catalyst (Figure 1-10). The fracture energy of the hydrogels was investigated and that the alkyl chain length and the cationic charge number of the viologen units increased, the energy of the obtained hydrogels also increased. The fracture energy is closely related to the dissociation energy between the CD and viologen units. Changing the size of the CD cavity, alkyl chain length, and number of cationic species could also control the dissociation energy. The dependence on the number of cationic species led to the finding that the mechanical properties of the hydrogels can be changed by redox stimuli. The mechanical properties changed due to reducing conditions because of the formation of a radical cation dimer between the viologen units, which indicated that the host-guest inclusion complex and radical cation dimer cooperatively functioned as dual cross-linking points.

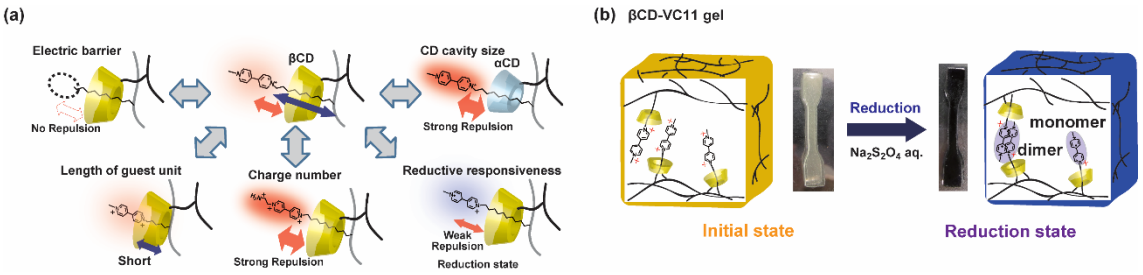

Figure 1-10. (**a**) Effect of an electric barrier, the CD cavity size, the length of the guest unit, the charge number, and the reduction responsiveness to the mechanical properties of CD-based supramolecular hydrogels. (**b**) *β*CD-VC11 gel before and after immersion in a 1M Na_2SO_4 aqueous solution. Reprinted with permission from ref. 117. Copyright 2017 American Chemical Society.

1.7. Supramolecular elastomer

The host-guest interactions between CD molecules and guest molecules in hydrogel state have been well summarized. However, stress dispersion in hydrogel state is not applicable for general purposes where hydrophobic bulk polymers are employed. Therefore, elastomers were prepared using CD molecules and guest molecules with hydrophobic acrylates as the side-chain polymer.[119] Since hydrophilic CD monomers are insoluble in hydrophobic acrylates, the CD monomers were modified by Williamson ether synthesis or acetylation to transform them into permethylated CD monomers (PM*γ*-CDAAmMe) or peracetylated CD monomers (PAc*β*-CDAAmMe and PAc*γ*-CDAAmMe), respectively. An elastomer was prepared by mixing the modified CD monomers with a

guest monomer [2-ethyladamantyl acrylate (AdEtA) and fluorooctyl acetate (H2F6)] in an acrylate monomer [ethyl acrylate (EA) and butyl acrylate (BA)] and then sonicating them mixture to form the inclusion complex. The homogenous mixture was bulk-copolymerized using UV irradiation with a photoinitiator to obtain an elastomer and then was dried in a vacuum oven at 80ºC to remove residual acrylate monomer. The elastomer showed tough and flexible properties with self-healing ability (Figure 1-11).

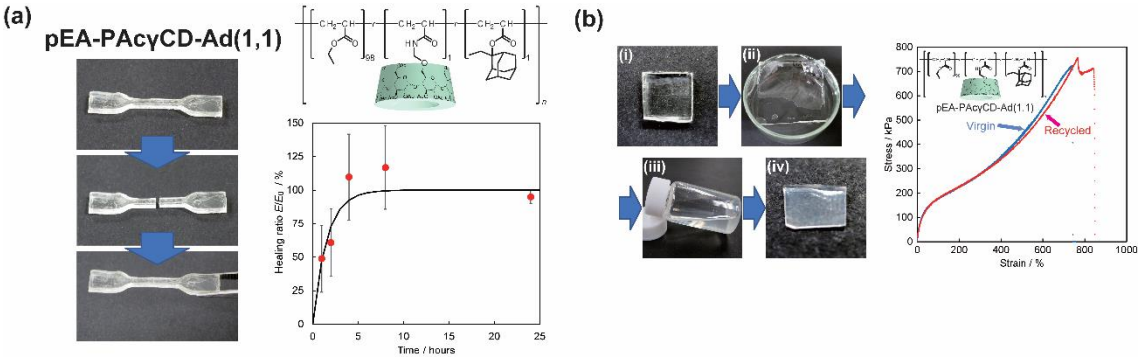

Figure 1-11. (**a**) Self-healing properties and (**b**) recycling experiments of supramolecular elastomer pEA-PAc*γ*-CD-Ad(1,1). Reprinted with permission from ref. 119. Copyright 2019 American Chemical Society.

To test the self-healing ability of the elastomer, a dumbbell-shaped sample was divided by a knife and then re-joined. The fractured sample completely recovered to 95% within only 4 hours of adhesion time at 80 °C. Beside the self-healing ability, supramolecular elastomer also can be recycled to recover its mechanical properties. The self-healing ability of the supramolecular elastomer also enabled the, which is useful for moulding and shaping by manufacturers.

1.8. Ionic liquids

Ionic liquids (ILs), also known as molten salts or liquids that just composed by ions, have great physicochemical properties such as great ionic conductivity, negligible volatility, non-flammability, and high thermal and electrochemical stability in room temperature.[120-122] Recently, ILs utilized as electrolyte salts in polymer networks because of their low glass transition (T_g) and low melting point (T_m), and capability to form (supercooled) liquids at room temperature. These properties will preserve high ionic conductivity, high electrochemical stability, and compatibility with the host polymers.[123-

[124] There are many known ILs with formed by various cations and anions structures. imidazolium, pyrrolidinium, guanidinium, pyridinium, alkylammonium, alkylphosphonium, and alkylpyrrolidinium are several common cations used in IL. Anions in IL usually selected from inorganic compound such as halides (Cl^-, Br^-, I^-), polyatomic inorganics (PF_6^-, BF_4^-), polyoxometallates, or more topically such as NO_3^- and $TFSI^-$]. Figure 1-12 shows common IL cations and anions structures with their.[125] The combination of cation and anion affected the properties of ILs such as hydrophobicity, conductivity, melting point, solubility, viscosity, etc.

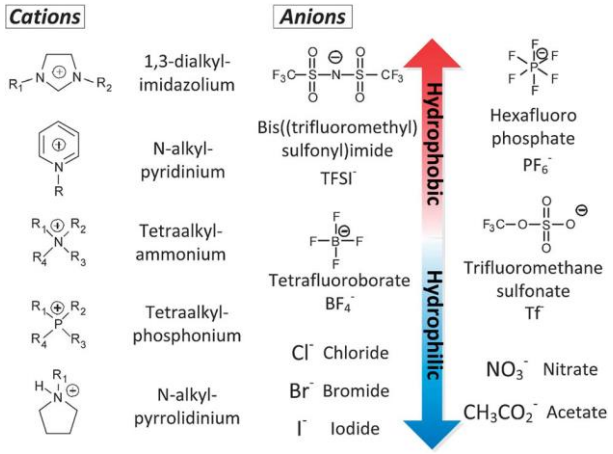

Figure 1-12. Common cations and anions compound used as ionic liquids with their in hydrophilic–hydrophobic properties. Reproduced from ref. 125 with permission from The Royal Society of Chemistry.

Since ILs have been popular for their properties then recently ILs were considered to be applied in electrochemical devices including lithium ion batteries, fuel cells, and solar batteries. However, applying ILs is not a good idea because of their leakage possibility during application. Therefore, ILs are utilized with polymers to form ionic liquid gels (IGs) that more preferable for application while still maintaining their physicochemical properties.

1.9. Scope and outline of this thesis

This thesis focus on utilization of ionic liquid in supramolecular materials cross-linked by host-guest interactions. Host-guest interactions used in this thesis are constructed from inclusion complex between CD as host molecules and guest molecules. Since ionic liquid utilized then ionic conductivity was expected to be detected in the supramolecular materials. Additionally, supramolecular materials formed by CD as host molecules also expected to show good mechanical properties and self-healing properties.

In *chapter 2*, supramolecular polymeric ionic liquid gel (IG) based on host-guest interaction was prepared from host-guest inclusion complex between peracetylated γ-CD monomer and 2-ethyl-2-adamantane monomer in acrylate (ethyl acrylate or butyl acrylate) monomer then followed by immersion in 1-ethyl-3-methylimidazolium bis(trifluoromethylsulfonyl)imide (EMIm TFSI) ionic liquid. The ionic conductivity of the supramolecular polymeric IG with host-guest interactions was higher than those of the chemically cross-linked IG which showed the importance of host-guest interaction in supramolecular polymeric IG.

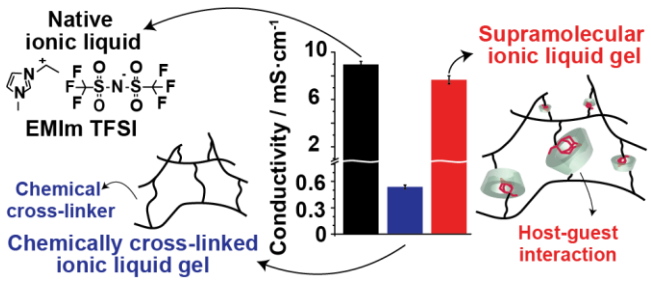

In *chapter 3*, the mechanical and self-recovery properties of supramolecular polymeric elastomers immersed in an ionic liquid (IEs) were investigated. Furthermore, the investigation also included relation between ionic liquid content with mechanical properties. The supramolecular polymeric IEs were prepared in the preparation method with supramolecular materials in *chapter 2* but more acrylate variation was used (methyl acrylate, ethyl acrylate, butyl acrylate, methyl methacrylate). The supramolecular polymeric IEs show a self-recovery capability, which conventional chemically cross-linked IEs cannot achieve.

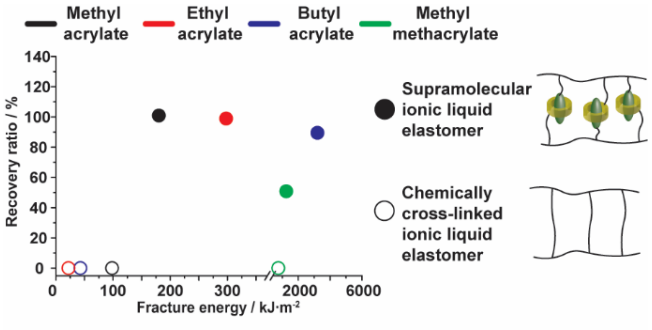

In *chapter 4*, the author prepared cellulose nanofibers (CNFs)-reinforced supramolecular materials. The method was dissolving CNFs in 1-butyl-3-methylimidazolium chloride (BMIm Cl). Then, dissolved CNFs were mixed with host-guest inclusion complex between peracetylated γ-CD monomer and 12-(acrylamide) dodecanoic acid monomer in the presence of 2-hydroxyethyl acrylate to obtain CNFs-reinforced supramolecular materials. CNFs-reinforced supramolecular materials showed higher mechanical properties and self-healing recovery ratio compared to supramolecular materials without CNFs.

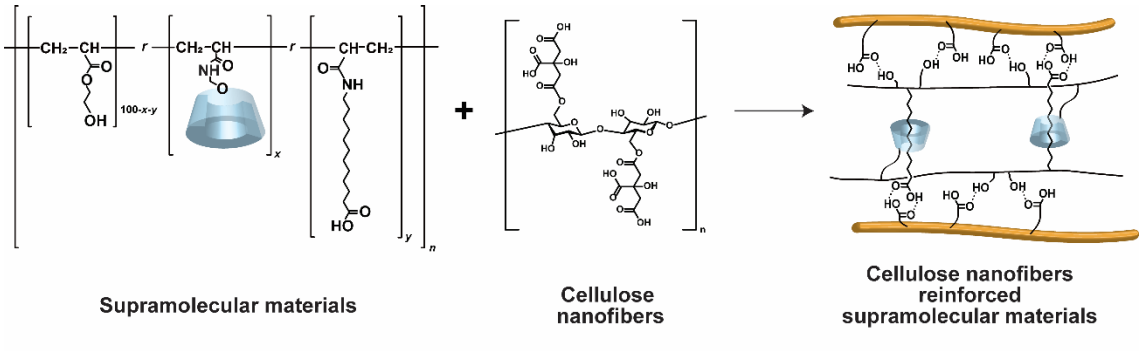

References

1. Lehn, J. M., *Acc. Chem. Res.* **1978,** *11*, 49-57.
2. Fischer, E., *Berichte der deutschen chemischen Gesellschaft* **1894,** *27*, 2985-2993.
3. Lehn, J.-M., *Angew. Chem. Int. Ed.* **1988,** *27*, 89-112.
4. Cram, D. J., *Angew. Chem. Int. Ed.* **1988,** *27*, 1009-1020.
5. Pedersen, C. J., *Angew. Chem. Int. Ed.* **1988,** *27*, 1021-1027.
6. Toohey, K. S.; Sottos, N. R.; Lewis, J. A.; Moore, J. S.; White, S. R., *Nat. Mater.* **2007,** *6*, 581.
7. Reutenauer, P.; Buhler, E.; Boul, P. J.; Candau, S. J.; Lehn, J.-M., *Chemistry – A European Journal* **2009,** *15*, 1893-1900.
8. Cordier, P.; Tournilhac, F.; Soulié-Ziakovic, C.; Leibler, L., *Nature* **2008,** *451*, 977.
9. Burattini, S.; Colquhoun, H. M.; Fox, J. D.; Friedmann, D.; Greenland, B. W.; Harris, P. J. F.; Hayes, W.; Mackay, M. E.; Rowan, S. J., *Chem. Commun.* **2009,** 6717-6719.
10. Fox, J.; Wie, J. J.; Greenland, B. W.; Burattini, S.; Hayes, W.; Colquhoun, H. M.; Mackay, M. E.; Rowan, S. J., *J. Am. Chem. Soc.* **2012,** *134*, 5362-5368.
11. Burnworth, M.; Tang, L.; Kumpfer, J. R.; Duncan, A. J.; Beyer, F. L.; Fiore, G. L.; Rowan, S. J.; Weder, C., *Nature* **2011,** *472*, 334.
12. Wojtecki, R. J.; Meador, M. A.; Rowan, S. J., *Nat. Mater.* **2010,** *10*, 14.
13. Wang, Q.; Mynar, J. L.; Yoshida, M.; Lee, E.; Lee, M.; Okuro, K.; Kinbara, K.; Aida, T., *Nature* **2010,** *463*, 339.
14. Tuncaboylu, D. C.; Sari, M.; Oppermann, W.; Okay, O., *Macromolecules* **2011,** *44*, 4997-5005.
15. Campanella, A.; Döhler, D.; Binder, W. H., *Macromol. Rapid Commun.* **2018,** *39*, 1700739.
16. Yang, Y.; Urban, M. W., *Adv. Mater. Interfaces* **2018,** *5*, 1800384.
17. Tan, S.; Ladewig, K.; Fu, Q.; Blencowe, A.; Qiao, G. G., *Macromol. Rapid Commun.* **2014,** *35*, 1166-1184.
18. Yang, X.; Yu, H.; Wang, L.; Tong, R.; Akram, M.; Chen, Y.; Zhai, X., *Soft Matter* **2015,** *11*, 1242-1252.
19. Appel, E. A.; del Barrio, J.; Loh, X. J.; Scherman, O. A., *Chem. Soc. Rev.* **2012,** *41*, 6195-6214.
20. Cram, D. J.; Cram, J. M., *Acc. Chem. Res.* **1978,** *11*, 8-14.
21. Rekharsky, M. V.; Inoue, Y., *Chem. Rev.* **1998,** *98*, 1875-1918.
22. Seiffert, S.; Sprakel, J., *Chem. Soc. Rev.* **2012,** *41*, 909-930.
23. Pedersen, C. J., *J. Am. Chem. Soc.* **1967,** *89*, 7017-7036.
24. Pedersen, C. J., *J. Am. Chem. Soc.* **1967,** *89*, 2495-2496.
25. Freeman, W. A.; Mock, W. L.; Shih, N. Y., *J. Am. Chem. Soc.* **1981,** *103*, 7367-7368.
26. Kim, J.; Jung, I.-S.; Kim, S.-Y.; Lee, E.; Kang, J.-K.; Sakamoto, S.; Yamaguchi, K.; Kim, K., *J. Am. Chem. Soc.* **2000,** *122*, 540-541.
27. Day, A.; Arnold, A. P.; Blanch, R. J.; Snushall, B., *J. Org. Chem.* **2001,** *66*, 8094-8100.
28. Gutsche, C. D.; Dhawan, B.; No, K. H.; Muthukrishnan, R., *J. Am. Chem. Soc.* **1981,** *103*, 3782-3792.
29. Böhmer, V., *Angew. Chem. Int. Ed.* **1995,** *34*, 713-745.
30. Ogoshi, T.; Yamagishi, T.-a.; Nakamoto, Y., *Chem. Rev.* **2016,** *116*, 7937-8002.
31. Xue, M.; Yang, Y.; Chi, X.; Zhang, Z.; Huang, F., *Acc. Chem. Res.* **2012,** *45*, 1294-1308.
32. Ogoshi, T.; Kanai, S.; Fujinami, S.; Yamagishi, T.-a.; Nakamoto, Y., *J. Am. Chem. Soc.* **2008,** *130*, 5022-5023.
33. Strutt, N. L.; Zhang, H.; Schneebeli, S. T.; Stoddart, J. F., *Acc. Chem. Res.* **2014,** *47*, 2631-2642.
34. Bender, M. L.; Komiyama, M., *Cyclodextrin Chemistry*. Springer-Verlag: Berlin, 1978.

35. Easton, C. J.; Lincoln, S. F., *Modified Cyclodextrins: Scaffolds and Templates for Supramolecular Chemistry*. Imperial College Press: London, 1999.
36. Harada, A.; Takashima, Y.; Yamaguchi, H., *Chem. Soc. Rev.* **2009,** *38*, 875-882.
37. Harada, A.; Furue, M.; Nozakura, S.-i., *Macromolecules* **1976,** *9*, 701-704.
38. Raymo, F. M.; Stoddart, J. F., *Chem. Rev.* **1999,** *99*, 1643-1664.
39. Wenz, G.; Han, B.-H.; Müller, A., *Chem. Rev.* **2006,** *106*, 782-817.
40. Harada, A.; Hashidzume, A.; Yamaguchi, H.; Takashima, Y., *Chem. Rev.* **2009,** *109*, 5974-6023.
41. Bosman, A. W.; Sijbesma, R. P.; Meijer, E. W., *Mater. Today* **2004,** *7*, 34-39.
42. de Greef, T. F. A.; Meijer, E. W., *Nature* **2008,** *453*, 171.
43. Krieg, E.; Bastings, M. M. C.; Besenius, P.; Rybtchinski, B., *Chem. Rev.* **2016,** *116*, 2414-2477.
44. Harada, A.; Takashima, Y.; Nakahata, M., *Acc. Chem. Res.* **2014,** *47*, 2128-2140.
45. Kim, S.; Healy, K. E., *Biomacromolecules* **2003,** *4*, 1214-1223.
46. Beaty, C. E.; Saltzman, W. M., *J. Controlled Release* **1993,** *24*, 15-23.
47. Mahoney, M. J.; Anseth, K. S., *Biomaterials* **2006,** *27*, 2265-2274.
48. Petka, W. A.; Harden, J. L.; McGrath, K. P.; Wirtz, D.; Tirrell, D. A., *Science* **1998,** *281*, 389-392.
49. Shen, W.; Lammertink, R. G. H.; Sakata, J. K.; Kornfield, J. A.; Tirrell, D. A., *Macromolecules* **2005,** *38*, 3909-3916.
50. Hennink, W. E.; van Nostrum, C. F., *Adv. Drug Delivery Rev.* **2002,** *54*, 13-36.
51. Amiel, C.; Sebille, B., *J. Inclusion Phenom.* **1996,** *25*, 61-67.
52. Weickenmeier, M.; Wenz, G.; Huff, J., *Macromol. Rapid Commun.* **1997,** *18*, 1117-1123.
53. Burckbuchler, V.; Kjøniksen, A.-L.; Galant, C.; Lund, R.; Amiel, C.; Knudsen, K. D.; Nyström, B., *Biomacromolecules* **2006,** *7*, 1871-1878.
54. Wintgens, V.; Daoud-Mahammed, S.; Gref, R.; Bouteiller, L.; Amiel, C., *Biomacromolecules* **2008,** *9*, 1434-1442.
55. van de Manakker, F.; van der Pot, M.; Vermonden, T.; van Nostrum, C. F.; Hennink, W. E., *Macromolecules* **2008,** *41*, 1766-1773.
56. Amiel, C.; Moine, L.; Sandier, A.; Brown, W.; David, C.; Hauss, F.; Renard, E.; Gosselet, M.; Sébille, B., Macromolecular Assemblies Generated by Inclusion Complexes between Amphipathic Polymers and β-Cyclodextrin Polymers in Aqueous Media. In *Stimuli-Responsive Water Soluble and Amphiphilic Polymers*, American Chemical Society: 2000; Vol. 780, pp 58-81.
57. Guo, X.; Wang, J.; Li, L.; Pham, D.-T.; Clements, P.; Lincoln, S. F.; May, B. L.; Chen, Q.; Zheng, L.; Prud'homme, R. K., *Macromol. Rapid Commun.* **2010,** *31*, 300-304.
58. Kretschmann, O.; Choi, S. W.; Miyauchi, M.; Tomatsu, I.; Harada, A.; Ritter, H., *Angew. Chem. Int. Ed.* **2006,** *45*, 4361-4365.
59. Wang, J.; Pham, D.-T.; Guo, X.; Li, L.; Lincoln, S. F.; Luo, Z.; Ke, H.; Zheng, L.; Prud'homme, R. K., *Ind. Eng. Chem. Res.* **2010,** *49*, 609-612.
60. Koopmans, C.; Ritter, H., *Macromolecules* **2008,** *41*, 7418-7422.
61. Tomatsu, I.; Hashidzume, A.; Harada, A., *J. Am. Chem. Soc.* **2006,** *128*, 2226-2227.
62. Tamesue, S.; Takashima, Y.; Yamaguchi, H.; Shinkai, S.; Harada, A., *Angew. Chem. Int. Ed.* **2010,** *49*, 7461-7464.
63. Nakahata, M.; Takashima, Y.; Hashidzume, A.; Harada, A., *Angew. Chem. Int. Ed.* **2013,** *52*, 5731-5735.
64. White, S. R.; Sottos, N. R.; Geubelle, P. H.; Moore, J. S.; Kessler, M. R.; Sriram, S. R.; Brown, E. N.; Viswanathan, S., *Nature* **2001,** *409*, 794-797.
65. Diesendruck, C. E.; Sottos, N. R.; Moore, J. S.; White, S. R., *Angew. Chem. Int. Ed.* **2015,** *54*, 10428-10447.

66. White, S. R.; Moore, J. S.; Sottos, N. R.; Krull, B. P.; Santa Cruz, W. A.; Gergely, R. C. R., *Science* **2014,** *344*, 620-623.
67. Binder, W. H., *Self-Healing Polymers: From Principles to Applications*. Wiley-VCH Verlag GmbH & Co. KGaA: Weinheim, 2013.
68. Burattini, S.; Greenland, B. W.; Chappell, D.; Colquhoun, H. M.; Hayes, W., *Chem. Soc. Rev.* **2010,** *39*, 1973-1985.
69. Yang, Y.; Urban, M. W., *Chem. Soc. Rev.* **2013,** *42*, 7446-7467.
70. Wool, R. P., *Soft Matter* **2008,** *4*, 400-418.
71. Roy, N.; Bruchmann, B.; Lehn, J.-M., *Chem. Soc. Rev.* **2015,** *44*, 3786-3807.
72. Yanagisawa, Y.; Nan, Y.; Okuro, K.; Aida, T., *Science* **2018,** *359*, 72-76.
73. Kang, J.; Tok, J. B. H.; Bao, Z., *Nat. Electron.* **2019,** *2*, 144-150.
74. Ono, T.; Nobori, T.; Lehn, J.-M., *Chem. Commun.* **2005,** 1522-1524.
75. Ono, T.; Fujii, S.; Nobori, T.; Lehn, J.-M., *Chem. Commun.* **2007,** 46-48.
76. Chow, C.-F.; Fujii, S.; Lehn, J.-M., *Angew. Chem. Int. Ed.* **2007,** *46*, 5007-5010.
77. Ono, T.; Fujii, S.; Nobori, T.; Lehn, J.-M., *Chem. Commun.* **2007,** 4360-4362.
78. Fukuda, K.; Shimoda, M.; Sukegawa, M.; Nobori, T.; Lehn, J.-M., *Green Chem.* **2012,** *14*, 2907-2911.
79. Brunsveld, L.; Folmer, B. J. B.; Meijer, E. W.; Sijbesma, R. P., *Chem. Rev.* **2001,** *101*, 4071-4098.
80. Harada, A., *Supramolecular Polymer Chemistry*. Wiley-VCH Verlag & Co. KGaA: Weinheim, 2012.
81. Lehn, J. M., *Supramolecular Chemistry: Concepts and Perspectives*. Wiley-VCH Verlag & Co. KGaA: Weinheim, 1995.
82. Zhang, X.; Waymouth, R. M., *J. Am. Chem. Soc.* **2017,** *139*, 3822-3833.
83. Moutos, F. T.; Freed, L. E.; Guilak, F., *Nat. Mater.* **2007,** *6*, 162.
84. Harada, A.; Kobayashi, R.; Takashima, Y.; Hashidzume, A.; Yamaguchi, H., *Nat. Chem.* **2011,** *3*, 34.
85. Nakahata, M.; Takashima, Y.; Yamaguchi, H.; Harada, A., *Nat. Commun.* **2011,** *2*, 511.
86. Kakuta, T.; Takashima, Y.; Nakahata, M.; Otsubo, M.; Yamaguchi, H.; Harada, A., *Adv. Mater.* **2013,** *25*, 2849-2853.
87. Kakuta, T.; Takashima, Y.; Harada, A., *Macromolecules* **2013,** *46*, 4575-4579.
88. Kakuta, T.; Takashima, Y.; Sano, T.; Nakamura, T.; Kobayashi, Y.; Yamaguchi, H.; Harada, A., *Macromolecules* **2015,** *48*, 732-738.
89. Nakahata, M.; Takashima, Y.; Harada, A., *Macromol. Rapid Commun.* **2016,** *37*, 86-92.
90. Shibayama, M., *Soft Matter* **2012,** *8*, 8030-8038.
91. Zhao, X., *Soft Matter* **2014,** *10*, 672-687.
92. Gong, J. P.; Katsuyama, Y.; Kurokawa, T.; Osada, Y., *Adv. Mater.* **2003,** *15*, 1155-1158.
93. Ducrot, E.; Chen, Y.; Bulters, M.; Sijbesma, R. P.; Creton, C., *Science* **2014,** *344*, 186-189.
94. Sato, K.; Nakajima, T.; Hisamatsu, T.; Nonoyama, T.; Kurokawa, T.; Gong, J. P., *Adv. Mater.* **2015,** *27*, 6990-6998.
95. Haraguchi, K.; Takehisa, T., *Adv. Mater.* **2002,** *14*, 1120-1124.
96. Okumura, Y.; Ito, K., *Adv. Mater.* **2001,** *13*, 485-487.
97. Bin Imran, A.; Esaki, K.; Gotoh, H.; Seki, T.; Ito, K.; Sakai, Y.; Takeoka, Y., *Nat. Commun.* **2014,** *5*, 5124.
98. Sakai, T.; Matsunaga, T.; Yamamoto, Y.; Ito, C.; Yoshida, R.; Suzuki, S.; Sasaki, N.; Shibayama, M.; Chung, U.-i., *Macromolecules* **2008,** *41*, 5379-5384.
99. Kondo, S.; Hiroi, T.; Han, Y.-S.; Kim, T.-H.; Shibayama, M.; Chung, U.-i.; Sakai, T., *Adv. Mater.* **2015,** *27*, 7407-7411.
100. Sun, J.-Y.; Zhao, X.; Illeperuma, W. R. K.; Chaudhuri, O.; Oh, K. H.; Mooney, D. J.; Vlassak, J. J.; Suo, Z., *Nature* **2012,** *489*, 133.

101. Fantner, G. E.; Hassenkam, T.; Kindt, J. H.; Weaver, J. C.; Birkedal, H.; Pechenik, L.; Cutroni, J. A.; Cidade, G. A. G.; Stucky, G. D.; Morse, D. E.; Hansma, P. K., *Nat. Mater.* **2005,** *4*, 612-616.
102. Takashima, Y.; Sawa, Y.; Iwaso, K.; Nakahata, M.; Yamaguchi, H.; Harada, A., *Macromolecules* **2017,** *50*, 3254-3261.
103. Stuart, M. A. C.; Huck, W. T. S.; Genzer, J.; Müller, M.; Ober, C.; Stamm, M.; Sukhorukov, G. B.; Szleifer, I.; Tsukruk, V. V.; Urban, M.; Winnik, F.; Zauscher, S.; Luzinov, I.; Minko, S., *Nat. Mater.* **2010,** *9*, 101.
104. Zhuang, J.; Gordon, M. R.; Ventura, J.; Li, L.; Thayumanavan, S., *Chem. Soc. Rev.* **2013,** *42*, 7421-7435.
105. Lenhardt, J. M.; Black, A. L.; Craig, S. L., *J. Am. Chem. Soc.* **2009,** *131*, 10818-10819.
106. Karthikeyan, S.; Potisek, S. L.; Piermattei, A.; Sijbesma, R. P., *J. Am. Chem. Soc.* **2008,** *130*, 14968-14969.
107. Piermattei, A.; Karthikeyan, S.; Sijbesma, R. P., *Nat. Chem.* **2009,** *1*, 133.
108. Chen, Y.; Spiering, A. J. H.; Karthikeyan, S.; Peters, G. W. M.; Meijer, E. W.; Sijbesma, R. P., *Nat. Chem.* **2012,** *4*, 559.
109. Imato, K.; Irie, A.; Kosuge, T.; Ohishi, T.; Nishihara, M.; Takahara, A.; Otsuka, H., *Angew. Chem. Int. Ed.* **2015,** *54*, 6168-6172.
110. Zheng, Y.; Hashidzume, A.; Harada, A., *Macromol. Rapid Commun.* **2013,** *34*, 1062-1066.
111. Zheng, Y.; Hashidzume, A.; Takashima, Y.; Yamaguchi, H.; Harada, A., *ACS Macro Lett.* **2012,** *1*, 1083-1085.
112. Koopmans, C.; Ritter, H., *J. Am. Chem. Soc.* **2007,** *129*, 3502-3503.
113. Taguchi, K., *J. Am. Chem. Soc.* **1986,** *108*, 2705-2709.
114. Fleischmann, C.; Cheng, J.; Tabatabai, M.; Ritter, H., *Macromolecules* **2012,** *45*, 5343-5346.
115. Fleischmann, C.; Ritter, H., *Macromol. Rapid Commun.* **2013,** *34*, 1085-1089.
116. Takashima, Y.; Yonekura, K.; Koyanagi, K.; Iwaso, K.; Nakahata, M.; Yamaguchi, H.; Harada, A., *Macromolecules* **2017,** *50*, 4144-4150.
117. Takashima, Y.; Otani, K.; Kobayashi, Y.; Aramoto, H.; Nakahata, M.; Yamaguchi, H.; Harada, A., *Macromolecules* **2018,** *51*, 6318-6326.
118. Kawaguchi, Y.; Harada, A., *J. Am. Chem. Soc.* **2000,** *122*, 3797-3798.
119. Nomimura, S.; Osaki, M.; Park, J.; Ikura, R.; Takashima, Y.; Yamaguchi, H.; Harada, A., *Macromolecules* **2019,** *52*, 2659-2668.
120. Rogers, R. D.; Seddon, K. R., *Science* **2003,** *302*, 792-793.
121. Welton, T., *Chem. Rev.* **1999,** *99*, 2071-2083.
122. Wilkes, J. S.; Zaworotko, M. J., *J. Chem. Soc., Chem. Commun.* **1992,** 965-967.
123. Angell, C. A.; Liu, C.; Sanchez, E., *Nature* **1993,** *362*, 137-139.
124. Watanabe, M.; Yamada, S.-I.; Sanui, K.; Ogata, N., *J. Chem. Soc., Chem. Commun.* **1993,** 929-931.
125. Ye, Y. S.; Rick, J.; Hwang, B. J., *J. Mater. Chem. A* **2013,** *1*, 2719-2743.

Chapter 2

Preparation of supramolecular ionic liquid gels based on host-guest interactions and their swelling and ionic conductive properties

2.1. Introduction

In recent year, various demands for ionic liquid materials have also prompted the development of ionic liquid gel with high fracture energy. Ionic liquid gels (IGs),[1-2] which was prepared through swelling the polymeric materials in an ionic liquid, have been received much attention because of its high ionic conductivity (σ). These IGs have been applied as actuators,[3-4] solid electrolytes,[5-10] capacitors,[11-12] membranes,[13-14] dye-sensitized solar cells,[15-17] and so on.[18-20] Of course, these applications are basically utilized from physicochemical properties of ionic liquids as molten salts.[21-23] Ionic liquid low glass transition (T_g) and low melting point (T_m) preserve σ and electrochemical stability while utilized in polymeric materials,[24-25] there were a few reports physicochemical properties of ionic liquid gels based on a design of polymer networks. Covalently bonded polymers as polymer backbone have been popular to be used as IGs, whereas non-covalently bonded polymers in ionic liquid gels have not been brought to attentions for materials design because the cationic properties of ionic liquids will be inhibit non-covalent interactions (cation-anion, cation-π, π-π, etc). Ionic liquid gels based on supramolecular materials, "supramolecular ionic liquid gels", were supposed to show further high σ and electrochemical stability.

Recently, there are some report concerning about supramolecular polymeric gels cross-linking by non-covalent interaction such as hydrogen bonds,[26] π-π stacking,[27-28] electrostatic interactions,[29] metal-ligand interactions,[30-31] and hydrophobic interactions[32]. Host-guest interactions based on cyclodextrins (CDs) and hydrophobic guest molecules will be a breakthrough method because other non-covalent interactions are affected by the cationic properties of ionic liquids. Previously, supramolecular hydrogels and elastomers cross-linked by the inclusion complex between CDs and guest molecules on polymer main chain have been reported. The fracture energy of the resulting supramolecular materials were higher compared to the chemically cross-linked materials.

Herein, supramolecular elastomers as IGs based on CD and adamantane derivatives were employed, [PAc*γ*-CD-Ad-R IG(*x*,*y*)] (Figure 2-1). The supramolecular polymeric IG containing CD as host molecules and Ad as guest molecules was prepared by preparing supramolecular elastomer through bulk copolymerization then followed by immersion in ionic liquid. 1-Ethyl-3-methylimidazolium bis(trifluoromethylsulfonyl)imide (EMIm TFSI) was renowned for its highest σ value among other hydrophobic ionic liquid available.[2, 33-34] Chemically cross-linked IGs, R IG, PAc*γ*-CD-R IG, and Ad-R IG were also prepared for comparison of the σ and fracture energy between PAc*γ*-CD-Ad-R IG and the chemically cross-linked IGs. The results show that σ of PAc*γ*-CD-Ad-R IGs are higher than those of the chemically cross-linked IGs due to host-guest interactions.

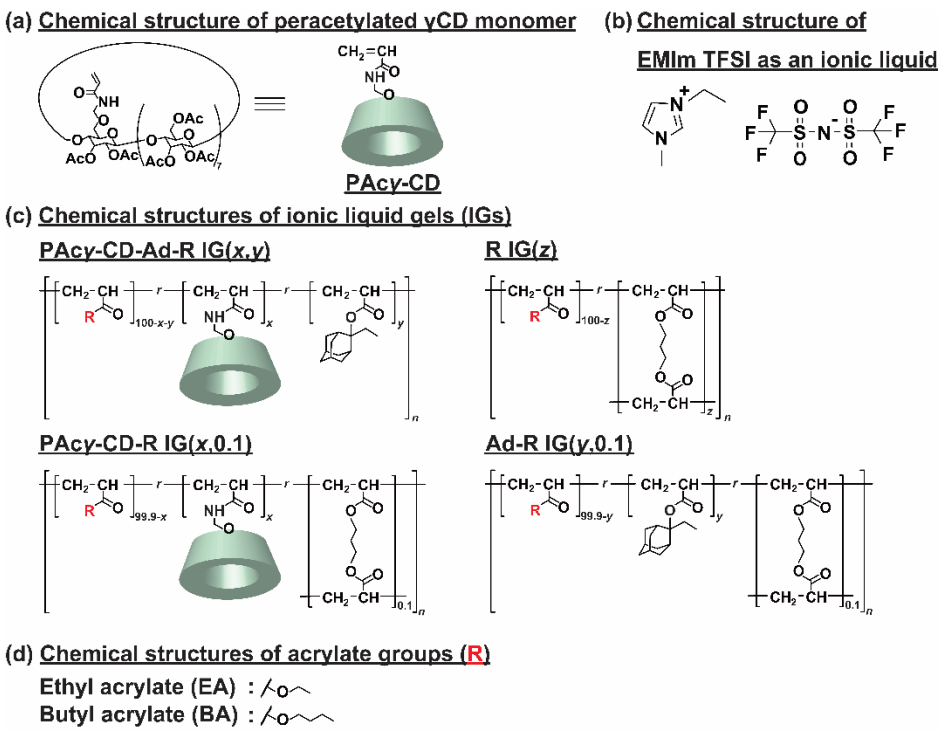

Figure 2-1. Chemical structures of (**a**) peracetylated 6–acrylamido methylether–*γ*-CD monomer (PAc*γ*-CD) as host monomer, (**b**) 1-ethyl-3-methylimidazolium bis(trifluoromethylsulfonyl)imide (EMIm TFSI) as an ionic liquid, and (**c**) ionic liquid gels (PAc*γ*-CD-Ad-R IG, R-IG, PAcγ-CD-R IG, Ad-R IG). (**d**) Group of main chain monomers (R). The mol% of PAc*γ*-CD, Ad, and 1,4-butanediol diacrylate (BDA) units were indicated as *x*, *y*, and *z* , respectively.

2.2. Experimental section

2.2.1. Materials

γ-CD was purchased from Junsei Chemical Co., Ltd. Ad was purchased from Osaka Organic Chemical Industry Ltd. 1-Hydroxy cyclohexyl phenyl ketone (IRGACURE 184, Ciba) was obtained from BASF Japan Co., Ltd. Ethyl acrylate (EA) and butyl acrylate (BA) were obtained from Toagosei Co., Ltd. Acetic anhydride, 1,4-butanediol diacrylate (BDA), and bromoethane were obtained from Nacalai Tesque Inc. Lithium bis(trifluoromethanesulfonyl)imide (LiTFSI) was obtained from Tokyo Chemical Industry Co., Ltd. $CDCl_3$ and pyridine were obtained from Wako Pure Chemical Industries, Ltd. DMSO–d_6 was purchased from Merck & Co., Inc. Water used for the preparation was purified with a Millipore Elix 5 system. Other reagents were used as received.

2.2.2. Measurements.

^1H, ^{13}C, and ^{19}F NMR spectra were recorded at 500 MHz with a JEOL-ECA-500 NMR spectrometer at 25 ºC. Solid–state ^1H field gradient magic angle spinning (FGMAS) and difussion-ordered spectroscopy (DOSY) NMR spectra were recorded at 400 MHz with a JEOL-ECA-400 NMR spectrometer. FGMAS NMR sample spinning rate was 7 kHz. In all NMR measurements, chemical shifts were referenced to the solvent values [^1H NMR: δ = 0 ppm for tetramethylsilane (TMS) and 2.49 ppm for DMSO–d_6, ^{13}C NMR: δ = 0 ppm for TMS and 39.5 ppm for DMSO–d_6)]. ^{19}F NMR spectra were calibrated using external standard $CFCl_3$ (δ = 0 ppm). Mass spectrometry was performed using Bruker autoflex speed positive-ion matrix-assisted laser desorption/ionization time-of-flight (MALDI-TOF MS) mass spectrometer using 2,5-dihydroxybenzoic acid as matrix. Young's modulus of ionic liquid gels were measured using universal tensile test machine Autograph AG-X plus with a 50 N load cell with deformation rate 1 mm/s until 10% strain. Conductivity of ionic liquid gels were measured by Hewlett-Packard 4284A Precision LCR [inductance (L), capacitance (C), and resistance (R)] meter with frequency 20 Hz–1 MHz using electrode made from stainless steel with sample size 20 mm in diameter

2.2.3. Preparation of materials

Preparation of peracetylated 6–acrylamido methylether–*γ*-CD (PAc*γ*-CD)[35-36]

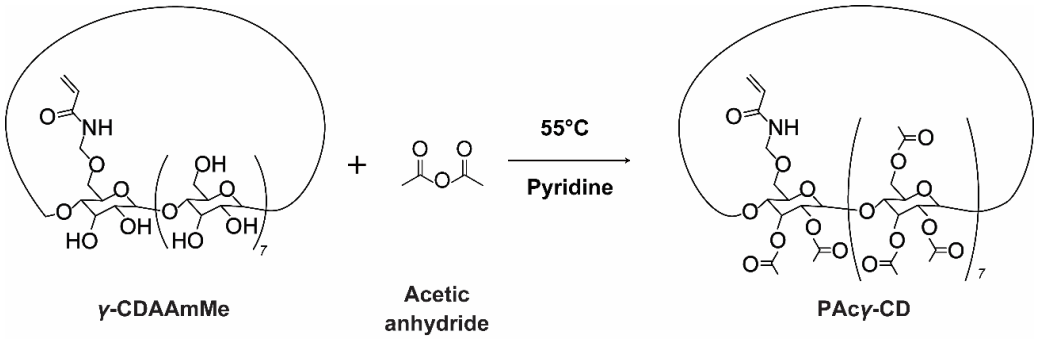

Scheme 2-1. Preparation of PAc*γ*-CD.

6–Acrylamido methylether–*γ*-CD (*γ*-CDAAmMe) was prepared according to previous reports.[37] *γ*-CDAAmMe (20 g, 15 mmol) and acetic anhydride (0.17 kg, 1.7 mol) were dissolved in pyridine (0.30 L) and stirred at 55 ºC for overnight. The solution was cooled to room temperature and put in ice bath and then methanol (50 mL) was added to quench the reaction. The solution was evaporated until 0.20 L and then precipitated in cooled water (1.5 L). Precipitate was filtered and dissolved again in acetone (0.20 L) and then precipitated again in cooled water (1.5 L). After second filtration, the precipitate was washed twice with water (0.50 L) and then dried under reduced pressure at 40 ºC for 48 hours. Yield: 81%.

^{1}H NMR (500MHz, Chloroform-*d*) of PAc*γ*-CD: δ = 6.90 (t, 1H, -CON*H*-), 6.31 (dd, 1H, C*H*$_2$CH-), 6.13 (d, 1H, C*H*$_2$CH-), 5.69 (d, 1H, CH$_2$C*H*-), 5.33 (m, 8H, C(3)*H* of CD), 5.15 (m, 8H, C(1)*H* of CD), 4.91 (dd, 2H,-NHC*H*$_2$O-), 4.73 (m, 8H, C(2)*H* of CD), 4.45 (m, 16H, C(6)*H* of CD), 4.00 (m, 8H, C(5)*H* of CD), 3.69 (m, 8H, C(4)*H* of CD), 2.11 (m, C*H*$_3$ of acetyl overlaps with HOD).

^{13}C NMR (125 MHz, Chloroform-*d*) of PAc*γ*-CD: δ = 170.7, 170.4, 170.4, 169.4, 169.4, 169.4, 165.9, 130.6, 127.6, 76.3, 76.2, 75.8, 75.6, 71.4, 71.1, 70.9, 70.8, 70.6, 70.5, 70.4, 70.3, 70.2, 70.0, 69.8, 69.7, 69.6, 66.3, 62.9, 62.7, 62.5, 62.5, 20.8.

MALDI TOF MS of PAc*γ*-CD: Found : *m*/*z* = 2368.8, 2384.9.

Calcd. : $[C_{98}H_{131}NO_{64}Na]^+$ = 2368.7, $[C_{98}H_{131}NO_{64}K]^+$ = 2384.7.

Preparation of 1-ethyl-3-methylimidazolium bromide (EMIm Br)

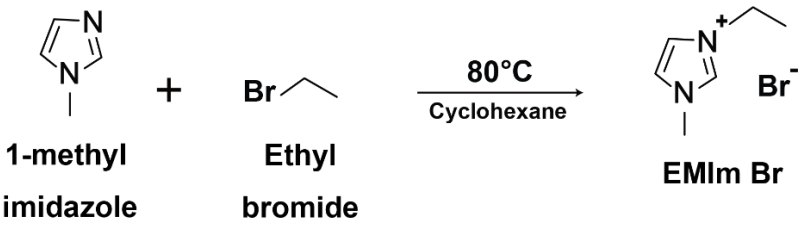

Scheme 2-2. Preparation of EMIm Br.

1-methyl imidazole (37 g, 0.50 mol) and ethyl bromide (0.15 kg, 1.4 mol) were dissolved in cyclohexane (0.20 L) and the solution was stirred at 80 °C for 24 h. After reaction, the mixture separated into 2 layers and then poured into beaker glass to room temperature. Lower layer turned into solid phase and then poured away the liquid phase. Solid phase was recrystallized using ethyl acetate : 2-propanol (1:1 by volume). The crystalized sample was melted at 83 °C for 24 h under vacuum to give EMIm Br. Yield: 91%.

^{1}H NMR (500 MHz, DMSO-d_6) of EMIm Br: δ = 9.37 (s, 1H,-NC*H*N-), 7.86 (t, *J* = 1.8 Hz, 1H,-NC*H*CH-), 7.76 (t, *J* = 1.8 Hz, 1H,-NCHC*H*-), 4.19 (q, *J* = 7.3 Hz, 2H,-NCH_2-), 3.84 (s, 3H,-NCH_3), 1.36 (t, *J* = 7.3 Hz, 3H, -CH_2CH_3).

^{13}C NMR (125 MHz, DMSO-d_6) of EMIm Br: δ = 136.8, 124.0, 122.5, 44.6, 36.3, 15.7.

Preparation of 1-ethyl-3-methylimidazolium bis(trifluoromethylsulfonyl)imide (EMIm TFSI)

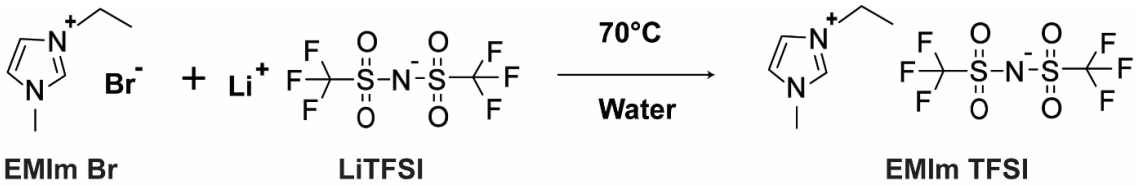

Scheme 2-3. Preparation of EMIm TFSI.

EMIm Br (5.0 g, 26 mmol) was dissolved in water (10 mL), and then bis(trifluoromethylsulfonyl)imide lithium salt (LiTFSI, 8.3 g, 29 mmol) was also dissolved in water (10 mL). These solutions were mixed together and stirred at 70 °C for 24 h. The mixture separated into 2 layers and poured into separating funnel. The lower layer was washed three times with water. After washing, it was dried under reduced pressure at 120 °C for 72 h to obtain EMIm TFSI ionic liquid. Yield: 84%.

^{19}F NMR (470 MHz, DMSO-d_6) of EMIm TFSI: δ = -78.80.

^{1}H NMR (500 MHz, DMSO-d_6) of EMIm TFSI: δ = 9.06 (s, 1H,-NC*H*N-), 7.71 (t, *J* = 1.8 Hz, 1H,-NC*H*CH-), 7.63 (t, *J* = 1.8 Hz, 1H,-NCHC*H*-), 4.20 (q, *J* = 7.3 Hz, 2H,-NCH_2-), 3.83 (s, 3H,-NCH_3), 1.42 (t, *J* = 7.3 Hz, 3H,-CH_2CH_3).

^{13}C NMR (125 MHz, DMSO-d_6) of EMIm TFSI: δ = 136.76, 124.05, 122.43, 121.31, 118.75, 44.67, 36.12, 15.42.

Preparation of elastomers

In order to form the inclusion complexes, host monomers (PAc*γ*-CD) and guest monomers (Ad) were dissolved in acrylate monomers and the solution was sonicated for 2 h at room temperature. The monomer solution was polymerized by 1-hydroxycyclohexyl phenyl ketone (IRGACURE 184) as photo-induced radical initiator to give PAc*γ*-CD-Ad-R(*x, y*) elastomer. The reference samples, R(*z*) elastomers, PAc*γ*-CD-R(*x,* 0.1) elastomers, and Ad-R(*y,* 0.1) elastomers were prepared by similar methods using BDA as chemical cross-linker. *x, y*, and *z* indicate the mol% of PAc*γ*-CD, Ad, and BDA units, respectively.

Table 2-1. Preparation of PAc*γ*-CD-Ad-EA(*x, y*) elastomers.

Molar ratio (*x, y*)	PAc*γ*-CD / g	Ad / g	EA / g	IRGACURE 184 / mg
(0.5, 0.5)	0.59	0.059	5.0	16
(1, 1)	1.2	0.12	5.0	16
(2, 2)	2.4	0.24	5.0	16

Table 2-2. Preparation of PAc*γ*-CD-Ad-BA(*x, y*) elastomers.

Molar ratio (*x, y*)	PAc*γ*-CD / g	Ad /g	BA / g	IRGACURE 184 / mg
(0.5, 0.5)	0.46	0.046	5.0	16
(1, 1)	0.93	0.093	5.0	16
(2, 2)	1.9	0.19	5.0	16

Table 2-3. Preparation of EA(*z*) elastomers.

Molar ratio (*z*)	BDA / g	EA / g	IRGACURE 184 / mg
(0.5)	0.050	5.0	16
(1)	0.10	5.0	16
(2)	0.20	5.0	16

Table 2-4. Preparation of BA(*z*) elastomers.

Molar ratio (*z*)	BDA / g	BA / g	IRGACURE 184 / mg
(0.5)	0.040	5.0	16
(1)	0.080	5.0	16
(2)	0.16	5.0	16

Table 2-5. Preparation of PAc*γ*-CD-EA(*x*, 0.1) elastomers.

Molar ratio (*x*, 0.1)	PAc*γ*-CD / g	BDA / mg	EA / g	IRGACURE 184 / mg
(0.5, 0.1)	0.59	9.9	5.0	16
(1, 0.1)	1.2	10	5.0	16
(2, 0.1)	2.4	10	5.0	16

Table 2-6. Preparation of PAc*γ*-CD-BA(*x*, 0.1) elastomers.

Molar ratio (*x*, 0.1)	PAc*γ*-CD / g	BDA / mg	BA / g	IRGACURE 184 / mg
(0.5, 0.1)	0.46	7.8	5.0	16
(1, 0.1)	0.93	7.8	5.0	16
(2, 0.1)	1.9	7.9	5.0	16

Table 2-7. Preparation of Ad-EA(*y*, 0.1) elastomers.

Molar ratio (*y*, 0.1)	Ad / g	BDA / mg	EA / g	IRGACURE 184 / mg
(0.5, 0.1)	0.059	9.9	5.0	16
(1, 0.1)	0.12	10	5.0	16
(2, 0.1)	0.24	10	5.0	16

Table 2-8. Preparation of Ad-BA(*y*, 0.1) elastomers.

Molar ratio (*y*, 0.1)	Ad / g	BDA / mg	BA / g	IRGACURE 184 / mg
(0.5, 0.1)	0.046	7.8	5.0	16
(1, 0.1)	0.093	7.8	5.0	16
(2, 0.1)	0.19	7.9	5.0	16

2.3. Results and discussion

2.3.1. Preparation of supramolecular ionic liquid gels

Figure 2-2 shows the procedure to prepare PAc*γ*-CD-Ad-R IG(*x*,*y*). PAc*γ*-CD (Scheme 2-1) as a host monomer and Ad as a guest monomer were sonicated in acrylate monomer (EA or BA) to form inclusion complex. The mixture was added with IRGACURE 184 as a photo radical initiator then irradiated with ultraviolet (UV) light (λ = 365 nm) to form supramolecular elastomer (PAc*γ*-CD-Ad-R elastomer) (Figure 2-2a, Tables 2-1 and 2-2).

EMIm TFSI was prepared through two steps,[2] first step is quaternization of 1-methyl imidazole by bromoethane to obtain white crystalline hygroscopic 1-ethyl-3-methyl imidazolium (EMIm Br), then second step is heating EMIm Br with equimolar lithium bis(trifluoromethanesulfonyl)imide (LiTFSI) to EMIm TFS. The PAc*γ*-CD-Ad-R elastomer was immersed in the EMIm TFSI to obtain the PAc*γ*-CD-Ad-R IG (Schemes 2-2 and 2-3, Figure 2-2b). R IG, PAc*γ*-CD-R IG, and Ad-R IG (Fig. 1c), were prepared by similar methods as reference samples, instead BDA was used as chemical cross-linker (Tables 2-3 –2-8).

x, *y*, and *z* indicate the mol% of the PAc*γ*-CD, Ad, and BDA units in IGs [PAc*γ*-CD-Ad-R IG(*x*,*y*), R IG(*z*), PAc*γ*-CD-R IG(*x*,0.1), and Ad-R IG(*y*,0.1)]. The notation 0.1 indicates the 0.1 mol% of BDA units at PAc*γ*-CD-R IG(*x*,0.1) and Ad-R IG(*y*,0.1).

Solid–state ^{1}H field gradient magic angle spinning (FGMAS) NMR was used to characterize PAc*γ*-CD-Ad-R elastomer and PAc*γ*-CD-Ad-R IG (Figures 2-3 – 2-6). Young's modulus of IGs were measured to confirm the host-guest cross-linking point at PAc*γ*-CD-Ad-R IG (Figure 2-7).

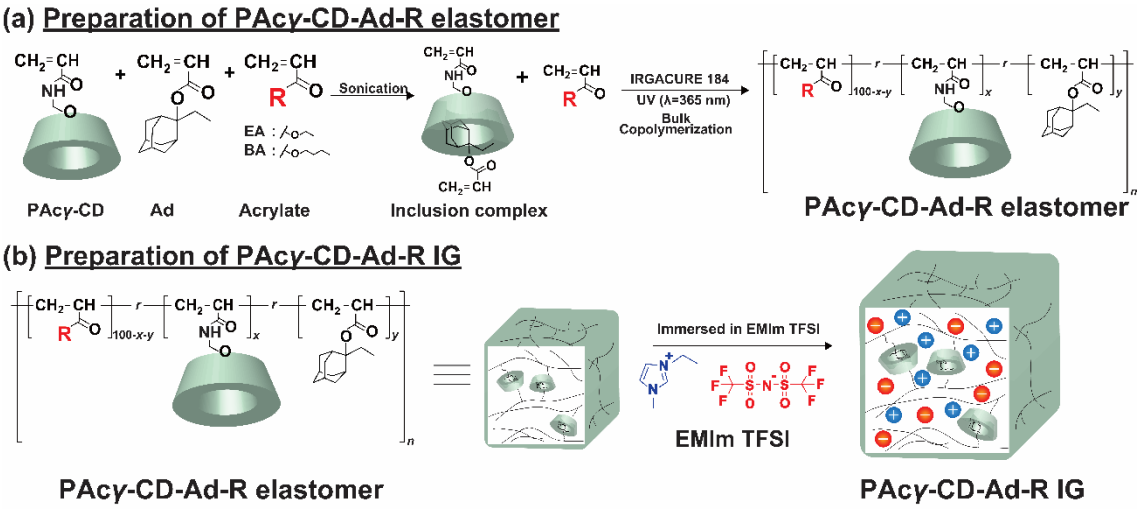

Figure 2-2. (**a**) Preparation of the PAc*γ*-CD-Ad-R elastomer(*x*,*y*) by bulk polymerization. (**b**) Immersion of PAc*γ*-CD-Ad-R elastomer(*x*,*y*) in the EMIm TFSI to obtain PAc*γ*-CD-Ad-R IG(*x*,*y*).

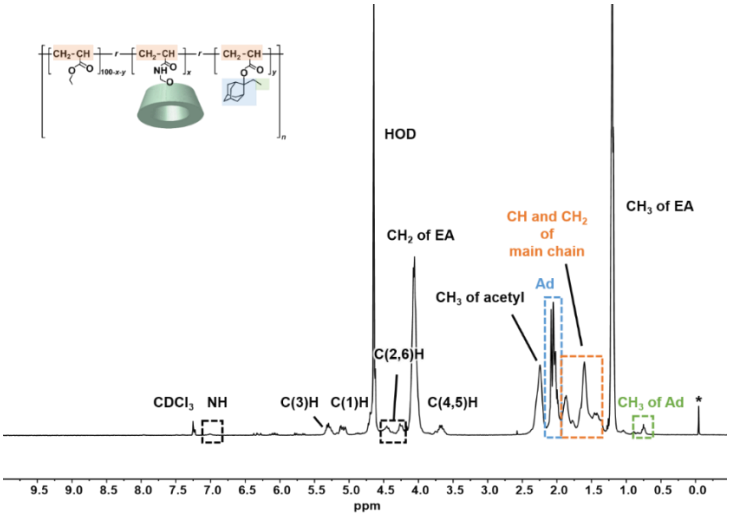

Figure 2-3. Solid-state ^{1}H FGMAS NMR spectrum of PAc*γ*-CD-Ad-EA elastomer(1,1) (TMS for standard, 400 MHz, 25 ºC, rotation frequency = 7 kHz).

^{1}H NMR (400 MHz, Chloroform-*d*): δ = 7.05 (-N*H*-), 5.38-5.29 (C(3)*H* of CD), 5.17-5.10 (C(1)*H* of CD), 4.52-4.27 (C(2,6)*H* of CD), 4.16-4.04 (-C*H*$_2$CH$_3$ of EA), 3.80-3.68 (C(4,5)*H* of CD), 2.35-2.29 (-C*H*$_3$ of acetyl), 2.15-2.03 (-C*H*-, -C*H*$_2$-, and -C*H*$_2$CH$_3$ of Ad), 1.97-1.41 (-C*H*$_2$C*H*- of main chain), 1.30-1.23 (-C*H*$_3$ of EA), 0.82-0.78 (-C*H*$_3$ of Ad).

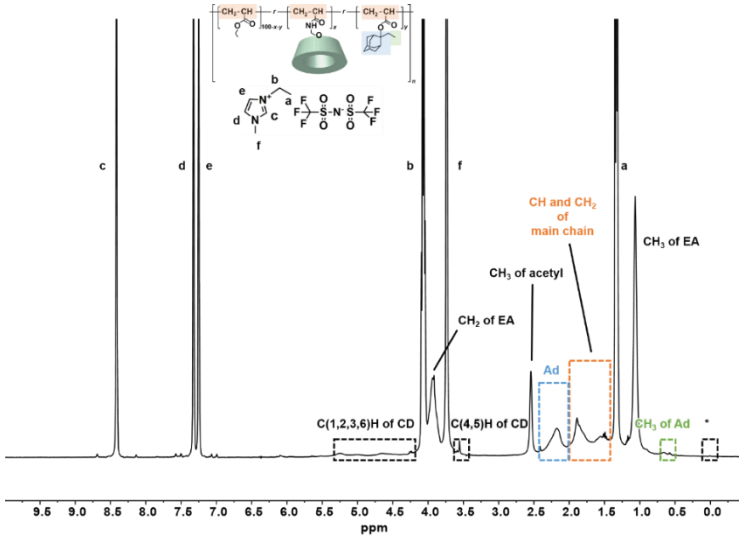

Figure 2-4. Solid-state ^{1}H FGMAS NMR spectrum of PAcγ-CD-Ad-EA IG(1,1) (TMS for standard, 400 MHz, 25 ºC, rotation frequency = 7 kHz).

^{1}H NMR (400 MHz, Chloroform-*d*): δ = 8.47 (-NC*H*N- of EMIm TFSI), 7.38 (-NC*H*CH- of EMIm TFSI), 7.31 (-NC*H*CH- of EMIm TFSI), 5.31-4.70 (C(1,2,3,6)*H* of CD), 4.14 (-NCH_2- of EMIm TFSI), 3.99-3.95 (-CH_2CH$_3$ of EA), 3.80 (-NCH_3 of EMIm TFSI), 2.59 (-CH_3 of acetyl), 2.24 (-C*H*-, -CH_2-, and -CH_2CH$_3$ of Ad), 1.95-1.61 (-CH_2C*H*- of main chain), 1.39 (-CH$_2$CH_3 of EMIm TFSI), 1.12 (-CH_3 of EA), 0.68 (-CH_3 of Ad).

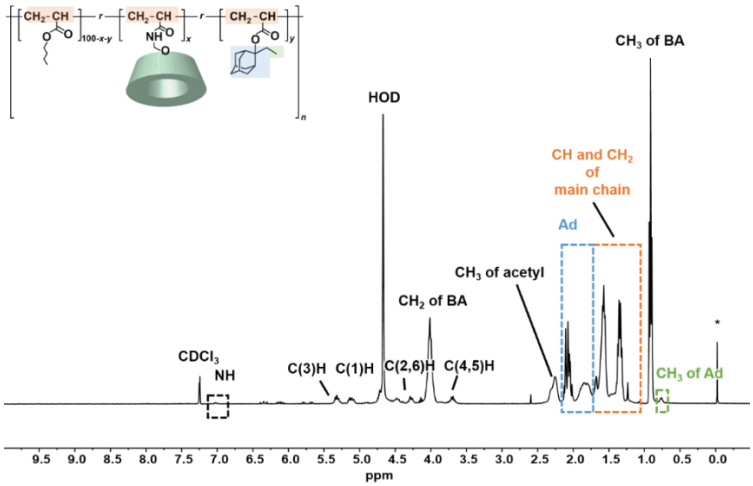

Figure 2-5. Solid-state ^{1}H FGMAS NMR spectrum of PAcγ-CD-Ad-BA elastomer(1,1) (TMS for standard, 400 MHz, 25 ºC, rotation frequency = 7 kHz).

^{1}H NMR (400 MHz, Chloroform-*d*): δ = 7.03 (-N*H*-), 5.38-5.32 (C(3)*H* of CD), 5.18-5.10 (C(1)*H* of CD), 4.50-4.16 (C(2,6)*H* of CD), 4.09-3.98 (-CH_2CH_2- of BA), 3.76-3.69 (C(4,5)*H* of CD), 2.28-2.26 (-CH_3 of acetyl), 2.15-1.70 (-C*H*-, -CH_2-, and -CH_2CH$_3$ of Ad), 1.66-1.26 (-CH_2C*H*- of main chain), 0.95-0.92 (-CH_3 of BA), 0.79 (-CH_3 of Ad).

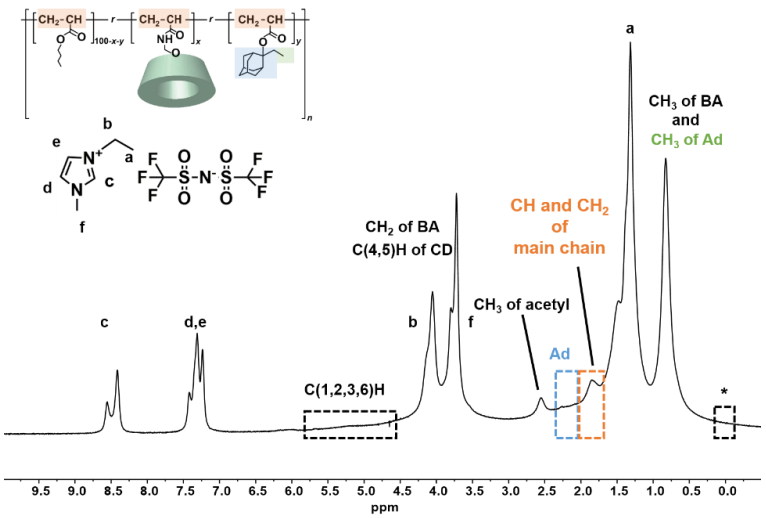

Figure 2-6. Solid-state ^{1}H FGMAS NMR spectrum of PAcγ-CD-Ad-BA IG(1,1) (TMS for standard, 400 MHz, 25 ºC, rotation frequency = 7 kHz).

^{1}H NMR (400 MHz, Chloroform-*d*): δ = 8.63-8.50 (-NC*H*N- of EMIm TFSI), 7.50-7.31 (-NC*H*C*H*- of EMIm TFSI), 5.80-4.71 (C(1,2,3,6)*H* of CD) 4.14 (-NCH_2- of EMIm TFSI), 3.88-3.80 (-CH_2CH_2- of BA, C(4,5)*H* of CD, and -NCH_2- of EMIm TFSI), 2.64 (-CH_3 of acetyl), 2.25 (-C*H*-, -CH_2-, and -CH_2CH$_3$ of Ad), 1.92 (-CH_2C*H*- of main chain), 1.39 (-CH$_2$CH_3 of EMIm TFSI), 0.91-0.70 (-CH_3 of BA and -CH_3 of Ad).

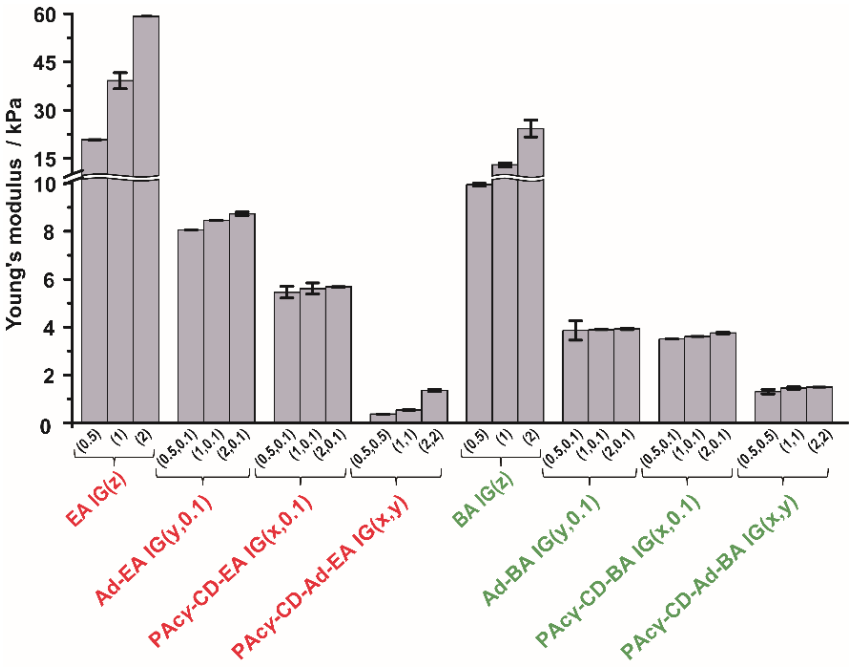

Figure 2-7. Young's modulus of ionic liquid gels.

2.3.2. Swelling ratio of ionic liquid gels

After immersion in the EMIm TFSI for 24 hours, swelling ratio of the elastomers (PAcγ-CD-Ad-R, PAcγ-CD-R, Ad-R, and R elastomers) were investigated by the following equation:

$$\text{Swelling ratio of elastomer} = \frac{W_{\text{IG}}\text{-}W_{\text{elastomer}}}{W_{\text{elastomer}}} \times 100\%$$

where $W_{\text{elastomer}}$ is weight of elastomers (before immersion in EMIm TFSI) and W_{IG} is weight of IGs (after immersion in EMIm TFSI).

Elastomers based on EA main chain polymer showed higher swelling ratios higher than those of the elastomers based on the BA main chain polymer because the EMIm TFSI is more compatible with EA main chain polymer (Figure 2-8a). The swelling ratio of the PAcγ-CD-Ad-EA elastomer(1,1) was larger than chemical cross-linked EA elastomer(1). Also, PAcγ-CD-Ad-EA elastomer(1,1) showed higher swelling ratio than those of the PAcγ-CD-EA elastomer(1,0.1) and the Ad-EA elastomer(1,0.1) even though the concentration of the cross-linking unit in PAcγ-CD-Ad-EA elastomer(1,1) was 10 times higher. This caused by relaxed cross-linking points of host-guest interaction in the PAcγ-CD-Ad-EA elastomer(1,1) during immersion in the EMIm TFSI. The ionic liquid content also closely related with in the swelling ratio in elastomer, higher ionic liquid content resulted in larger swelling ratio (Figure 2-9).

$$\text{Ionic liquid content (\%)} = \frac{W_{\text{IG}}\text{-}W_{\text{elastomer}}}{W_{\text{IG}}} \times 100\%$$

where $W_{\text{elastomer}}$ is weight of elastomer (before immersion in EMIm TFSI) and W_{IG} is weight of IGs (after elastomer immersion in EMIm TFSI).

Swelling ratio of IGs also correlated with cross-link density in IGs which can be determined through Young's modulus (Figure 2-8b). PAcγ-CD-Ad-EA IG(1,1) showed lowest Young's modulus compared to EA IG(1,1), Ad-EA IG(1,0.1), and PAcγ-CD-EA IG(1,0.1) because of the flexible and reversible interactions between CD and Ad units.

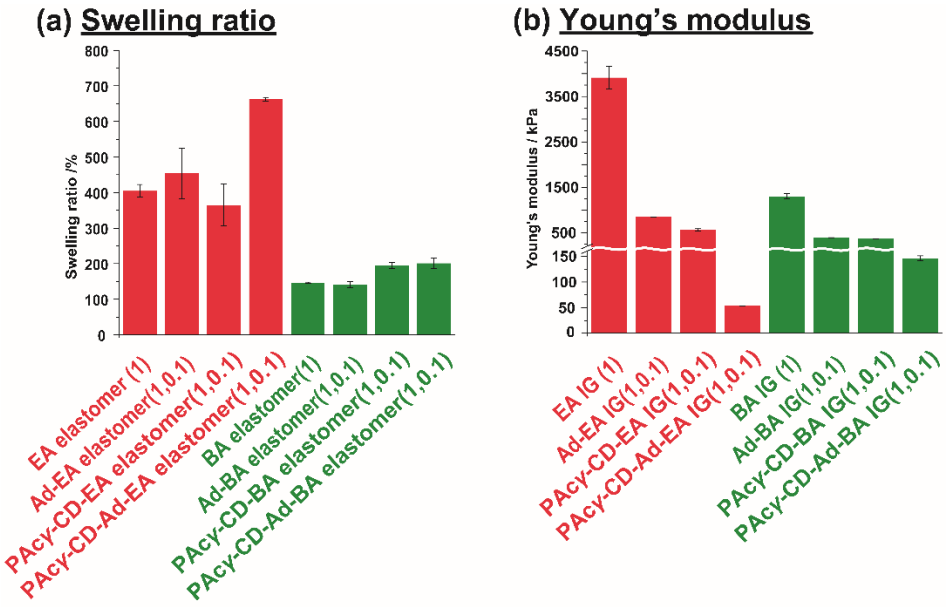

Figure 2-8. (**a**) Swelling ratio and (**b**) Young's modulus of ionic liquid gels.

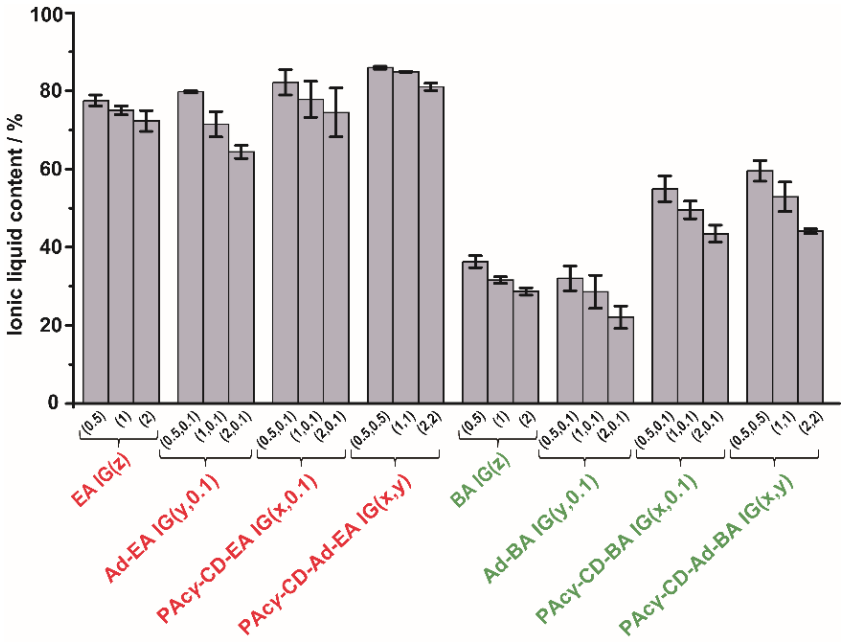

Figure 2-9. Ionic liquid content of ionic liquid gels.

2.3.3. Conductivity of ionic liquid gels

σ was measured using LCR meter with frequency 20 Hz-1 MHz. Measurement was conducted at constant temperature 25 °C. Data acquired from LCR Meter then calculated as using equation to obtain conductivity in AC current (σ_{ac}) as follows:

$$\sigma_{ac} = \omega\varepsilon_0\varepsilon'\tan(\delta) \qquad \text{where} \qquad \tan(\delta) = \frac{\varepsilon''}{\varepsilon'}$$

σ_{ac} is conductivity of AC current. ω is angular frequency. ε_0 is vacuum permittivity with value 8.85×10^{-12} F m^{-1}. ε' is dielectric constant and ε" is dielectric loss factor. Then, the result of σ_{ac} was plotted with frequency (f) in log graph to obtain graph that accordance to *Jonscher's Universal Power Law*[38] shows According to *Jonscher's Universal Power Law*, "plateau region" in plotted graph means conductivity that independent to frequency (σ_{dc}) (Figure 2-10a).

Figure 2-10b shows the sample calculation for conductivity of EMIm TFSI.[39] The plotted graph for EMIm TFSI showed that the frequency response of conductivity from EMIm TFSI exist in two different regions: electrode polarization region led to independent ionic motion and plateau region as frequency-dependent ionic transport in high frequency.

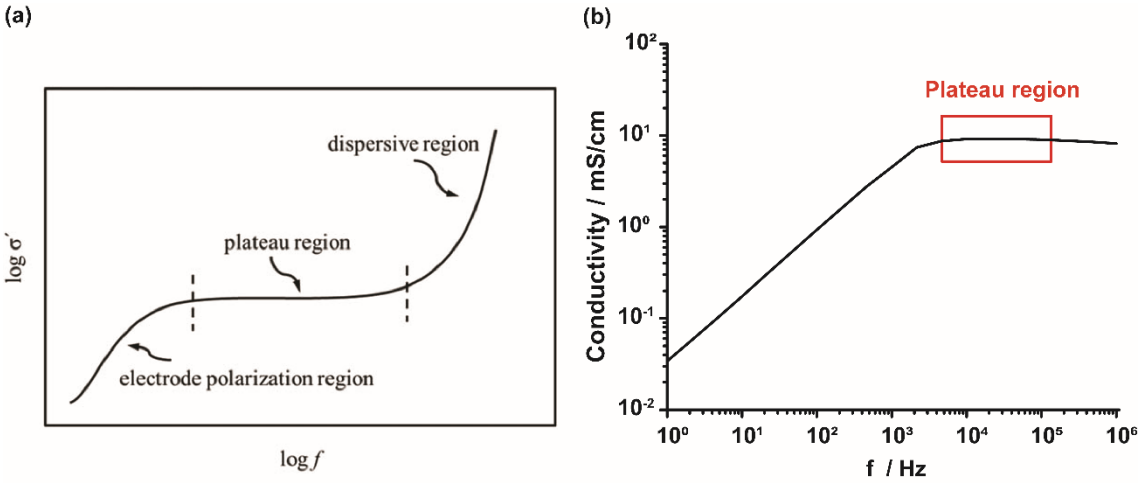

Figure 2-10. (**a**) *Jonscher's Universal Power Law* graph. (**b**) Plotted graph for ionic conductivity calculation of EMIm TFSI.

Figure 2-11a shows the illustration of ionic conductive measurement system. The σ of EMIm TFSI as native ionic liquid and IGs showed as Figure 2-11b. The σ of EMIm TFSI native ionic liquid was 9.0 mS/cm. The σ values of EA main chain polymer based IGs were higher than those of on BA main chain polymer based IGs. The σ of IGs either based EA main chain polymer or BA main chain polymer was lower than that of EMIm TFSI due to suppression while dispersed of in the polymer networks. The self-diffusion

coefficient will be discussed later in the section 2.3.4 to explain dispersion properties of EMIm TFSI.

The σ of PAcγ-CD-Ad-EA IG(1,1) (8.0 mS/cm) was higher than those of the EA IG(1) (0.54 mS/cm), Ad-EA IG(1,0.1) (0.50 mS/cm), and PAcγ-CD-EA IG(1,0.1) (1.6 mS/cm). The σ of PAcγ-CD-Ad-EA IG(1,1) (8.0 mS/cm) showed similar result with EMIm TFSI (9.0 mS/cm). These results showed that host-guest interaction raises the σ of IGs. Although the σ of BA main chain polymer based IGs were low, the trend was similar to EA main chain polymer based IGs (Figure 2-11b). The σ of IGs slightly depended on the molar ratio of cross-linkers (0.5-2 mol%), however it did not make any significant difference on σ (Figure 2-12).

Figure 2-11c compares the σ of similar ionic liquid content of EA main chain polymer based IGs. The σ of the PAcγ-CD-Ad-EA IG(0.5,0.5) (8.0 mS/cm) was 13 times higher than that of the EA IG(0.5) (0.61 mS/cm). The σ of the PAcγ-CD-Ad-EA IG(0.5,0.5) was also 13 and 4 times higher than those of Ad-EA IG(0.5,0.1) and PAcγ-CD-EA IG(0.5,0.1), respectively. Therefore, the host-guest interactions working as cross-linking point in supramolecular polymeric IGs is an effective network structure to increase the σ.

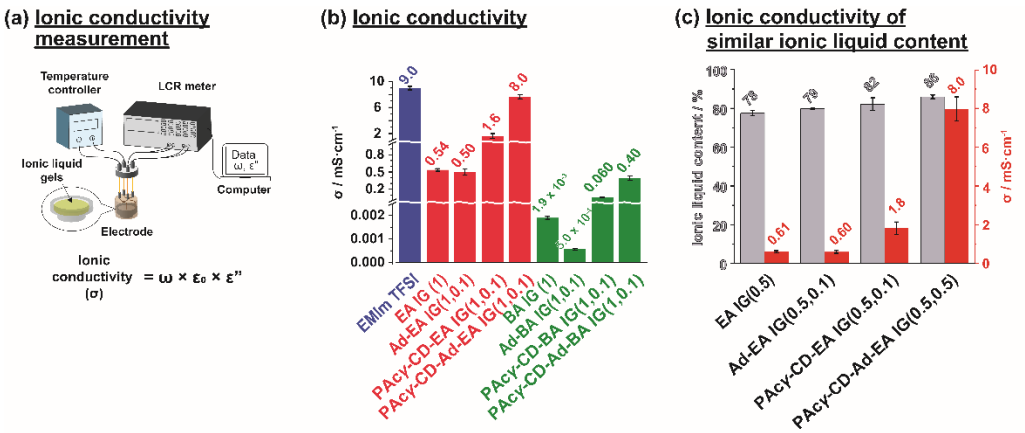

Figure 2-11. (**a**) Measurement apparatus for ionic conductivity. (**b**) Ionic conductivity of EMIm TFSI as native ionic liquid and ionic liquid gels [R IG(1), Ad-R IG(1,0.1), PAcγ-CD-R IG(1,0.1), and PAcγ-CD-Ad-R IG(1,1)].

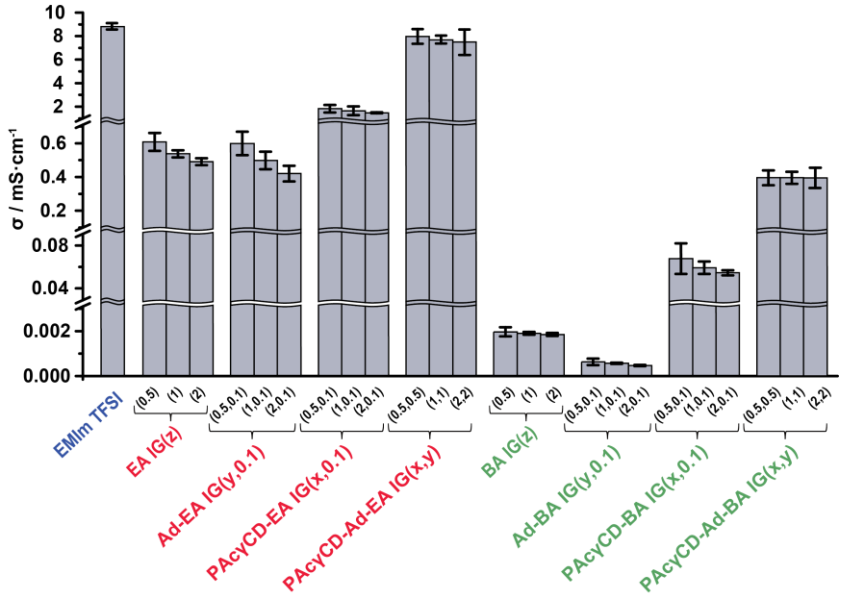

Figure 2-12. Ionic conductivity of EMIm TFSI and ionic liquid gels

2.3.4. Self-diffusion coefficient of ionic liquid gels

High σ of IGs is correlated with high mobility of the constituent ionic liquid. Higher σ in the IGs affected by fast mobility of ionic liquid constituent. The self-diffusion coefficient (D) of the EMIm TFSI was determined from mobility of ionic liquid constituent which measured by diffusion-ordered spectroscopy (DOSY) NMR, (Figures 2-21 – 2-29). DOSY NMR results show EMIm peaks from EMIm TFSI and acrylate peaks (Peaks from PAcγ-CD and Ad are very weak so that they can't be seen from DOSY NMR). Since the diffusion of the TFSI substituent was slower than EMIm substituent therefore D of IGs was determined only from EMIm substituent.[2]

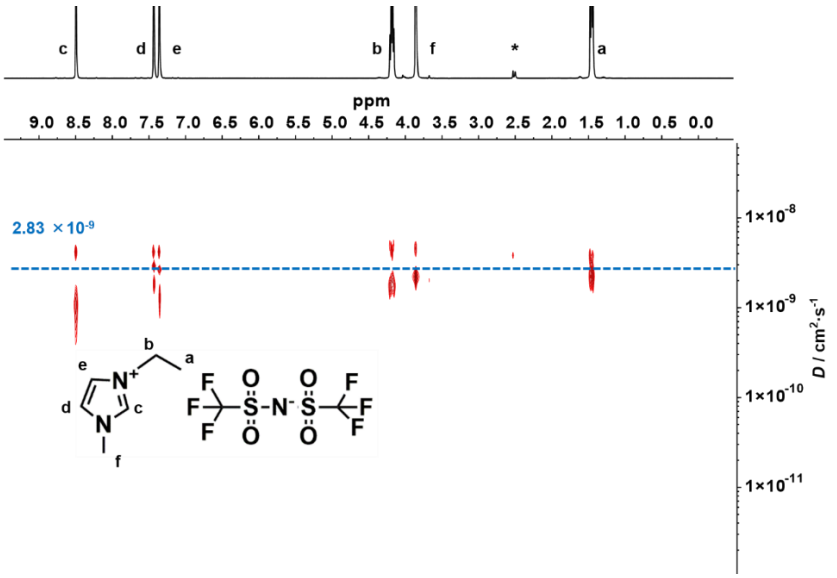

Figure 2-13. 2D DOSY NMR spectrum of EMIm constituent in EMIm TFSI ionic liquid (DMSO-d_6 for standard, 400 MHz, 25 ºC).

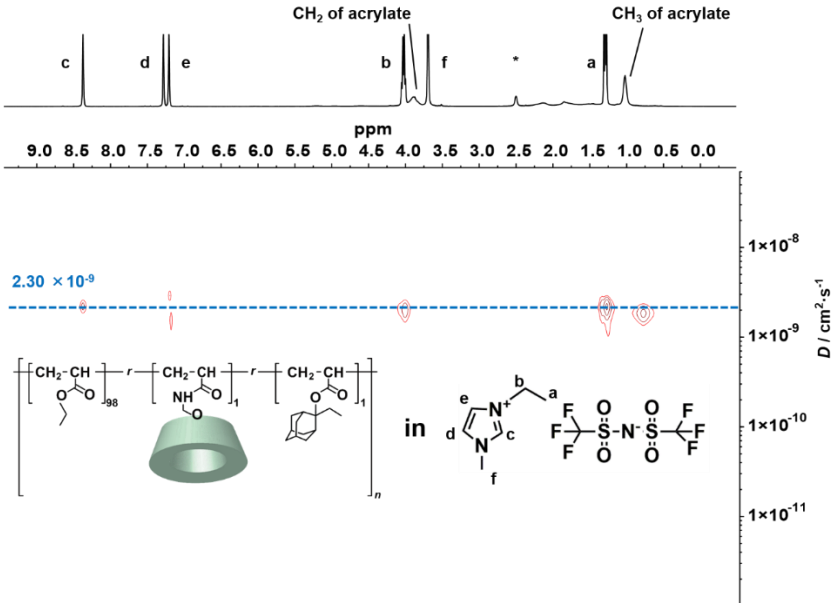

Figure 2-14. 2D DOSY NMR spectrum of EMIm constituent in supramolecular ionic liquid gel with ethyl acrylate main chain polymer [PAcγ-CD-Ad-EA IG(1,1)] (DMSO-d_6 for standard, 400 MHz, 25 ºC).

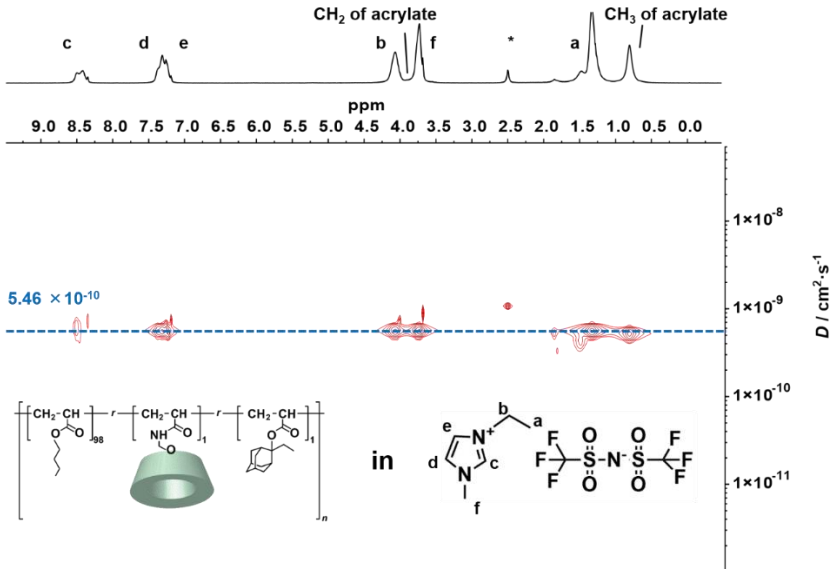

Figure 2-15. 2D DOSY NMR spectrum of EMIm constituent in supramolecular ionic liquid gel with butyl acrylate main chain polymer [PAcγ-CD-Ad-BA IG(1,1)] (DMSO-d_6 for standard, 400 MHz, 25 ºC).

Figure 2-16a shows the *D* of the EMIm substituent in the IGs. PAcγ-CD-Ad-EA IG(1,1) (Figures 2-14) showed faster *D* than the PAcγ-CD-Ad-EA IG(1,1) (Figures 2-15) because EA main chain polymer based IGs has shorter main chain compare with BA main chain polymer based IGs. The *D* of PAcγ-CD-Ad-EA IG(1,1) (2.30×10^{-9} cm^2/s) was faster than those of the EA IG(1) (7.99×10^{-10} cm^2/s), Ad-EA IG(1,0.1) (2.49×10^{-10} cm^2/s), or PAcγ-CD-EA IG(1,0.1) (1.09×10^{-9} cm^2/s). The *D* of PAcγ-CD-Ad-EA IG(1,1) (2.30×10^{-9} cm^2/s) showed similar result with EMIm TFSI (2.83×10^{-9} cm^2/s, Figure 2-13). These results showed that flexible and reversible host-guest interaction makes the ionic liquid easier to mobile in the polymer structure. EMIm substituent mobile faster in PAcγ-CD-Ad-R IG compared to EMIm substituent in chemically cross-linked IGs.

Figure 2-16b schematically illustrates the mobility of ionic liquid constituent in the IGs. Ionic liquid constituent almost static in the chemically cross-linked IGs due to anchored network, whereas in the PAcγ-CD-Ad-R IGs shows high mobility of ionic liquid constituent due the flexible and reversible host-guest cross-linking point. Therefore, the supramolecular polymeric ionic liquid gels has faster ionic mobility than those in chemically cross-linked ionic liquid gels.

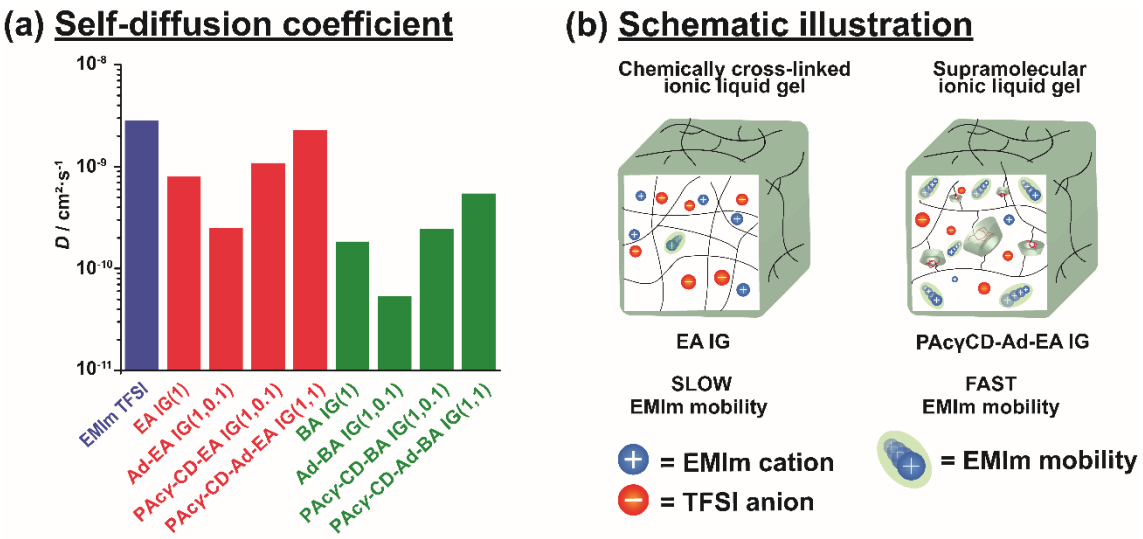

Figure 2-16. (**a**) Self-diffusion coefficient of EMIm constituent from EMIm and ionic liquid gels [R IG(1), Ad-R IG(1,0.1), PAc*γ*-CD-R IG(1,0.1), and PAc*γ*-CD-Ad-R IG(1,1)]. (**b**) Schematic illustration for EMIm TFSI constituent mobility in IGs.

2.3.5. Mobility and number of ions in the ionic liquid gels

From previous section, D of ionic liquid gels were successfully measured then the mobility of EMIm substituent (μ) can be proved by solving Einstein-Smoluchowski equation:

$$\mu = \frac{D \cdot q}{k_B \cdot T}$$

also number of ion carriers in IGs (n) can be calculated through Nernst-Einstein equation:

$$n = \frac{q \cdot \mu}{\sigma}$$

where q is electrical charge of a particle in this case is EMIm substituent which is 1, D is self-diffusion coefficient which obtained from previous section, k_B is Boltzmann's constant (1.38×10^{-23} J/K), T is temperature which is constant 25ºC (298 K), and σ is ionic conductivity which can be value obtained from ionic conductivity section. Table 2-9 summarizes the μ and n of ionic liquid gels.

The μ of PAc*γ*-CD-Ad-EA IG(1,1) as faster those that of the EA IG(1), Ad-EA IG(1,0.1), or PAc*γ*-CD-EA IG(1,0.1) which is consequence with D results. The trend also similar in BA main chain polymer. Since the mobility of PAc*γ*-CD-Ad-EA IG(1,1) is high therefore the number of ions in PAc*γ*-CD-Ad-EA IG(1,1) is the lowest compared to other IGs.

Table 2-9. Mobility and number of EMIm constituent from ionic liquid gels [R IG(1), Ad-R IG(1,0.1), PAc*γ*-CD-R IG(1,0.1), and PAc*γ*-CD-Ad-R IG(1,1)].

Chemical structures	$\mu \times 10^6$/ $m^2 \cdot V^{-1} \cdot s^{-1}$	$n \times 10^7$
EA IG(1)	20	36
Ad-EA IG(1,0.1)	6.1	16
PAc*γ*-CD-EA IG(1,0.1)	26	12
PAc*γ*-CD-Ad-EA IG(1)	55	7.3
BA IG(1)	4.5	2400
Ad-BA IG(1,0.1)	1.3	2300
PAc*γ*-CD-BA IG(1,0.1)	6	100
PAc*γ*-CD-Ad-BA IG(1)	13	34

2.3.6. Correlation between ionic conductivity and Young's modulus

Panzer et al.[40] reported relationship between σ and Young's modulus. They demonstrated that materials with low Young's modulus expected to show high σ. However, preparing materials less than 50 kPa is big challenge because this kind of materials will be soft and brittle. Herein, supramolecular polymeric IGs (PAc*γ*-CD-Ad-R IGs) solved this problem with lower Young's modulus and also high σ. Figure 2-17a and 2-17b summarize the correlation between Young's modulus and σ of IGs. The σ of PAc*γ*-CD-Ad-R IG was higher than those of R IG, Ad-R IG, and PAc*γ*-CD-R IG although it showed low Young's modulus. These results successfully shown that host-guest interactions with low cross-linking density still showed high σ.

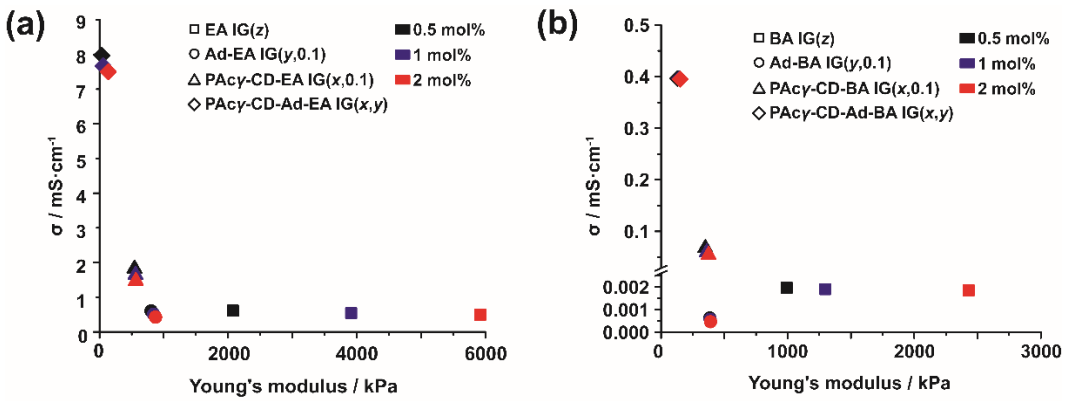

Figure 2-17. Correlation between ionic conductivity and Young's modulus for (**a**) EA main chain polymer based IGs and (**b**) BA main chain polymer based IGs. [□: R IG(*z*), ○: Ad-R IG(*y*,0.1), △: PAc*γ*-CD-R IG(*x*,0.1), ◇: PAc*γ*-CD-Ad-R IG(*x*,*y*); Black, blue, and red color for 0.5, 1, and 2 mol%, respectively].

2.4. Conclusion

Supramolecular polymeric IGs were prepared from immersion of elastomer made from bulk copolymerization between PAc*γ*-CD and Ad containing acrylate monomers in EMIm TFSI. The PAc*γ*-CD-Ad-R elastomer showed largest swelling ratio compared the other chemically cross-linked elastomers. This caused by during immersion in EMIm TFSI, host-guest cross-linking point in PAc*γ*-CD-Ad-R elastomer relaxed which made EMIm TFSI easier to penetrate to PAc*γ*-CD-Ad-R elastomer compared to the chemically cross-linked elastomers. The σ of IGs is in consequence with Young's modulus and D of EMIm substituent from EMIm TFSI in the IGs. The PAc*γ*-CD-Ad-R IGs showed lower Young's modulus than those of the chemically cross-linked IGs, indicating that the cross-linking density of the PAc*γ*-CD-Ad-R IGs was the lowest. This low cross-linking density of PAc*γ*-CD-Ad-R IG made EMIm substituent from EMIm TFSI easier to mobile compared to the chemically cross-linked IGs which resulted into higher σ. The σ and D of PAc*γ*-CD-Ad-EA IG were almost similar with EMIm TFSI as native ionic liquid. In conclusion, host-guest interaction in the supramolecular polymeric IGs is an important part for preparing low cross-linking density materials which show high σ. This supramolecular polymeric IGs based on host-guest interaction also expectable to be applied as electrochemical materials in the future because minimum σ required to prepare electrochemical materials is equal or over 0.1 mS/cm.[41]

References

1. Armand, M.; Endres, F.; MacFarlane, D. R.; Ohno, H.; Scrosati, B., *Nat. Mater.* **2009,** *8*, 621-629.
2. Susan, M. A.; Kaneko, T.; Noda, A.; Watanabe, M., *J. Am. Chem. Soc.* **2005,** *127*, 4976-4983.
3. Ding, J.; Zhou, D. Z.; Spinks, G.; Wallace, G.; Forsyth, S.; Forsyth, M.; MacFarlane, D. R., *Chem. Mater.* **2003,** *15*, 2392-2398.
4. Imaizumi, S.; Kokubo, H.; Watanabe, M., *Macromolecules* **2012,** *45*, 401-409.
5. Guyomard-Lack, A.; Abusleme, J.; Soudan, P.; Lestriez, B.; Guyomard, D.; Le Bideau, J., *Adv. Energy Mater.* **2014,** *4*, 1301570.
6. Horowitz, A. I.; Panzer, M. J., *J. Mater. Chem.* **2012,** *22*, 16534-16539.
7. Horowitz, A. I.; Panzer, M. J., *Angew. Chem., Int. Ed.* **2014,** *53*, 9780-9783.
8. Kim, D.; Lee, G.; Kim, D.; Ha, J. S., *ACS Appl. Mater. Interfaces* **2015,** *7*, 4608-4615.
9. Le Bideau, J.; Ducros, J. B.; Soudan, P.; Guyomard, D., *Adv. Funct. Mater.* **2011,** *21*, 4073-4078.
10. Wang, S.; Hsia, B.; Carraro, C.; Maboudian, R., *J. Mater. Chem. A* **2014,** *2*, 7997-8002.
11. Lewandowski, A.; Zajder, M.; Frackowiak, E.; Beguin, F., *Electrochim. Acta* **2001,** *46*, 2777-2780.
12. Sato, T.; Masuda, G.; Takagi, K., *Electrochim. Acta* **2004,** *49*, 3603-3611.
13. Gin, D. L.; Noble, R. D., *Science* **2011,** *332*, 674-676.
14. Hoarfrost, M. L.; Segalman, R. A., *Macromolecules* **2011,** *44*, 5281-5288.
15. Li, B.; Wang, L. D.; Kang, B. N.; Wang, P.; Qiu, Y., *Sol. Energy Mater. Sol. Cells* **2006,** *90*, 549-573.
16. Snaith, H. J.; Schmidt-Mende, L., *Adv. Mater.* **2007,** *19*, 3187-3200.
17. Yang, H. X.; Huang, M. L.; Wu, J. H.; Lan, Z.; Hao, S. C.; Lin, J. M., *Mater. Chem. Phys.* **2008,** *110*, 38-42.
18. Lu, J. M.; Yan, F.; Texter, J., *Prog. Polym. Sci.* **2009,** *34*, 431-448.
19. Mecerreyes, D., *Prog. Polym. Sci.* **2011,** *36*, 1629-1648.
20. Ye, Y. S.; Rick, J.; Hwang, B. J., *J. Mater. Chem. A* **2013,** *1*, 2719-2743.
21. Rogers, R. D.; Seddon, K. R., *Science* **2003,** *302*, 792-793.
22. Welton, T., *Chem. Rev.* **1999,** *99*, 2071-2083.
23. Wilkes, J. S.; Zaworotko, M. J., *J. Chem. Soc., Chem. Commun.* **1992,** 965-967.
24. Angell, C. A.; Liu, C.; Sanchez, E., *Nature* **1993,** *362*, 137-139.
25. Watanabe, M.; Yamada, S.-I.; Sanui, K.; Ogata, N., *J. Chem. Soc., Chem. Commun.* **1993,** 929-931.
26. Cordier, P.; Tournilhac, F.; Soulié-Ziakovic, C.; Leibler, L., *Nature* **2008,** *451*, 977.
27. Burattini, S.; Colquhoun, H. M.; Fox, J. D.; Friedmann, D.; Greenland, B. W.; Harris, P. J. F.; Hayes, W.; Mackay, M. E.; Rowan, S. J., *Chem. Commun.* **2009,** 6717-6719.
28. Fox, J.; Wie, J. J.; Greenland, B. W.; Burattini, S.; Hayes, W.; Colquhoun, H. M.; Mackay, M. E.; Rowan, S. J., *J. Am. Chem. Soc.* **2012,** *134*, 5362-5368.
29. Wang, Q.; Mynar, J. L.; Yoshida, M.; Lee, E.; Lee, M.; Okuro, K.; Kinbara, K.; Aida, T., *Nature* **2010,** *463*, 339.
30. Burnworth, M.; Tang, L.; Kumpfer, J. R.; Duncan, A. J.; Beyer, F. L.; Fiore, G. L.; Rowan, S. J.; Weder, C., *Nature* **2011,** *472*, 334.
31. Wojtecki, R. J.; Meador, M. A.; Rowan, S. J., *Nat. Mater.* **2010,** *10*, 14.
32. Tuncaboylu, D. C.; Sari, M.; Oppermann, W.; Okay, O., *Macromolecules* **2011,** *44*, 4997-5005.
33. Galiński, M.; Lewandowski, A.; Stępniak, I., *Electrochim. Acta* **2006,** *51*, 5567-5580.
34. Le Bideau, J.; Viau, L.; Vioux, A., *Chem. Soc. Rev.* **2011,** *40*, 907-925.

35. Jicsinszky, L.; Martina, K.; Caporaso, M.; Cintas, P.; Zanichelli, A.; Cravotto, G., *Phys. Chem. Chem. Phys.* **2015,** *17*, 17380-17390.
36. Uccello-Barretta, G.; Sicoli, G.; Balzano, F.; Salvadori, P., *Carbohydr. Res.* **2003,** *338*, 1103-1107.
37. Takashima, Y.; Sawa, Y.; Iwaso, K.; Nakahata, M.; Yamaguchi, H.; Harada, A., *Macromolecules* **2017,** *50*, 3254-3261.
38. Greenhoe Brian, M.; Hassan Mohammad, K.; Wiggins Jeffrey, S.; Mauritz Kenneth, A., *J. Polym. Sci., Part B: Polym. Phys.* **2016,** *54*, 1918-1923.
39. Jonscher, A. K., *Nature* **1977,** *267*, 673.
40. Visentin, A. F.; Panzer, M. J., *ACS Appl. Mater. Interfaces* **2012,** *4*, 2836-2839.
41. Meyer Wolfgang, H., *Adv. Mater.* **1999,** *10*, 439-448.

Chapter 3

Mechanical and self-recovery properties of supramolecular ionic liquid elastomers based on host-guest interaction and correlation with ionic liquid content

3.1. Introduction

Supramolecular materials[1-3] based on noncovalent interactions, including hydrophobic interactions,[4] π-π stacking,[5-6] metal-ligand interactions,[7-8] electrostatic interactions,[9] and hydrogen bonds,[10] have attracted attention for their mechanical properties. Host-guest interactions are noncovalent interactions that can easily be introduced into self-healing materials.[11-12] Crown ethers, [13-14] calixarenes,[15-16] cucurbiturils,[17-19] pillararenes,[20-21] and cyclodextrins (CDs)[22-24] are common macrocylic molecules that act as host molecules. Previously,[25] by polymerizing CD and guest monomers, supramolecular materials were prepared with enhanced mechanical properties compared to covalently cross-linked materials.

Recently, ionic liquids have been utilized in polymer networks because of their great physicochemical properties, such as negligible volatility, high thermal and electrochemical stability, non-flammability, and great ionic conductivity at room temperature.[26-28] The purpose of utilizing in polymer networks was to prevent leakage of ionic liquids during practical application.[29] There are several methods used to incorporate ionic liquids into polymer networks, such as polymerizing the monomers,[30-31] using as polymerization solvents,[32-36] and swelling the elastomeric films.[37-43]

Several types of ionic gels with high ionic conductivity (σ) have been reported.[44-49] Previously,[50-51] supramolecular materials with self-healing and tough materialwere reported but these materials were in a hydrogel state therefore it is hard to be used in electrochemical application. Herein, supramolecular polymeric ionic liquid elastomers [PAcγ-CD-Ad-Acrylate IE(x)] were prepared using peracetylated acrylamide-methyl ether-modified γ-CD host molecules (PAcγ-CD, Figure 3-1a) and 2-ethyl-2-adamanthyl acrylate (Ad) guest molecules in the presence of various acrylates [methyl acrylate (MA), ethyl acrylate (EA), n-butyl acrylate (BA), and methyl methacrylate (MMA)] to form

supramolecular polymeric materials. The acrylates as the side chains tethered the host and guest units. The supramolecular polymeric materials were swelled in 1-ethyl-3-methylimidazolium bis(trifluoro-methylsulfonyl)imide (EMIm TFSI) ionic liquid (Figure 3-1b). The PAc*γ*-CD-Ad-Acrylate IE(*x*) higher fracture energy than chemically cross-linked IEs although in low cross-linking density (low Young's modulus). In addition, the PAc*γ*-CD-Ad-Acrylate IE(*x*) can be self-recovered which chemically cross-linked IEs cannot achieve.

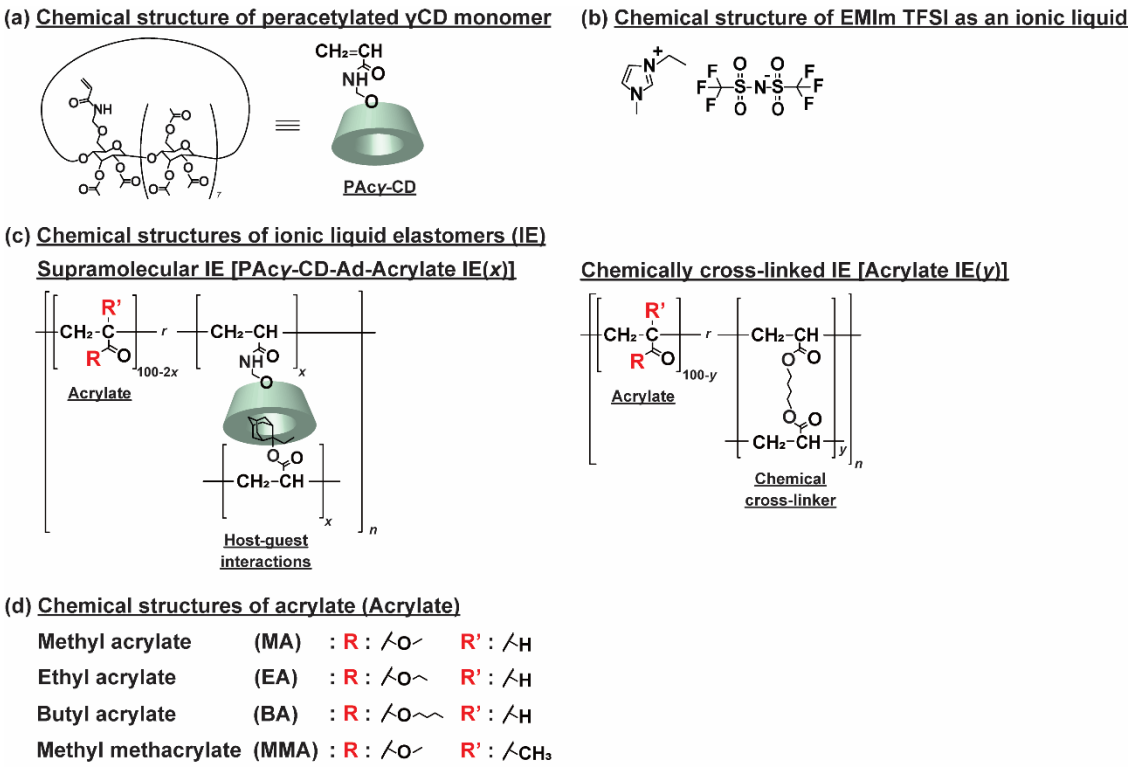

Figure 3-1. Chemical structures of (**a**) the host monomer: peracetylated 6-acrylamido methylether-*γ*-CD (PAc*γ*-CD), (**b**) ionic liquid: 1-ethyl-3-methylimidazolium bis(trifluoromethylsulfonyl) imide (EMIm TFSI), and (**c**) supramolecular polymeric elastomer swollen with EMIm TFSI [PAc*γ*-CD-Ad-Acylate IE(*x*)] and chemically cross-linked elastomer swollen with EMIm TFSI [Acrylate IE(*y*)]. (**d**) Group of side chain monomers (Acrylate): methyl acrylate (MA), ethyl acrylate (EA), butyl acrylate (BA), and methyl methacrylate (MMA). The mol% content of cross-linking unit of the host-guest inclusion complex (PAc*γ*-CD and Ad) and BDA units indicated as *x* and *y*, respectively.

3.2. Experimental section

3.2.1. Materials

γ-CD was purchased from Junsei Chemical Co., Ltd. MA, EA, BA, and MMA were obtained from Toagosei Co., Ltd. 1-Hydroxy cyclohexyl phenyl ketone (IRGACURE 184, Ciba) was purchased from BASF Japan Co., Ltd. Ad was purchased from Osaka Organic Chemical Industry Ltd. Acetic anhydride, 1,4-butanediol diacrylate (BDA), and bromoethane were obtained from Nacalai Tesque Inc. Lithium bis(trifluoromethanesulfonyl)imide (LiTFSI) was obtained from Tokyo Chemical Industry Co., Ltd. PAc*γ*-CD was prepared according to Scheme 2-1 in *chapter 2*. EMIm TFSI was also prepared according to Schemes 2-2 – 2-3 in *chapter 2*. $CDCl_3$ and pyridine were obtained from Wako Pure Chemical Industries, Ltd. DMSO–d_6 was obtained from Merck & Co., Inc. Water used for the preparation of the aqueous solutions was purified with a Millipore Elix 5 system. Other reagents were used without further purification.

3.2.2. Characterization

^1H, ^{13}C, and ^{19}F nuclear magnetic resonance (NMR) spectra were recorded with JEOL-ECA-500 spectrometer at 25 °C. at 500 MHz (for ^1H), 125 MHz (for ^{13}C), and 470 MHz (for ^{19}F), Solid–state ^1H field gradient magic angle spinning (FGMAS) NMR spectra was recorded at 400 MHz with a JEOL JNM–ECA 400 NMR spectrometer with a sample spinning rate of 7 kHz. In all the solid-state NMR measurements, the chemical shifts were referenced to residual protons values of the deuterated solvent [^1H NMR: δ = 0 ppm for tetramethylsilane (TMS) and 2.49 ppm for DMSO-d_6; ^{13}C NMR: δ = 0 ppm for TMS and 39.52 ppm for DMSO-d_6]. ^{19}F NMR spectra were calibrated using the external standard $CFCl_3$ (δ = 0 ppm). Mass spectrometry was performed using Bruker autoflex speed positive-ion matrix-assisted laser desorption/ionization time-of-flight (MALDI-TOF MS) mass spectrometer using 2,5-dihydroxybenzoic acid as matrix. The mechanical properties of the IEs were measured using universal tensile test machine Autograph AG-X plus with 50 N load cell at deformation rate 1.0 mm/s. The conductivity of the IEs was measured by a Hewlett-Packard 4284A Precision LCR [inductance (L), capacitance (C), and resistance (R)] meter at a frequency of 20 Hz-1 MHz using electrode made from stainless steel with sample size 20 mm in diameter.

3.3. Results and discussion

3.3.1. Preparation of the supramolecular ionic liquid elastomer

The supramolecular polymeric IEs based on inclusion complex between CD with guest unit [PAc*γ*-CD-Ad-Acrylate IE(*x*)] with similar procedure as in *chapter 2* (Scheme 3-1).[53] PAc*γ*-CD as a host monomer and Ad as a guest monomer were sonicated in an acrylate monomer (MA, EA, BA, or MMA) to form inclusion complex. To produce the supramolecular elastomer, IRGACURE 184 was added to perform bulk radical copolymerization with irradiation of UV 365 nm. Then, supramolecular elastomer was swollen in the EMIm TFSI to obtain PAc*γ*-CD-Ad-Acrylate IE(*x*) (Tables 3-1 – 3-4). Chemically cross-linked IEs [Acrylate IE (*y*), Figure 3-1c and Tables 3-5 – 3-8] were prepared for a comparison of the mechanical properties with similar methods using BDA as chemical cross-linker.

Solid–state ^{1}H field gradient magic angle spinning (FGMAS) NMR was used to characterize PAc*γ*-CD-Ad-Acrylate elastomer(*x*) and PAc*γ*-CD-Ad-Acrylate IE(*x*) (Figures 3-2 – 3-9).

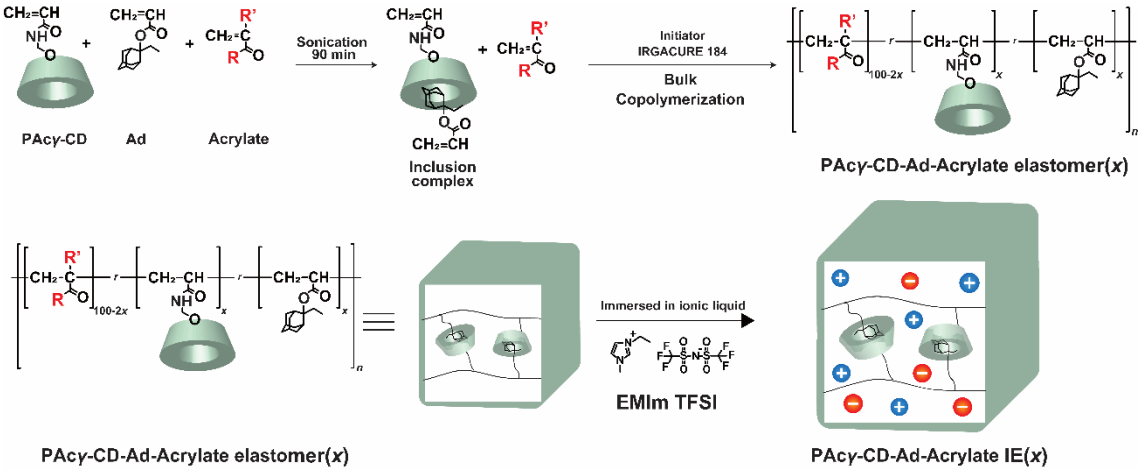

Scheme 3-1. Preparation of the PAc*γ*-CD-Ad-Acrylate IE(*x*). *x* indicate the mol% of cross-linker from host guest inclusion complex between PAc*γ*-CD and Ad units. Group of side chain monomers (Acrylate): methyl acrylate (MA), ethyl acrylate (EA), butyl acrylate (BA), and methyl methacrylate (MMA).

Table 3-1. Preparation of PAc*γ*-CD-Ad-MA elastomer(*x*).

x	PAc*γ*-CD / g	Ad / g	1 / g	IRGACURE 184 / g
0.5	0.69	0.07	5.00	0.02
1	1.38	0.14	5.00	0.02
2	2.78	0.28	5.00	0.02

Table 3-2. Preparation of PAc*γ*-CD-Ad-EA elastomer(*x*).

x	PAc*γ*-CD / g	Ad / g	2 / g	IRGACURE 184 / g
0.5	0.59	0.06	5.00	0.02
1	1.20	0.12	5.00	0.02
2	2.44	0.24	5.00	0.02

Table 3-3. Preparation of PAcγ-CD-Ad-BA elastomer(*x*).

x	PAc*γ*-CD / g	Ad /g	3 / g	IRGACURE 184 / g
0.5	0.46	0.05	5.00	0.02
1	0.93	0.09	5.00	0.02
2	1.91	0.19	5.00	0.02

Table 3-4. Preparation of PAcγ-CD-Ad-MMA elastomer(*x*).

x	PAc*γ*-CD / g	Ad /g	4 / g	IRGACURE 184 / g
0.5	0.59	0.06	5.00	0.02
1	1.20	0.12	5.00	0.02
2	2.44	0.24	5.00	0.02

Table 3-5. Preparation of MA elastomer(*y*).

y	BDA / g	1 / g	IRGACURE 184 / g
0.5	0.06	5.00	0.02
1	0.12	5.00	0.02
2	0.23	5.00	0.02

Table 3-6. Preparation of EA elastomer(*y*).

y	BDA / g	2 / g	IRGACURE 184 / g
0.5	0.05	5.00	0.02
1	0.10	5.00	0.02
2	0.20	5.00	0.02

Table 3-7. Preparation of BA elastomer(*y*).

y	BDA / g	3 / g	IRGACURE 184 / g
0.5	0.04	5.00	0.02
1	0.08	5.00	0.02
2	0.16	5.00	0.02

Table 3-8. Preparation of MMA elastomer(*y*).

y	BDA / g	4 / g	IRGACURE 184 / g
0.5	0.05	5.00	0.02
1	0.10	5.00	0.02
2	0.20	5.00	0.02

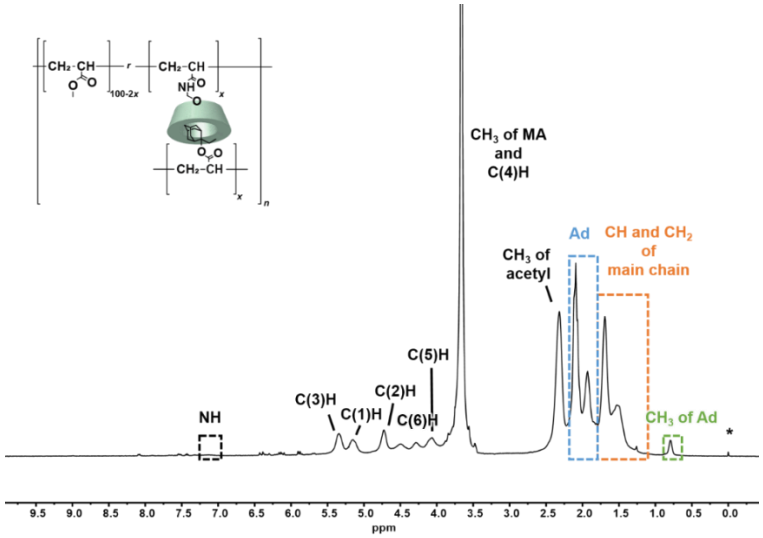

Figure 3-2. Solid-state ^{1}H FGMAS NMR spectrum of PAcγ-CD-Ad-MA elastomer(1) (TMS for standard, 400 MHz, 25 ºC, rotation frequency = 7 kHz).

^{1}H NMR (400 MHz, Chloroform-*d*): δ = 7.05 (-N*H*-), 5.42-5.28 (C(3)*H* of CD), 5.19-5.11 (C(1)*H* of CD), 4.81-4.66 (C(2)*H* of CD), 4.50-4.29 (C(6)*H* of CD), 4.13-4.01 (C(5)*H* of CD), 3.85-3.50 (-C*H*$_3$ of MA and C(4)*H* of CD), 2.45-2.20 (-C*H*$_3$ of acetyl), 2.15-1.88 (-C*H*-, -C*H*$_2$-, and -C*H*$_2$CH$_3$ of Ad), 1.78-1.17 (-C*H*$_2$C*H*- of side chain), 0.83-0.73 (-C*H*$_3$ of Ad).

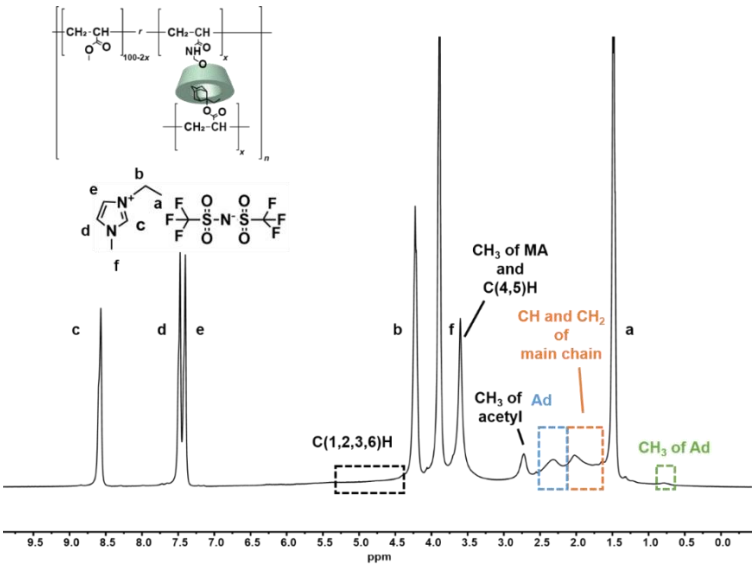

Figure 3-3. Solid-state ^{1}H FGMAS NMR spectrum of PAcγ-CD-Ad-MA IE(1) (TMS for standard, 400 MHz, 25 ºC, rotation frequency = 7 kHz).

^{1}H NMR (400 MHz, Chloroform-*d*): δ = δ 8.58 (-NC*H*N^{+}- of EMIm TFSI), 7.49 (-NC*H*CH- of EMIm TFSI), 7.40 (-N^{+}C*H*CH- of EMIm TFSI), 5.42-4.29 (C(1,2,3,6)*H* of CD), 4.22 (-N^{+}C*H*$_2$- of EMIm TFSI), 3.90 (-NC*H*$_3$ of EMIm TFSI), 3.70-3.43 (-C*H*$_3$ of MA and C(4)*H* of CD), 2.79-2.55 (-C*H*$_3$ of acetyl), 2.51-2.13 (-C*H*-, -C*H*$_2$-, and -C*H*$_2$CH$_3$ of Ad), 2.10-1.59 2.02 (-C*H*$_2$C*H*- of side chain), 1.48 (-CH$_2$C*H*$_3$ of EMIm TFSI), 0.88-0.68 (-C*H*$_3$ of Ad).

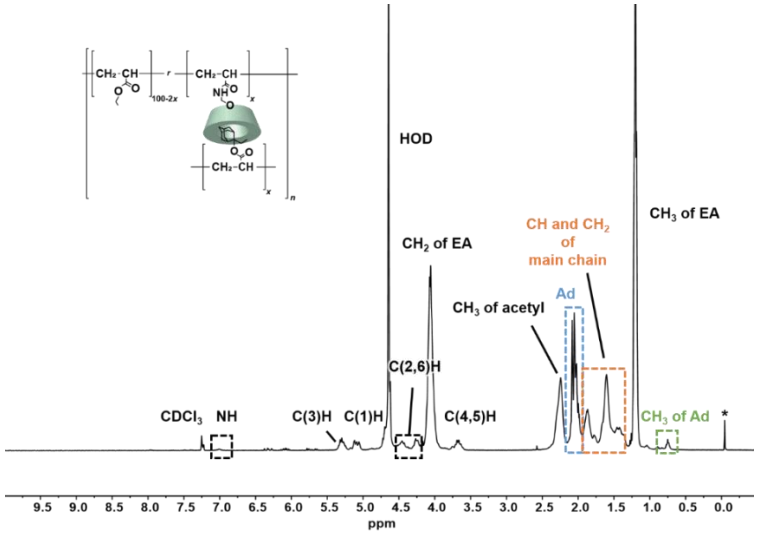

Figure 3-4. Solid-state ^{1}H FGMAS NMR spectrum of PAcγ-CD-Ad-EA elastomer(1) (TMS for standard, 400 MHz, 25 ºC, rotation frequency = 7 kHz).

^{1}H NMR (400 MHz, Chloroform-*d*): δ = 7.05 (-N*H*-), 5.38-5.29 (C(3)*H* of CD), 5.17-5.10 (C(1)*H* of CD), 4.52-4.27 (C(2,6)*H* of CD), 4.16-4.04 (-CH_2CH$_3$ of EA), 3.80-3.68 (C(4,5)*H* of CD), 2.35-2.29 (-CH_3 of acetyl), 2.15-2.03 (-C*H*-, -CH_2-, and -CH_2CH$_3$ of Ad), 1.97-1.41 (-CH_2C*H*- of side chain), 1.30-1.23 (-CH_3 of EA), 0.82-0.78 (-CH_3 of Ad).

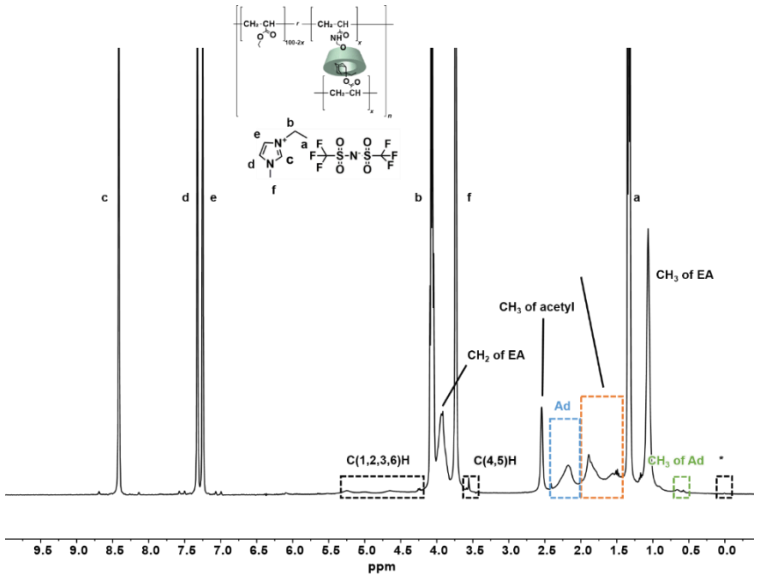

Figure 3-5. Solid-state ^{1}H FGMAS NMR spectrum of PAcγ-CD-Ad-EA IE(1) (TMS for standard, 400 MHz, 25 ºC, rotation frequency = 7 kHz).

^{1}H NMR (400 MHz, Chloroform-*d*): δ = 8.47 (-NC*H*N^{+}- of EMIm TFSI), 7.38 (-NC*H*CH- of EMIm TFSI), 7.31 (-N^{+}C*H*CH- of EMIm TFSI), 5.31-4.70 (C(1,2,3,6)*H* of CD), 4.14 (-N^{+}CH_2- of EMIm TFSI), 3.99-3.95 (-CH_2CH$_3$ of EA), 3.80 (-NCH_3 of EMIm TFSI), 2.59 (-CH_3 of acetyl), 2.24 (-C*H*-, -CH_2-, and -CH_2CH$_3$ of Ad), 1.95-1.61 (-CH_2C*H*- of side chain), 1.39 (-CH$_2$CH_3 of EMIm TFSI), 1.12 (-CH_3 of EA), 0.68 (-CH_3 of Ad).

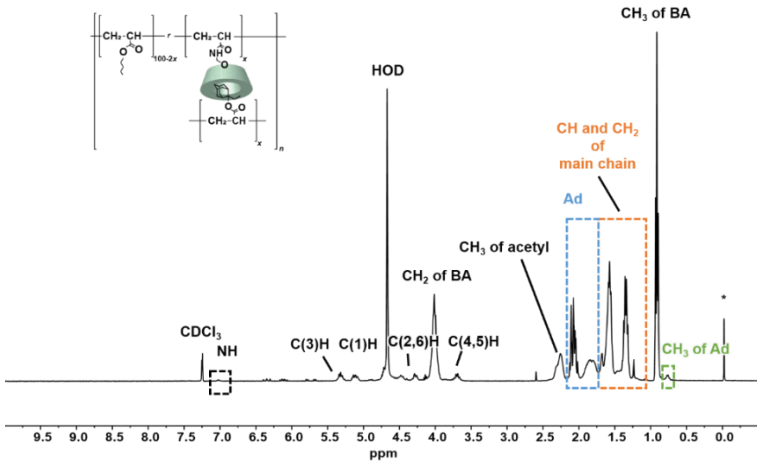

Figure 3-6. Solid-state ^{1}H FGMAS NMR spectrum of PAc*γ*-CD-Ad-BA elastomer(1) (TMS for standard, 400 MHz, 25 ºC, rotation frequency = 7 kHz).

^{1}H NMR (400 MHz, Chloroform-*d*): δ = 7.03 (-N*H*-), 5.38-5.32 (C(3)*H* of CD), 5.18-5.10 (C(1)*H* of CD), 4.50-4.16 (C(2,6)*H* of CD), 4.09-3.98 (-CH_2CH_2- of BA), 3.76-3.69 (C(4,5)*H* of CD), 2.28-2.26 (-CH_3 of acetyl), 2.15-1.70 (-C*H*-, -CH_2-, and -CH_2CH$_3$ of Ad), 1.66-1.26 (-CH_2C*H*- of side chain), 0.95-0.92 (-CH_3 of BA), 0.79 (-CH_3 of Ad).

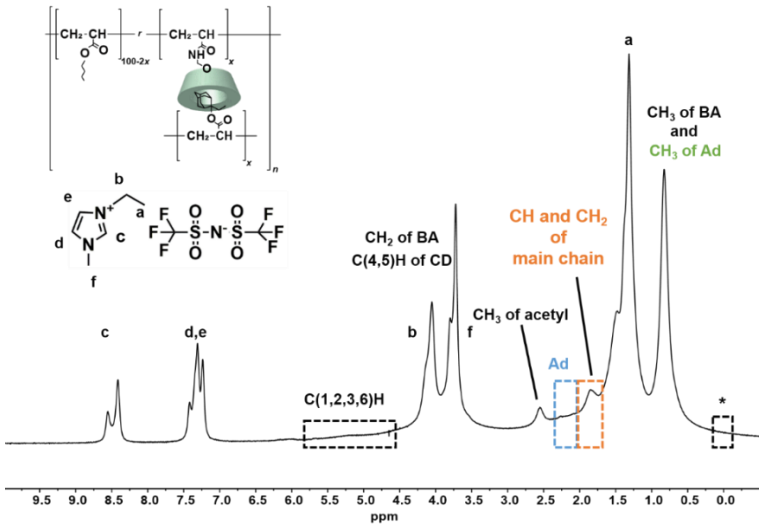

Figure 3-7. Solid-state ^{1}H FGMAS NMR spectrum of PAc*γ*-CD-Ad-BA IE(1) (TMS for standard, 400 MHz, 25 ºC, rotation frequency = 7 kHz).

^{1}H NMR (400 MHz, Chloroform-*d*): δ = 8.63-8.50 (-NC*H*N^{+}- of EMIm TFSI), 7.50-7.31 (-NC*HCH*N^{+}- of EMIm TFSI), 5.80-4.71 (C(1,2,3,6)*H* of CD), 4.14 (-N^{+}CH_2- of EMIm TFSI), 3.88-3.80 (-CH_2CH_2- of BA, C(4,5)*H* of CD, and -NCH_2- of EMIm TFSI), 2.64 (-CH_3 of acetyl), 2.25 (-C*H*-, -CH_2-, and -CH_2CH$_3$ of Ad), 1.92 (-CH_2C*H*- of side chain), 1.39 (-CH$_2$CH_3 of EMIm TFSI), 0.91-0.70 (-CH_3 of BA and -CH_3 of Ad).

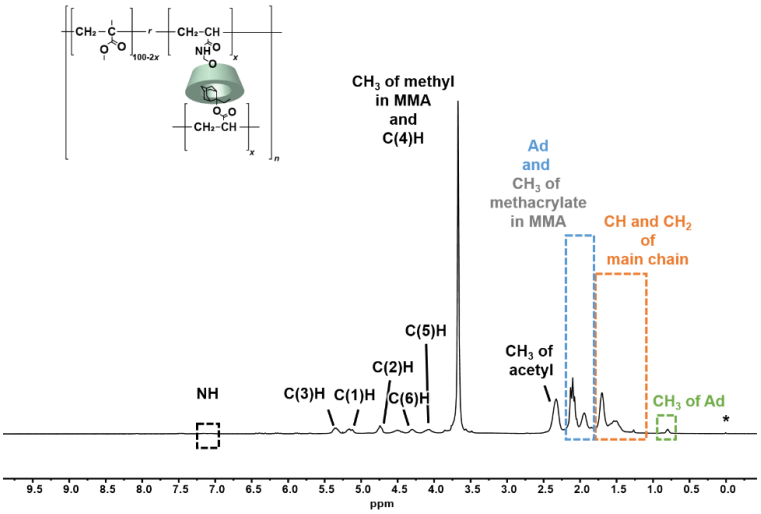

Figure 3-8. Solid-state ^{1}H FGMAS NMR spectrum of PAc*γ*-CD-Ad-MMA elastomer(1) (TMS for standard, 400 MHz, 25 ºC, rotation frequency = 7 kHz).

^{1}H NMR (400 MHz, Chloroform-*d*): δ = 7.05 (-N*H*-), 5.42-5.29 (C(3)*H* of CD), 5.24-5.10 (C(1)*H* of CD), 4.80-4.71 (C(2)*H* of CD), 4.56-4.23 (C(6)*H* of CD), 4.15-4.04 (C(5)*H* of CD), 3.80-3.57 (-CH_3 of methyl in MMA and C(4)*H* of CD), 2.43-2.18 (-CH_3 of acetyl), 2.18 – 1.83 (-C*H*-, -CH_2-, -CH_2CH$_3$ of Ad, and -CH_3 of methacrylate in MMA), 1.80-1.19 (-CH_2C*H*- of side chain), 0.85-0.74 (-CH_3 of Ad).

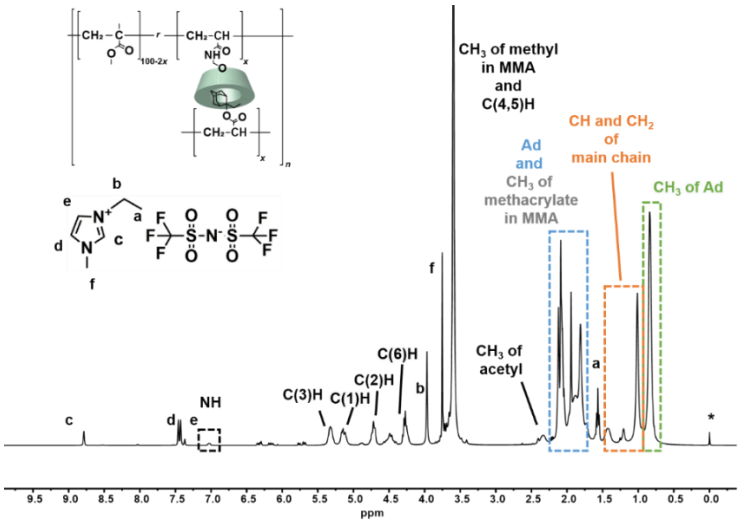

Figure 3-9. Solid-state ^{1}H FGMAS NMR spectrum of PAc*γ*-CD-Ad-MMA IE(1) (TMS for standard, 400 MHz, 25 ºC, rotation frequency = 7 kHz).

^{1}H NMR (400 MHz, Chloroform-*d*): δ = δ 8.78 (-NC*H*N^{+}- of EMIm TFSI), 7.48 (-NC*H*CH- of EMIm TFSI), 7.42 (-N^{+}C*H*CH- of EMIm TFSI), 7.32 (-N*H*-), 6.39-27 (C(3)*H* of CD), 6.22-6.06 (C(1)*H* of CD), 4.77-4.64 (C(2)*H* of CD), 4.69-4.18 (C(6)*H* of CD), 3.97 (-N^{+}CH_2- of EMIm TFSI), 3.76 (-NCH_3 of EMIm TFSI), 3.69-3.37 (-CH_3 of methyl in MMA and C(4,5)*H* of CD), 2.42-2.26 (-CH_3 of acetyl), 2.19-1.88 (-C*H*-, -CH_2-, -CH_2CH$_3$ of Ad, and -CH_3 of methacrylate in MMA), 1.68 (-CH$_2$CH_3 of EMIm TFSI), 1.50-0.94 (-CH_2C*H*- of side chain), 0.92-0.74 (-CH_3 of Ad).

3.3.2. Mechanical properties of the ionic liquid elastomers

The mechanical properties of the PAcγ-CD-Ad-Acrylate IE(x) were investigated and compared with the Acrylate IE(y). The stress and strain curves of the PAcγ-CD-Ad-Acrylate IE(x) and Acrylate IE(y) were evaluated while using tensile speed of 1.0 mm/s. Then from these strain-stress curves, mechanical properties such as ultimate strength, Young's modulus and fracture energy were measured and summarized as Table 3-9 and Figures 3-10 – 3-11. Every acrylate groups showed different ultimate strength. The PAcγ-CD-Ad-MMA IE(1) showed ultimate strength (8 MPa) which similar to the chemically cross-linked MMA IE(1) (8 MPa). However, PAcγ-CD-Ad-EA IE(1) showed more elastic properties with lower ultimate strength (0.1 MPa) compared to the chemically cross-linked EA IE(1) (0.18 MPa).

PAcγ-CD-Ad-MMA IE(1) also showed lower Young's modulus (34 MPa) compared to chemically cross-linked MMA IE(1) (66 MPa). PAcγ-CD-Ad-EA IE(1) with more elastic properties also showed lower Young's modulus: 0.01 MPa compared to chemically cross-linked EA IE(1) (0.81 MPa). These results are caused by the cross-linking points between CD and Ad units in PAcγ-CD-Ad-Acrylate IE(x) can associate and dissociate freely.

The fracture energy for the PAcγ-CD-Ad-Acrylate IE(1) and Acrylate IE(1) also investigated. The PAcγ-CD-Ad-MMA IE(1) showed fracture energy values comparable with the chemically cross-linked MMA IE(1). As for fracture energy, the PAcγ-CD-Ad-BA IE(1) showed a higher fracture energy (3200 kJ/m^2) compared to the chemically cross-linked BA IE(1) (43 kJ/m^2). PAcγ-CD-Ad-MA IE(1) and PAcγ-CD-Ad-EA IE(1) also showed same trends. These results showed that to increase the fracture energy of the IEs the host-guest interaction is important.

Table 3-9 Mechanical properties of supramolecular ionic liquid elastomer [PAc*γ*-CD-Ad-Acrylate IE(1)] and chemically cross-linked elastomer [Acrylate IE(1)]. Acrylate: methyl acrylate (MA), ethyl acrylate (EA), butyl acrylate (BA), and methyl methacrylate (MMA).

Chemical structures	Strength / MPa	Young's modulus / MPa	Fracture energy / $kJ \cdot m^{-2}$
PAc*γ*-CD-Ad-MA IE(1)	0.060	0.08	180
PAc*γ*-CD-Ad-EA IE(1)	0.10	0.01	310
PAc*γ*-CD-Ad-BA IE(1)	0.50	0.01	3200
PAc*γ*-CD-Ad-MMA IE(1)	8.0	34	870
MA IE(1)	0.40	1.4	98
EA IE(1)	0.20	0.80	22
BA IE(1)	0.20	0.90	43
MMA IE(1)	8.0	66	750

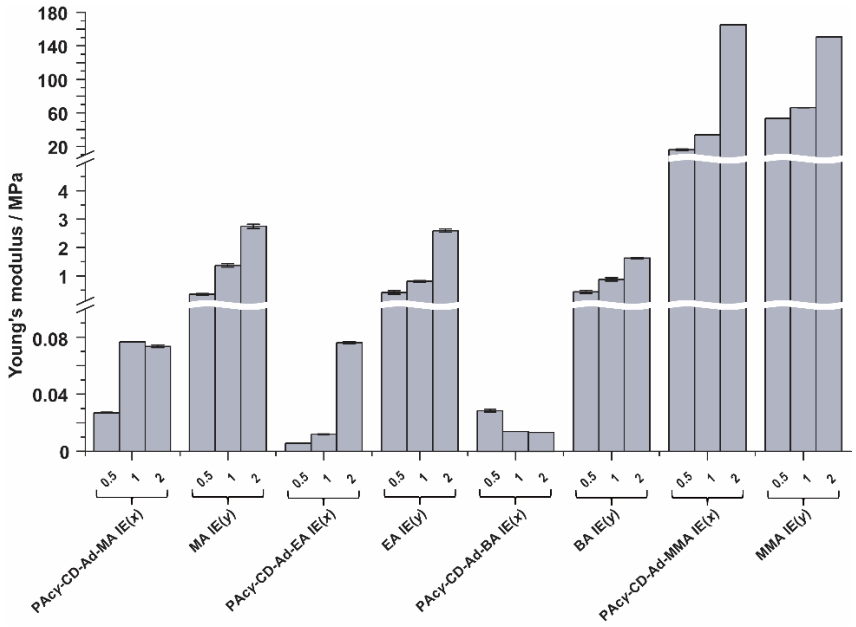

Figure 3-10. Young's modulus of elastomers swollen by EMIm TFSI.

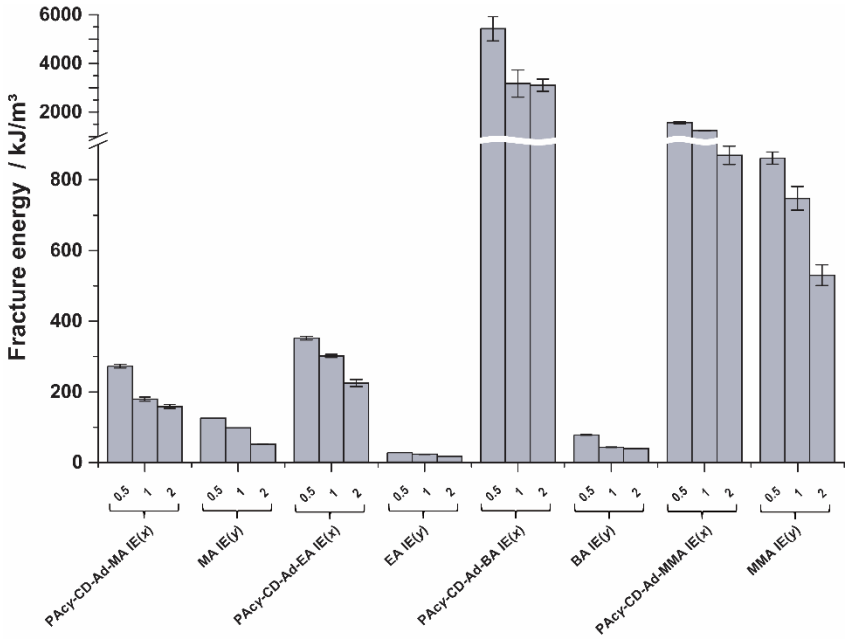

Figure 3-11. Fracture energy of elastomers swollen by EMIm TFSI.

EMIm TFSI content also show relationship with the fracture energy [Figure 3-12a for PAcγ-CD-Ad-Acrylate IE(x) and Figure 3-12b for Acrylate IE(y)]. EMIm TFSI content in IE was controlled by first calculating to mass of elastomer (W_E) and then EMIm TFSI that required for immersion (W_{IL}) was calculated to obtain controlled EMIm TFSI content in the sample.

$$IL=\frac{W_{IE}-W_E}{W_{IE}}\times 100\% \qquad \text{where} \qquad W_{IE}=W_{IL}+W_E$$

$$IL=\frac{(W_{IL}+W_E)-W_E}{(W_{IL}+W_E)}\times 100\%$$

IL is EMIm TFSI content in weight percent. W_{IE} is weight of elastomers after immersion in EMIm TFSI. W_E is weight of elastomers. W_{IL} is the weight of EMIm TFSI required for immersion. By solving the equation, W_{IL} required for the controlled EMIm TFSI content can be obtained.

The higher EMIm TFSI content often decreasing mechanical property values, however at a certain point around 20-60%, local maxima of the fracture energy were observed. The fracture energy of PAcγ-CD-Ad-MA IE(1)and PAcγ-CD-Ad-BA IE(1) decreased during the addition of ionic liquid content, but the fracture energy increased again to show peaks at a 41% and a 24% EMIm TFSI content, respectively. The PAcγ-CD-Ad-MMA IE(1) also showed a local peak of the fracture energy at a 5% EMIm TFSI content. Figure 3-12a and 3-12b also compares that in every EMIm TFSI content, PAcγ-

CD-Ad-Acrylate IE(x) shows higher fracture energy than Acrylate IE(y). These results indicate that at certain amounts of EMIm TFSI affecting the association and dissociation host-guest interactions in PAcγ-CD-Ad-Acrylate IE(x).

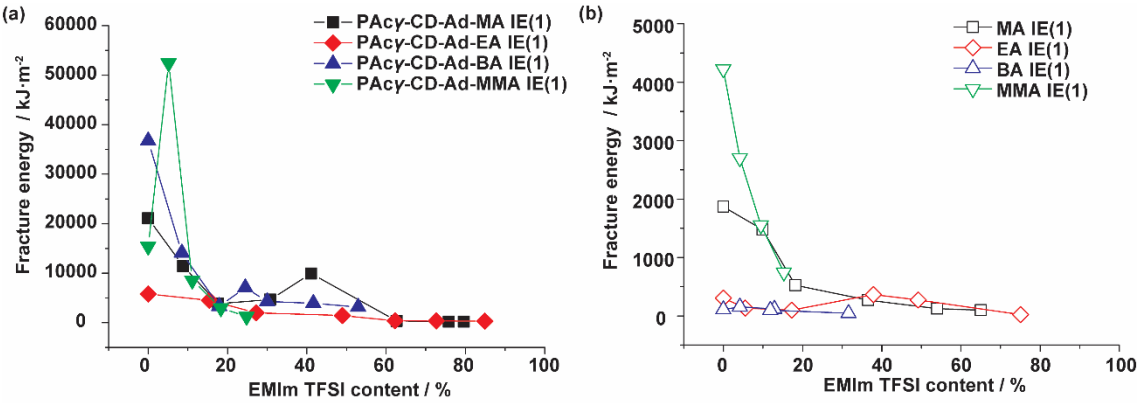

Figure 3-12. Relationship between the fracture energy and ionic liquid (EMIm TFSI) content for (a) supramolecular ionic liquid elastomer [PAcγ-CD-Ad-acrylate IE(1)] and (b) chemically cross-linked ionic liquid elastomer [Acrylate IE(1)]. [■: Methyl acrylate (MA), ◆: ethyl acrylate (EA), ▲: butyl acrylate (BA), and ▼: methyl methacrylate (MMA)].

3.3.3. Stress relaxation behavior of the ionic liquid elastomers

The stress relaxation test was used to the proof the behavior of the CD/Ad host-guest interactions in the IEs, the test was done for both PAcγ-CD-Ad-Acrylate IE(1) and Acrylate IE(1) in their maximum EMIm TFSI content. In the stress relaxation test, the IEs were stretched to a 5% strain using a universal test machine and keep the 5% strain for 1 hour then the stress was observed. Data acquired from universal tensile test machine then fitted with *Maxwell method* curve fitting. The stress-relaxation curves of supramolecular polymeric ionic liquid elastomers [PAcγ-CD-Ad-Acrylate IE(1)] were fitted with two-order exponential equation (τ' and τ) whereas chemically cross-linked ionic liquid elastomers [Acrylate IE(1)] were fitted with one-order exponential equation (τ) whereas

Fitting equation:

PAcγ-CD-Ad-Acrylate IE(1) $\sigma_t = \sigma_0 + G_1 e^{-\left(\frac{t}{\tau}\right)} + G_2 e^{-\left(\frac{t}{\tau'}\right)}$

Acrylate IE(1) $\sigma_t = \sigma_0 + G_1 e^{-\left(\frac{t}{\tau}\right)}$

σ_t is the stress at a certain time *t*; σ_0 is the peak stress; G_i is constant; τ is slow relaxation time constant for PAc*γ*-CD-Ad-Acrylate IE(1) and Acrylate IE(1), respectively; τ' is rapid relaxation time constant for PAc*γ*-CD-Ad-Acrylate IE(1). All stress values were normalized with initial stress normalized as 1 and plotted (Figure 3-13a).

The stress relaxation time constants were obtained from the curve fitting of the stress relaxation curve profile with exponential decreasing model. The PAc*γ*-CD-Ad-Acrylate IE(*x*) showed two relaxation modes (slow and rapid relaxation mode). On the other hand, Acrylate IE(*y*) showed single relaxation mode (slow relaxation mode). Figure 3-13b summarizes the stress relaxation time constants for slow relaxation mode (τ). The τ of PAc*γ*-CD-Ad-Acrylate IE(1) [PAc*γ*-CD-Ad-MA IE(1): 120 s, PAc*γ*-CD-Ad-EA IE(1): 160 s, PAc*γ*-CD-Ad-BA IE(1): 180 s, and PAc*γ*-CD-Ad-MMA IE(1): 170 s] were approximately one order higher than those of the chemically cross-linked Acrylate IE(1) [MA IE(1): 9.2 s, EA IE(1): 17 s, BA IE(1): 62 s, and MMA IE(1): 38 s]. Higher τ values suggest the presence of host-guest interactions in PAc*γ*-CD-Ad-Acrylate IE(*x*) due to slower molecular motions. The results also suggested longer size of side chain like PAc*γ*-CD-Ad-BA IE(1) and bulky size of side chain like PAc*γ*-CD-Ad-MMA IE(1) showed slower stress relaxation compared to smaller size of side chain such as PAc*γ*-CD-Ad-MA IE(1) and PAc*γ*-CD-Ad-EA IE(1).

The stress relaxation time constants for rapid relaxation mode (τ') only achieved PAc*γ*-CD-Ad-Acrylate IE(*x*) (Figure 3-13c). This because host-guest interactions between PAcγCD and Ad in the IEs PAc*γ*-CD-Ad-Acrylate IE(*x*) suggested fast association and dissociation which contribute to the effective stress dispersion mechanism of the PAc*γ*-CD-Ad-Acrylate IE(*x*).

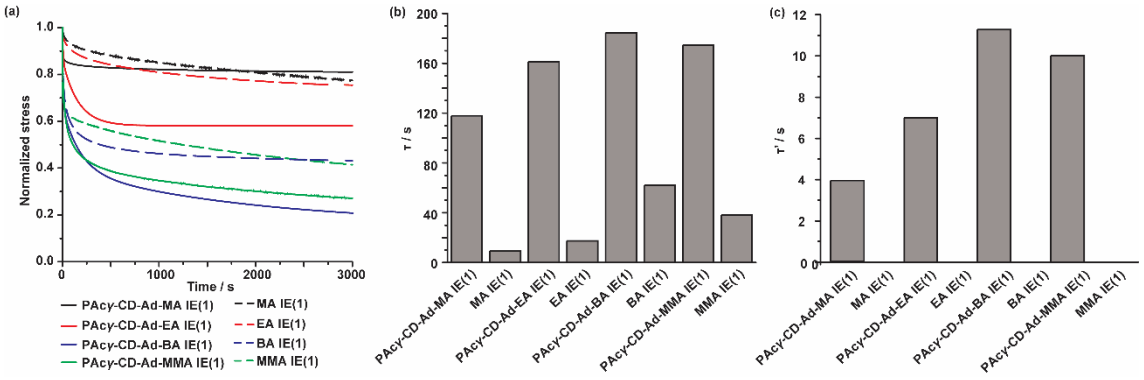

Figure 3-13. (**a**) Stress relaxation behavior of the supramolecular ionic liquid elastomer [PAc*γ*-CD-Acrylate IE(1), solid lines] and chemically cross-linked ionic liquid elastomer [Acrylate IE(1), dashed lines) in their maximum EMIm TFSI content stretched until 5% strain for 1 hour. (**b**) Slow relaxation time constant and (**c**) rapid relaxation time constant of the PAc*γ*-CD-Ad-Acrylate IE(1) and Acrylate IE (1).

3.3.4. Correlation between EMIm TFSI content and ionic conductivity of the ionic liquid elastomers

Utilizing an ionic liquid in the materials mean utilizing the ionic conductivity properties. The ionic conductivity (σ) was measured with same method as in *chapter* 2. The σ of EMIm TFSI, the PAc*γ*-CD-Ad-Acrylate IE(x), and the Acrylate IE(y) are shown at Figure 3-14. In this chapter, the relation of EMIm TFSI content with the σ in the PAc*γ*-CD-Ad-Acrylate IE(1) was observed (Figure 3-15). The results showed at approximately 60% of the EMIm TFSI content, the σ values supramolecular polymeric IEs in drastically increases. However, chemically cross-linked IEs did not show any significant increase of σ. Some chemically cross-linked IEs cannot even contain EMIm TFSI at high content (<60%). EMIm TFSI could penetrate through the PAc*γ*-CD-Ad-MA IE(1) and PAc*γ*-CD-Ad-EA IE(1) with a maximum content of over 60%, which makes PAc*γ*-CD-Ad-MA IE(1) and PAc*γ*-CD-Ad-EA IE(1) show high σ values, whereas the PAc*γ*-CD-Ad-BA IE(1) and PAc*γ*-CD-Ad-MMA IE(1) could only contain maximum of 53% and 25% of EMIm TFSI, respectively. Therefore, the PAc*γ*-CD-Ad-BA IE(1) and PAc*γ*-CD-Ad-MMA IE(1) showed lower σ values.

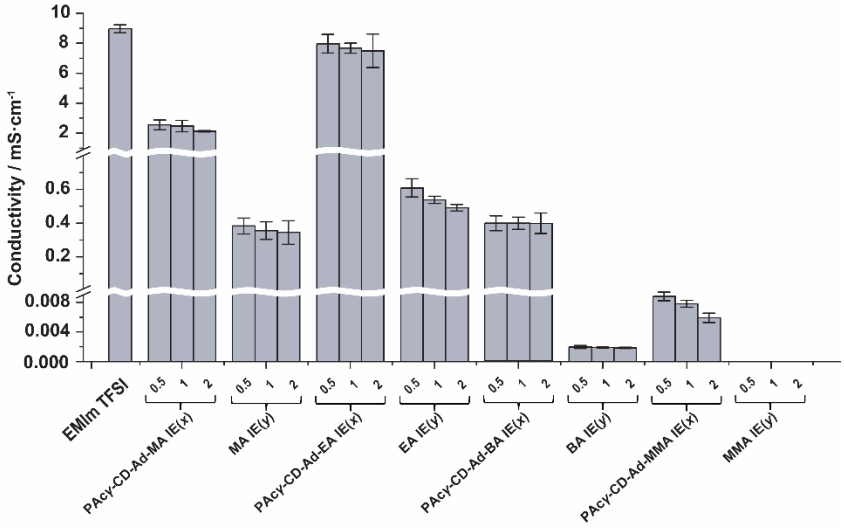

Figure 3-14. Ionic conductivity of EMIm TFSI and elastomers swollen in EMIm TFSI.

Figure 3-15 also shows the σ at similar EMIm TFSI between PAcγ-CD-Ad-Acrylate IE(1) and Acrylate IE(1). At 65% EMIm TFSI content, PAcγ-CD-Ad-MA IE(1) (σ=2.1 mS/cm) showed higher σ than MA IE(1) (σ=0.40 mS/cm) and also for around 75% EMIm TFSI content PAcγ-CD-Ad-EA IE(1) (σ=4.1 mS/cm) showed higher σ than EA IE(1) (σ=0.50 mS/cm). This result proved that reversible and elastic cross-linker in supramolecular IEs PAcγ-CD-Ad-MA IE(1) and PAcγ-CD-Ad-EA IE(1) makes mobility of substituents of EMIm TFSI are faster compared to mobility of substituents of EMIm TFSI inside the chemically cross-linked IE MA IE(1) and EA IE(1) which resulted into higher σ.

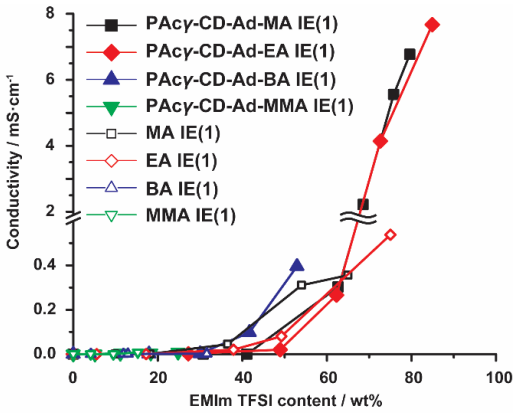

Figure 3-15. Relationship between the ionic conductivity (σ) and ionic liquid (EMIm TFSI) content for supramolecular ionic liquid elastomer [PAcγ-CD-Ad-Acrylate IE(1)] and chemically cross-linked ionic liquid elastomer [Acrylate IE (1)]. [■: Methyl acrylate (MA), ◆: ethyl acrylate (EA), ▲: butyl acrylate (BA), and ▼: methyl methacrylate (MMA)].

3.3.5. Self-recovery properties of supramolecular ionic liquid elastomers

Host-guest interactions are closely related to their self-recovery capability. The self-recovery of the PAc*γ*-CD-Ad-Acrylate IE(1) also investigated. Calculation of recovery ratio provided as Figure 3-16 and 3-17.

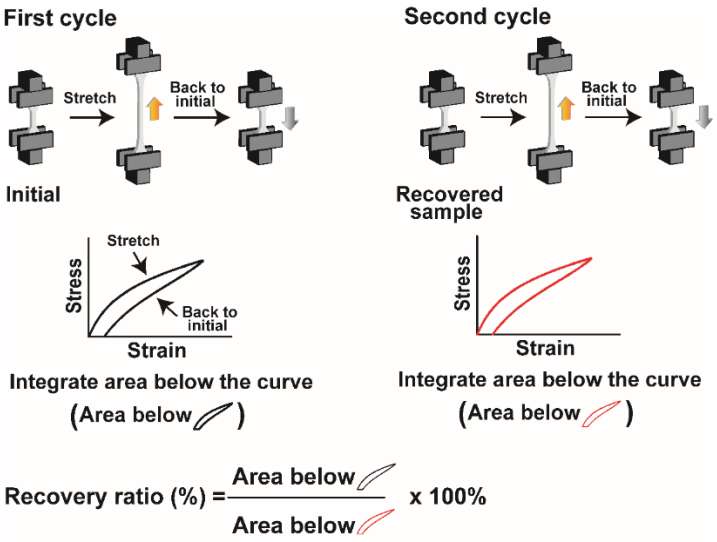

Figure 3-16. Recovery ratio calculation procedure

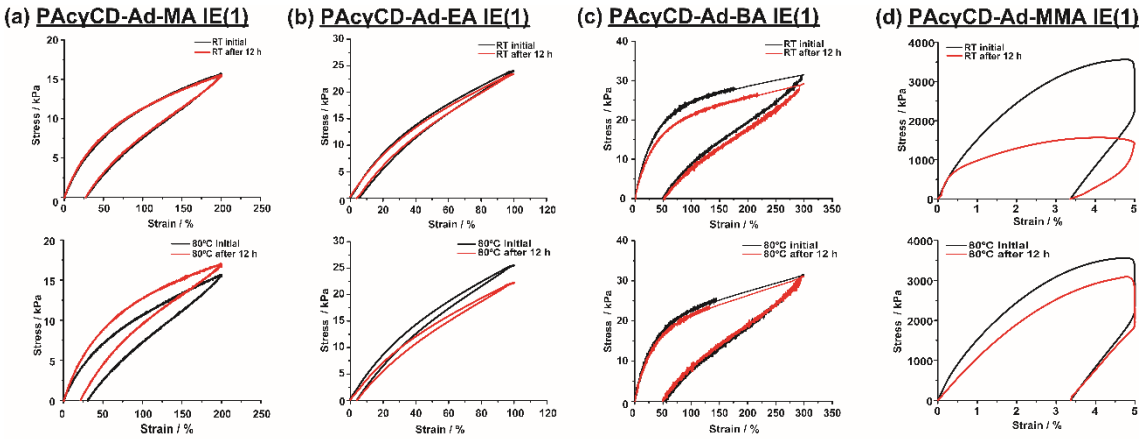

Figure 3-17. Cyclic test for first cycle / initial state (black line) and after 12 h rest (red line) at room temperature (upper figure) and 80 ºC (lower figure): (**a**) PAc*γ*-CD-Ad-MA IE(1), (**b**) PAc*γ*-CD-Ad-EA IE(1), (**c**) PAc*γ*-CD-Ad-BA IE(1), and (**d**) PAc*γ*-CD-Ad-MMA IE(1).

Figure 3-18a shows the self-recovery properties test procedure using a protocol from previous report.[56] The PAc*γ*-CD-Ad-Acrylate IE(1) was stretched into half of the plastic deformable region and then rested to the initial state. Then, the PAc*γ*-CD-Ad-Acrylate IE(1) was rested either at room temperature (RT) or 80 °C to investigate the temperature dependency on the self-recovery. After 12 hours, the PAc*γ*-CD-Ad-Acrylate IE(1**)** was stretched again with the same strain value.

Recovery ratio of supramolecular polymeric IE were calculated using hysteresis curve. First, supramolecular polymeric IE samples were stretched until half of the plastic deformable region then let it back to initial state. From this first cycle hysteresis curve was obtained and calculated to measure the area under the curve. Then, supramolecular polymeric IE samples were held either at RT or 80 ºC for 12 hours (different sample for both temperature). After 12 hours, similar procedure was performed again as same as first cycle to obtain second cycle's hysteresis curve and the area under the curve also calculated. Last, the result of second cycle hysteresis area was divided with first cycle hysteresis area and times it with 100% to obtain recovery ratio.

Figure 3-18b shows the recovery ratio of the PAc*γ*-CD-Ad-Acrylate IE(1) after two cycles at room temperature (RT) or 80 °C. The PAc*γ*-CD-Ad-MA IE(1) and PAc*γ*-CD-Ad-EA IE(1) showed full recovery results (100% and 99%, respectively) after 12 hours at room temperature and at 80 °C, but the PAc*γ*-CD-Ad-BA IE(1) and PAc*γ*-CD-Ad-MMA IE(1) were almost fully recovered (98% and 80%, respectively) only at 80 °C. These results show that PAc*γ*-CD-Ad-MA IE(1) and PAc*γ*-CD-Ad-EA IE(1) with smaller size of the side chain acrylate show faster stress relaxation compared to PAc*γ*-CD-Ad-BA IE(1) and PAc*γ*-CD-Ad-MMA IE(1), respectively. This phenomena is caused by longer size of side chain like BA and bulky size of side chain like MMA make the inclusion complex of PAcγCD and Ad units harder to re-join again after dissociation.

Figure 3-18c schematically illustrates mechanism of the self-recovery. Several host-guest interactions were dissociated when the PAc*γ*-CD-Ad-Acrylate IE(1) materials were stretched. This dissociate behavior contributes to the high fracture energy because of the stress dispersion of the material. Those host and guest units re-joined again through host-guest interactions to recover the cross-linking. Thus, the self-recovery properties can be shown through this the material.

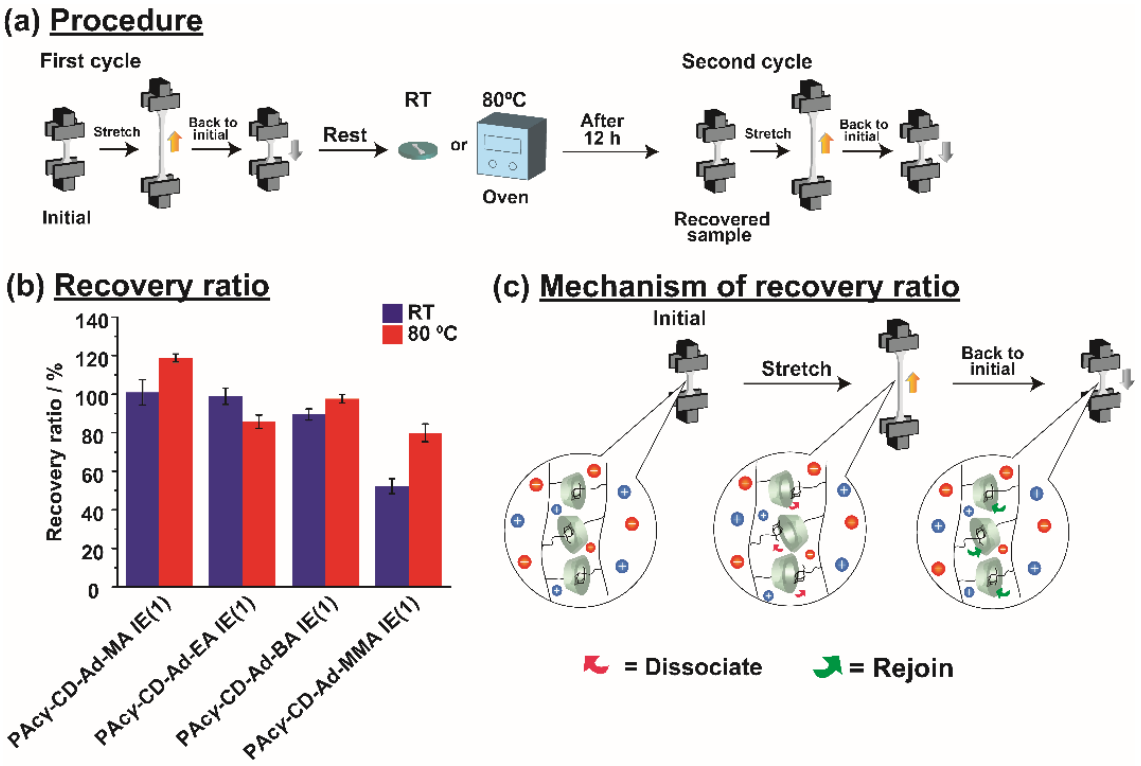

Figure 3-18. (**a**) Procedure for the self-recovery calculation. (**b**) Recovery ratio for supramolecular ionic liquid elastomer [PAc*γ*-CD-Ad-Acrylate IE(1)] in their maximum EMIm TFSI content after 12 h at room temperature and 80 °C. (**c**) Schematic illustration of the self-recovery mechanism.

PAc*γ*-CD-Ad-MA IE(1) interestingly showed more than 100% recovery ratio after rested at 80 ºC, because MA is the smallest size of side chain which make self-recovery easier than longer or bulkier side chain. This result was also supported by Young's modulus of PAc*γ*-CD-Ad-MA IE(1) during self-recovery test (Figure 3-19). PAc*γ*-CD-Ad-MA IE(1) sample rested in RT showed similar Young's modulus value with after first cycle (0.07 MPa). However, when the PAc*γ*-CD-Ad-MA IE(1) sample rested at 80 ºC, it showed higher Young's modulus (0.08 MPa) than the first cycle. These results confirmed that the PAc*γ*-CD-Ad-Acrylate IE(1) shows self-recovery properties.

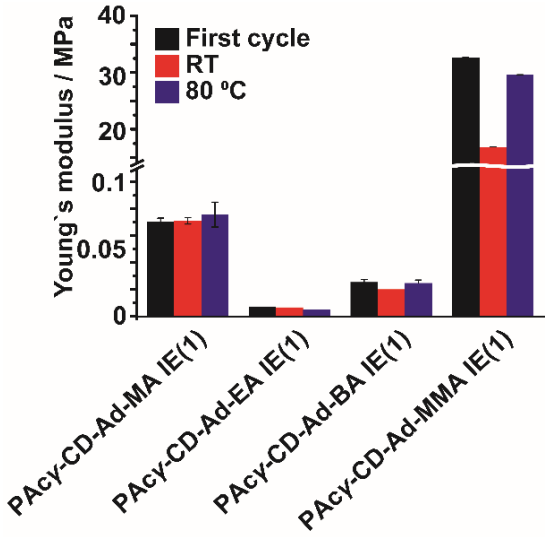

Figure 3-19. Young's modulus for self-recovery for PAcγ-CD-Ad-MA IE(1), PAcγ-CD-Ad-EA IE(1), PAcγ-CD-Ad-BA IE(1), and PAcγ-CD-Ad-MMA IE(1).

3.4. Conclusions

Supramolecular elastomer swollen by ionic liquid were successfully prepared. This materials were immersion of host-guest elastomer containing PAcγ-CD and Ad in EMIm TFSI. The PAcγ-CD-Ad-Acrylate IE(x) have a flexible cross-linking points which resulted to lower Young's modulus compared to the chemically cross-linked IEs. Usually materials with low Young's modulus materials are soft and brittle. Even though the PAcγ-CD-Ad-Acrylate IE(x) have low Young's modulus, the fracture energy is higher compared to the chemically cross-linked IEs. PAcγ-CD-Ad-MA IE(1) and PAcγ-CD-Ad-EA IE(1) also showed full recovery results both at 12 hours at room temperature and 80 °C. In conclusion, supramolecular polymeric IEs with high fracture energy and self-recovery properties are successfully prepared by using host-guest interactions. In the near future, supramolecular polymeric IEs based on host-guest interactions are promising for applications in self-recoverable electrochemical materials.

References

1. Brunsveld, L.; Folmer, B. J. B.; Meijer, E. W.; Sijbesma, R. P., *Chem. Rev.* **2001,** *101*, 4071-4098.
2. Harada, A., *Supramolecular Polymer Chemistry*. Wiley-VCH Verlag & Co. KGaA: Weinheim, 2012.
3. Lehn, J.-M., *Polym. Int.* **2002,** *51*, 825-839.
4. Tuncaboylu, D. C.; Sari, M.; Oppermann, W.; Okay, O., *Macromolecules* **2011,** *44*, 4997-5005.
5. Burattini, S.; Colquhoun, H. M.; Fox, J. D.; Friedmann, D.; Greenland, B. W.; Harris, P. J. F.; Hayes, W.; Mackay, M. E.; Rowan, S. J., *Chem. Commun.* **2009,** 6717-6719.
6. Fox, J.; Wie, J. J.; Greenland, B. W.; Burattini, S.; Hayes, W.; Colquhoun, H. M.; Mackay, M. E.; Rowan, S. J., *J. Am. Chem. Soc.* **2012,** *134*, 5362-5368.
7. Burnworth, M.; Tang, L.; Kumpfer, J. R.; Duncan, A. J.; Beyer, F. L.; Fiore, G. L.; Rowan, S. J.; Weder, C., *Nature* **2011,** *472*, 334.
8. Wojtecki, R. J.; Meador, M. A.; Rowan, S. J., *Nat. Mater.* **2010,** *10*, 14.
9. Wang, Q.; Mynar, J. L.; Yoshida, M.; Lee, E.; Lee, M.; Okuro, K.; Kinbara, K.; Aida, T., *Nature* **2010,** *463*, 339.
10. Cordier, P.; Tournilhac, F.; Soulié-Ziakovic, C.; Leibler, L., *Nature* **2008,** *451*, 977.
11. Chen, X.; Dam, M. A.; Ono, K.; Mal, A.; Shen, H.; Nutt, S. R.; Sheran, K.; Wudl, F., **2002,** *295*, 1698-1702.
12. Roy, N.; Bruchmann, B.; Lehn, J.-M., *Chem. Soc. Rev.* **2015,** *44*, 3786-3807.
13. Pedersen, C. J., *J. Am. Chem. Soc.* **1967,** *89*, 7017-7036.
14. Pedersen, C. J., *J. Am. Chem. Soc.* **1967,** *89*, 2495-2496.
15. Gutsche, C. D.; Dhawan, B.; No, K. H.; Muthukrishnan, R., *J. Am. Chem. Soc.* **1981,** *103*, 3782-3792.
16. Yan, X.; Wang, F.; Zheng, B.; Huang, F., *Chem. Soc. Rev.* **2012,** *41*, 6042-6065.
17. Barrow, S. J.; Kasera, S.; Rowland, M. J.; del Barrio, J.; Scherman, O. A., *Chem. Rev.* **2015,** *115*, 12320-12406.
18. Kim, J.; Jung, I.-S.; Kim, S.-Y.; Lee, E.; Kang, J.-K.; Sakamoto, S.; Yamaguchi, K.; Kim, K., *J. Am. Chem. Soc.* **2000,** *122*, 540-541.
19. Freeman, W. A.; Mock, W. L.; Shih, N. Y., *J. Am. Chem. Soc.* **1981,** *103*, 7367-7368.
20. Ogoshi, T.; Yamagishi, T.-a.; Nakamoto, Y., *Chem. Rev.* **2016,** *116*, 7937-8002.
21. Xue, M.; Yang, Y.; Chi, X.; Zhang, Z.; Huang, F., *Acc. Chem. Res.* **2012,** *45*, 1294-1308.
22. Takashima, Y.; Harada, A., *J. Inclusion Phenom. Macrocyclic Chem.* **2017,** *87*, 313-330.
23. Kato, K.; Okabe, Y.; Okazumi, Y.; Ito, K., *Chem. Commun.* **2015,** *51*, 16180-16183.
24. Koopmans, C.; Ritter, H., *Macromolecules* **2008,** *41*, 7418-7422.
25. Harada, A.; Takashima, Y.; Nakahata, M., *Acc. Chem. Res.* **2014,** *47*, 2128-2140.
26. Armand, M.; Endres, F.; MacFarlane, D. R.; Ohno, H.; Scrosati, B., *Nat. Mater.* **2009,** *8*, 621-629.
27. Rogers, R. D.; Seddon, K. R., *Science* **2003,** *302*, 792-793.
28. Welton, T., *Chem. Rev.* **1999,** *99*, 2071-2083.
29. Wu, A.; Lu, F.; Sun, P.; Qiao, X.; Gao, X.; Zheng, L., *Langmuir* **2017,** *33*, 13982-13989.
30. Ohno, H.; Ito, K., *Chem. Lett.* **1998,** *27*, 751-752.
31. Yuan, J. Y.; Antonietti, M., *Polymer* **2011,** *52*, 1469-1482.
32. Carmichael, A. J.; Haddleton, D. M.; Bon, S. A. F.; Seddon, K. R., *Chem. Commun.* **2000,** 1237-1238.
33. Harrisson, S.; Mackenzie, S. R.; Haddleton, D. M., *Chem. Commun.* **2002,** 2850-2851.
34. Harrisson, S.; Mackenzie, S. R.; Haddleton, D. M., *Macromolecules* **2003,** *36*, 5072-5075.
35. Kaar, J. L.; Jesionowski, A. M.; Berberich, J. A.; Moulton, R.; Russell, A. J., *J. Am. Chem. Soc.* **2003,** *125*, 4125-4131.

36. Noda, A.; Watanabe, M., *Electrochim. Acta* **2000,** *45*, 1265-1270.
37. Fujii, K.; Asai, H.; Ueki, T.; Sakai, T.; Imaizumi, S.; Chung, U.-i.; Watanabe, M.; Shibayama, M., *Soft Matter* **2012,** *8*, 1756-1759.
38. Harner, J. M.; Hoagland, D. A., *J. Phys. Chem. B* **2010,** *114*, 3411-3418.
39. Jansen, J. C.; Friess, K.; Clarizia, G.; Schauer, J.; Izák, P., *Macromolecules* **2011,** *44*, 39-45.
40. Klingshirn, M. A.; Spear, S. K.; Subramanian, R.; Holbrey, J. D.; Huddleston, J. G.; Rogers, R. D., *Chem. Mater.* **2004,** *16*, 3091-3097.
41. Matsumoto, K.; Endo, T., *Macromolecules* **2008,** *41*, 6981-6986.
42. Seki, S.; Susan, A. B. H.; Kaneko, T.; Tokuda, H.; Noda, A.; Watanabe, M., *J. Phys. Chem. B* **2005,** *109*, 3886-3892.
43. Susan, M. A.; Kaneko, T.; Noda, A.; Watanabe, M., *J. Am. Chem. Soc.* **2005,** *127*, 4976-4983.
44. Ding, Y.; Zhang, J. J.; Chang, L.; Zhang, X. Q.; Liu, H. L.; Jiang, L., *Adv. Mater.* **2017,** *29*.
45. Eiji, K.; Tomoki, Y.; Yu, I.; Ping, G. J.; Hideto, M., *Adv. Mater.* **2017,** *29*, 1704118.
46. Lodge, T. P., *Science* **2008,** *321*, 50-51.
47. Gu, Y. Y.; Zhang, S. P.; Martinetti, L.; Lee, K. H.; McIntosh, L. D.; Frisbie, C. D.; Lodge, T. P., *J. Am. Chem. Soc.* **2013,** *135*, 9652-9655.
48. Tamesue, S.; Ohtani, M.; Yamada, K.; Ishida, Y.; Spruell, J. M.; Lynd, N. A.; Hawker, C. J.; Aida, T., *J. Am. Chem. Soc.* **2013,** *135*, 15650-15655.
49. Xinhua, L.; Dongbei, W.; Huanlei, W.; Qigang, W., *Adv. Mater.* **2014,** *26*, 4370-4375.
50. Nakahata, M.; Takashima, Y.; Harada, A., *Macromol. Rapid Commun.* **2016,** *37*, 86-92.
51. Kakuta, T.; Takashima, Y.; Nakahata, M.; Otsubo, M.; Yamaguchi, H.; Harada, A., *Adv. Mater.* **2013,** *25*, 2849-2853.

Chapter 4

Self-healable cellulose nanofiber reinforced supramolecular polymeric materials based on host-guest interactions

4.1. Introduction

Designing materials that can be both strong and tough is challenging because those properties are contradict to each other.[1] Materials with less-strength will tend to be tougher because they are easier to dissipate the stress for enduring the deformation.[2] Many research effort has been done to prepare materials with higher strength and toughness.[3-4] Breakthrough approach comes up by reinforcing fiber into the materials to increase mechanical properties. By adding small amount of fiber into the materials, the mechanical properties of materials like plastics can be increased. Several materials such as carbon fibers,[5-7] carbon nanotubes,[8-10] and graphene[11-12] have been reported as fiber-reinforced composites. However, this fiber-reinforced composites have minus point in high production cost and recycling difficulty. This difficulties have prompted researchers to use bio-based materials from renewable biomass to devise the idea of low cost and sustainable materials.

In 2015, Hu et al. reported a nature inspired toughening mechanisms by using cellulose.[13] Hu et al. used cellulose-based nanopaper and found that cellulose simultaneously increased both the strength and toughness. Cellulose is the most abundant biomass and have been favorably utilized due to its renewability, nontoxicity, and chemical stability.[14-15] One kind of high-value-added cellulose is cellulose nanofibers (CNFs).[16] CNFs are wide available[17-18] and biocompatible,[19] as well as show excellent mechanical properties such as high elastic modulus (29-36 GPa)[20] and tensile strength (1-3 GPa)[21] with relatively low density (~1.5 g/cm^3).

Various CNFs reinforced materials have been reported by benefiting these excellent mechanical properties.[22-25] Recently, CNFs also introduced to reinforce supramolecular polymeric materials.[26-29] Supramolecular polymeric materials are popular for their self-healing ability.[30-39] Development of self-healing materials will reduce the waste from man-made polymers that threaten human health, wildlife, the oceans, and landfills. Based on these problems, the idea about collaborating

biocompatible CNFs with self-healable supramolecular polymeric materials came up and somehow will actualize polymer researchers about preparing maintenance free materials with high mechanical properties.

In this study, citric acid modified cellulose nanofiber (CAC) were introduced to reinforce supramolecular polymeric materials using host-guest interactions from peracetylated 6–acrylamido methylether–*γ*-CD (PAc*γ*-CD) and alkyl chain derivatives (Dod) with 2-hydroxyethyl acrylate (HEA) as main chain polymer [PAc*γ*-CD-Dod-HEA-CAC(1,*x*)]. Previously, that host-guest interactions were reported as the easiest supramolecular chemistry to introduce in materials and their flexible polymer network will help local stress dissipation by while also giving self-healing properties.[40-41] These properties are important in PAc*γ*-CD-Dod-HEA-CAC(1, *x*). The PAc*γ*-CD-Dod-HEA-CAC(1,*x*) was prepared by radical copolymerization of host-guest inclusion complex mixture containing CAC mixture. As a reference, supramolecular polymeric materials without CAC also prepared [PAc*γ*-CD-Dod-HEA(1)]. The results showed that CAC in PAc*γ*-CD-Dod-HEA-CAC(1, *x*) increased the fracture energy with also showed higher self-healing ratio than supramolecular polymeric materials without CAC.

4.2. Experimental section

4.2.1. Materials

HEA, 12-aminolauric acid, and acryloyl chloride were purchased from Tokyo Chemical Industry Co., Ltd. γ-Cyclodextrin (*γ*-CD) was purchased from Junsei Chemical Co. Ltd. IRGACURE 184 was purchased from BASF Japan Co., Ltd. 1,4-dioxane, ethyl acetate, sodium hydroxide (NaOH), hydrochloric acid (HCl), sodium sulfate (Na_2SO_4) were purchased from Nacalai Tesque Inc. 1-Butyl-3-methylimildazolium chloride (BMIm Cl) was purchased from Sigma Aldrich. Pyridine were purchased from Wako Pure Chemical Industries, Ltd. DMSO–d_6 was obtained from Merck & Co., Inc. Water used for the preparation of the aqueous solutions was purified with a Millipore Elix 5 system. Other reagents were used without further purification. PAc*γ*-CD as prepared according to Scheme 2-1 in *chapter 2*. CAC was kindly provided by Prof. Hiroshi Uyama in Division of Applied Chemistry, Graduate School of Engineering, Osaka University.

4.2.2. Measurements.

^{1}H and ^{13}C spectra were recorded at 500 MHz with a JEOL-ECA-500 NMR spectrometer at 25 ºC. In all NMR measurements, chemical shifts were referenced to the solvent values [^{1}H NMR: δ = 0 ppm for tetramethylsilane (TMS) and 2.49 ppm for DMSO–d_6, ^{13}C NM : δ = 0 ppm for TMS and 39.5 ppm for DMSO–d_6). Attenuated total reflectance Fourier-transform infrared spectroscopy (ATR-FTIR) were recorded using a JASCO FT/IR-6100 spectrometer in the wavenumber range from 4000 to 400 cm^{-1} in ATR method. Scanning electron microscope (SEM) images of surfaces were examined by JEOL JSM-7600F with accelerating voltage 2 kV. Mechanical properties (fracture energy and Young's modulus) of CAC reinforced supramolecular polymeric materials were measured using Autograph AG-X plus using a 50 N load cell with specific deformation rate 1 mm/s.

4.2.3. Preparation of materials

Preparation of 12-acrylamido dodecanoic acid (Dod)

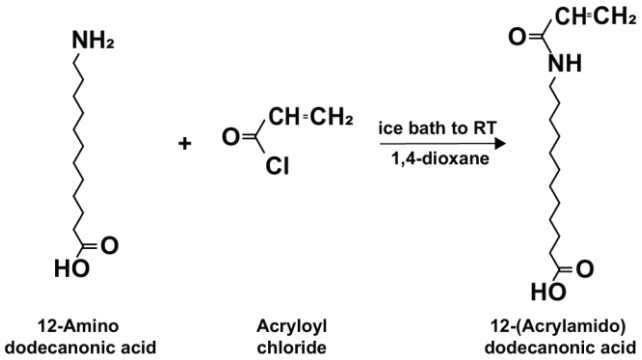

Scheme 4-1. Preparation of 12-acrylamido dodecanoic acid (Dod).

12-aminolauric acid (5 g, 323 mmol) and 2M NaOH (2.32 g NaOH in 29 mL water) were dissolved in 1,4-dioxane (0.10 L) and put in ice bath. After the solution was cooled, acryloyl chloride (3.15 g, 35 mmol) was added dropwise. The solution was stirred overnight in room temperature. Next day, HCl was added to solution until pH 2-3 and then the solution was extracted with ethyl acetate. After extraction, the organic phase was filtrated to remove the salt and then extracted again with ethyl acetate. Then, the solution was evaporated and dried at 40 ºC for 24 hours. Yield: 90%.

^{1}H NMR (500 MHz, DMSO-d_6) of Dod: δ = 11.92 (s, 1H, -N*H*), 7.99 (t, *J* = 5.6 Hz, 1H, -COO*H*), 6.16 (dd, *J* = 17.1, 10.1 Hz, 1H, CH_2CH-), 6.02 (dd, *J* = 17.1, 2.3 Hz, 1H, CH_2CH-), 5.51 (dd, *J* = 10.1, 2.3 Hz, 1H, CH_2CH-), 3.06 (td, *J* = 7.1, 5.7 Hz, 2H, -NHCH_2CH_2-), 2.14 (t, *J* = 7.4 Hz, 2H, -CH_2CH_2COOH-), 1.44 (t, *J* = 7.3 Hz, 2H,-$CH_2(CH_2)_{11}CH_2$COOH), 1.37 (q, *J* = 6.8 Hz, 2H,-$CH_2(CH_2)_{11}CH_2$COOH), 1.21 (t, *J* = 2.7 Hz, 14H,-$CH_2(CH_2)_{11}CH_2$COOH).

4.3. Results and discussion

4.3.1. Preparation of CNFs-reinforced supramolecular polymeric materials

Figure 4-2 shows the preparation method for the PAc*γ*-CD-Dod-HEA-CAC(1,*x*). Prior to mix with host-guest inclusion complex mixture, CAC was dissolved in BMIm Cl with 7.5wt% concentration at 100 ºC for 3 days (Figure 4-2a). Host-guest inclusion complex mixture were formed from peracetylated 6-monoacrylamide-methyl ether-modified monomer (PAc*γ*-CD; Scheme 2-1 in *chapter 2*) as a host monomer with 12-(acrylamido) dodecanoic acid (Dod; Scheme 4-1) as a guest monomer in 2-hydroxyethyl acrylate monomer (HEA) (Figure 4-2b) and sonication for 90 minutes. Radical copolymerization was carried by mixing CAC mixture into host-guest inclusion complex mixture using 1-hydroxycyclohexyl phenyl ketone (IRGACURE 184) as a photo induce radical initiator, successfully giving CAC reinforced supramolecular polymeric materials that still containing BMIm Cl. Then to remove BMIm Cl, CAC reinforced supramolecular polymeric materials was washed (with acetone and water) and dried to obtain PAc*γ*-CD-Dod-HEA-CAC(1,*x*) (Figure 4-2c). The notation 1 at PAc*γ*-CD-Dod-HEA-CAC (1,*x*) indicates mol% of host guest inclusion complex between PAc*γ*-CD and Dod units and *x* indicates the wt% of CAC (Table 4-1).

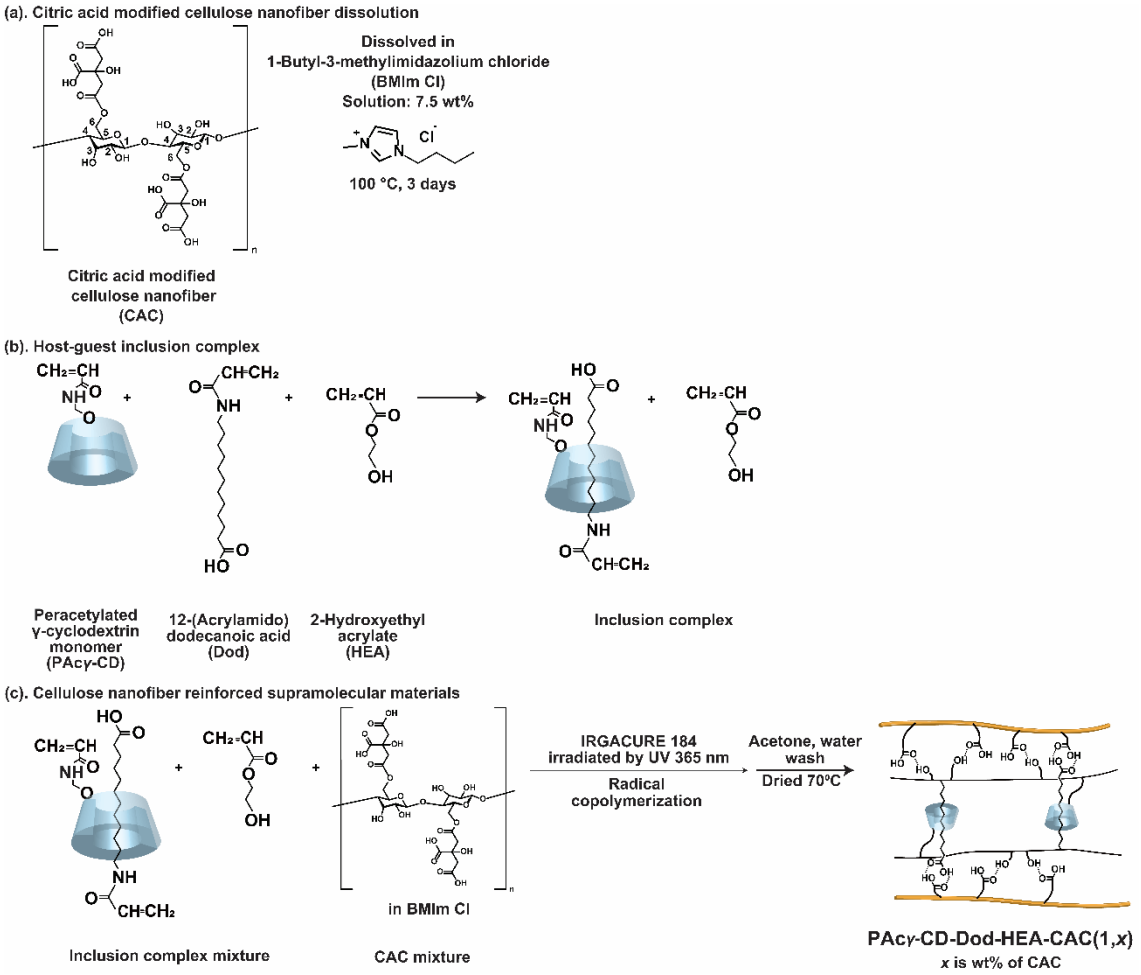

Figure 4-2. (**a**) Dissolving citric acid modified cellulose nanofibers (CAC) in 1-butyl-3-methylimidazolium chloride (BMIm Cl) ionic liquid. (**b**) Host-guest inclusion complex of peracetylated cyclodextrin (PAγcCD) and 12-(acrylamide) dodecanoic acid (Dod) in 2-hydroxyethyl acrylate (HEA). (**c**) Preparation of PAc*γ*-CD-Dod-HEA-CAC(1,*x*). Notation 1 indicates the mol% of host-guest interactions between PAc*γ*-CD and Dod, respectively and *x* indicates the wt% of CAC.

Table 4-1. Preparation of PAc*γ*-CD-Dod-HEA-CAC(1,*x*).

(1,*x*)	PAc*γ*-CD / g	Dod / g	HEA / g	CAC / g	IRGACURE 184 / mg
(1,0)	0.4	0.05	2	0	7
(1,1)	0.4	0.05	2	0.02	7
(1,3)	0.4	0.05	2	0.7	7
(1,5)	0.4	0.05	2	0.1	7

4.3.2. Characterization

Figure 4-3 shows the characterization of PAc*γ*-CD-Dod-HEA-CAC(1,*x*) using ATR-FTIR. BMIm Cl and water removal was confirmed by no detection of imidazole absorption (3054 and 1565 cm^{-1}) and –OH absorption from water at around 1640 cm^{-1}. The reinforcement of CAC into supramolecular polymeric materials also successfully done by confirmation of C-O-C asymmetric bridge and glicosidic deformation absorption peak from CAC at 1159 and 1027 cm^{-1} attached with C-O-C stretching of acetoxy group from PAc*γ*-CD at 1430 and 1370 cm^{-1}. The absorbance intensity of C-O-C vibration also enhanced with increasing CAC (*x*) in PAc*γ*-CD-Dod-HEA-CAC(1,*x*).

The most important characterization was confirmation of inter molecular hydrogen bond between CAC and supramolecular polymer in PAc*γ*-CD-Dod-HEA-CAC(1,*x*). Intra and inter molecular hydrogen bond could be observed from two separated peaks in broad –OH stretching absorption around 3600-3200 cm^{-1}, unfortunately these two peaks were not separated in PAc*γ*-CD-Dod-HEA-CAC(1,*x*) absorption. Therefore, it was not possible to identify the difference between intra and inter molecular hydrogen bond. The only information that could be observed from this broad –OH stretching absorption just the vibration enhanced by increasing *x* in PAc*γ*-CD-Dod-HEA-CAC(1,*x*). Thus, the important characterization of inter hydrogen bond between CAC and supramolecular polymer could be revealed from carbonyl group (C=O) absorption peak. The absorption of C=O was found at 1735 cm^{-1} from PAc*γ*-CD-Dod-HEA(1) and 1712 cm^{-1} from CAC. When CAC reinforced to supramolecular polymer, the wavenumber of C=O absorption was blue-shifted which confirmed the inter molecular hydrogen bond.[43] In addition, by increasing the *x* in PAc*γ*-CD-Dod-HEA-CAC(1,*x*), C=O stretching absorption also slightly blue-shifted [PAc*γ*-CD-Dod-HEA-CAC(1,1): 1725 cm^{-1}, PAc*γ*-CD-Dod-HEA-CAC(1,3): 1724 cm^{-1}, PAc*γ*-CD-Dod-HEA-CAC(1,5): 1723 cm^{-1}].

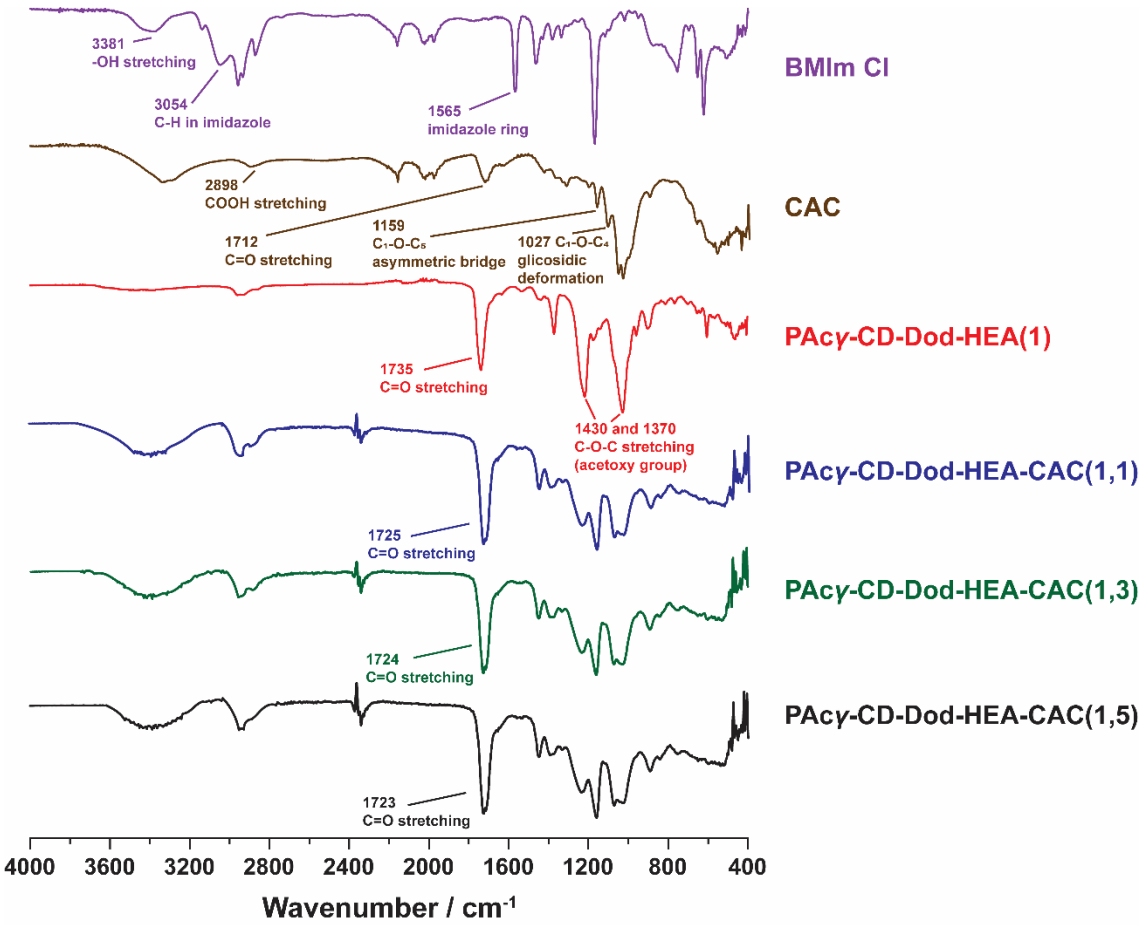

Figure 4-3. ATR-FTIR spectra of BMIm Cl, CAC, PAc*γ*-CD-Dod-HEA(1), PAc*γ*-CD-Dod-HEA-CAC(1,1), PAc*γ*-CD-Dod-HEA-CAC(1,3), and PAc*γ*-CD-Dod-HEA-CAC(1,5).

Figure 4-4 shows the surface SEM images of PAc*γ*-CD-Dod-HEA(1), PAc*γ*-CD-Dod-HEA-CAC(1,1), and PAc*γ*-CD-Dod-HEA-CAC(1,5). SEM image of PAc*γ*-CD-Dod-HEA(1) shows a flat surface without any fiber formation (Figure 4-4a) while PAc*γ*-CD-Dod-HEA-CAC(1,1) (Figure 4-4b) and PAc*γ*-CD-Dod-HEA-CAC(1,5) (Figure 4-4c) shows entangled formation of fiber. The tubular shape of fiber structure and bonding formation can be seen from SEM image of PAc*γ*-CD-Dod-HEA-CAC(1,*x*) (Figure 4-5). SEM image of PAc*γ*-CD-Dod-HEA-CAC(1,1) showed more separated fiber structure due to low content of CAC. SEM image of PAc*γ*-CD-Dod-HEA-CAC(1,5) showed more crowded fiber formation due to higher content of CAC (Figure 4-6). These SEM images proved that CAC successfully reinforced into supramolecular polymer.

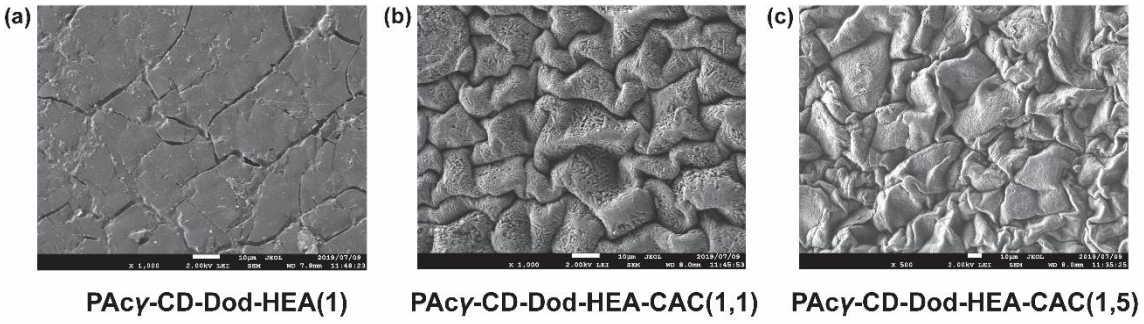

Figure 4-4. Surface SEM images of (**a**) PAc*γ*-CD-Dod-HEA(1), (**b**) PAc*γ*-CD-Dod-HEA-CAC(1,1), and (**c**) PAc*γ*-CD-Dod-HEA-CAC(1,5).

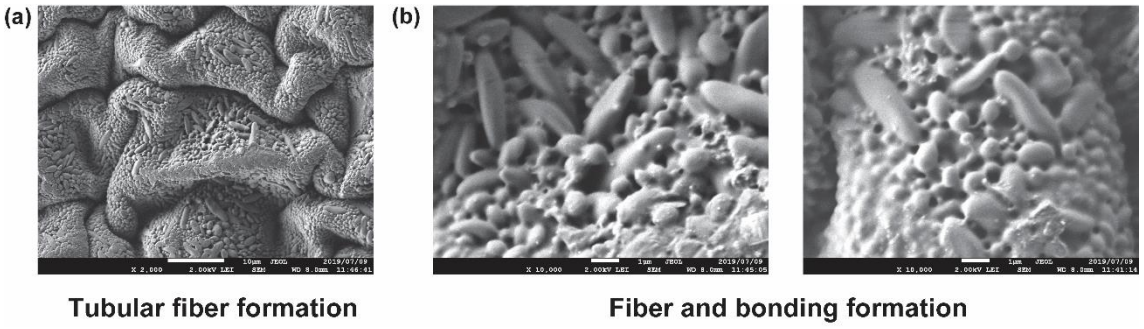

Figure 4-5. Surface SEM images of PAc*γ*-CD-Dod-HEA-CAC(1,1).

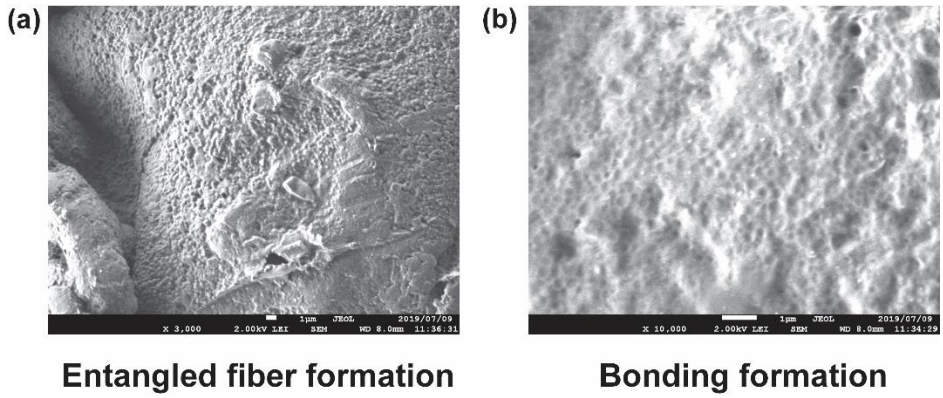

Figure 4-6. Surface SEM images of PAc*γ*-CD-Dod-HEA-CAC(1,5).

4.3.3. Mechanical properties

Mechanical properties of PAc*γ*-CD-Dod-HEA(1) and PAc*γ*-CD-Dod-HEA-CAC(1,*x*) were evaluated by tensile test as shown in Figure 4-7. PAc*γ*-CD-Dod-HEA(1) and PAc*γ*-CD-Dod-HEA-CAC(1,*x*) both showed high elongation (>1000%) (Figure 4-7). This result is interesting for PAc*γ*-CD-Dod-HEA-CAC(1,*x*) as usually fiber reinforced materials showed low elongation. This high elongation due to flexible polymer network in host-guest interactions.

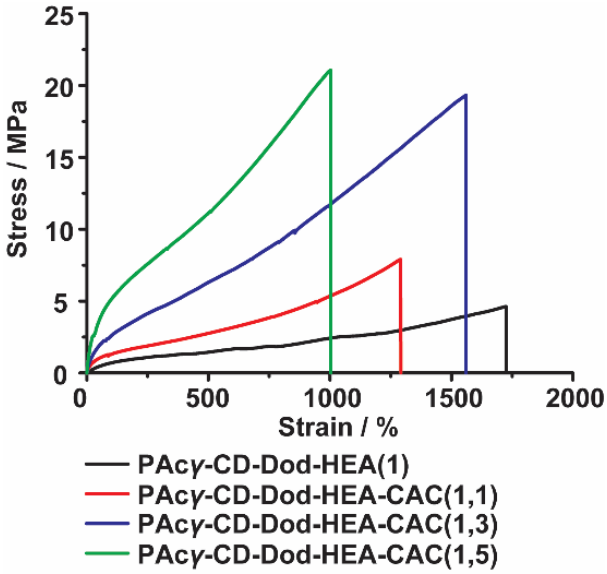

Figure 4-7. Stress-strain curve of PAc*γ*-CD-Dod-HEA(1), PAc*γ*-CD-Dod-HEA-CAC(1,1), PAc*γ*-CD-Dod-HEA-CAC(1,3), PAc*γ*-CD-Dod-HEA-CAC(1,5).

This condition was proven by preparing CAC reinforced supramolecular polymer materials without host-guest interactions as reference samples (Figure 4-8). Reference samples that not having host-guest interactions showed elongation break less than 1000% which proved the existence of flexible polymer network in host-guest interactions.

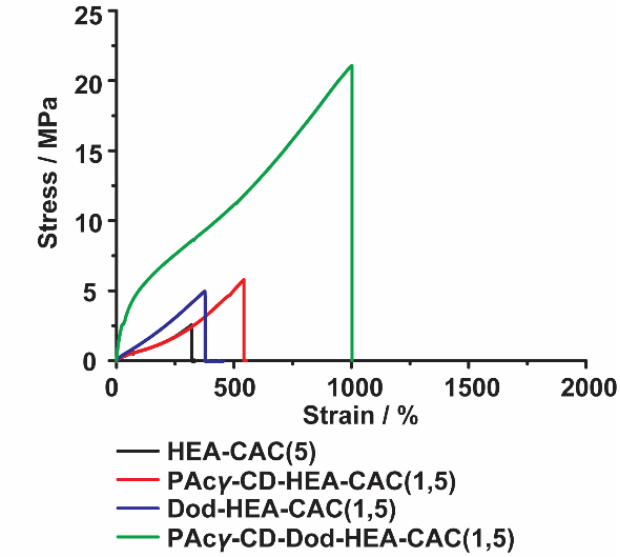

Figure 4-8. Stress-strain curve of HEA(1), PAc*γ*-CD-HEA-CAC(1,5), Dod-HEA-CAC(1,5), PAc*γ*-CD-Dod-HEA-CAC(1,5).

Figure 4-9 shows fracture energy and Young's modulus which measured from stress-strain curve. PAcγ-CD-Dod-HEA-CAC(1,1) (49 MJ/m^3) with low content CAC showed slightly higher fracture energy compared to PAcγ-CD-Dod-HEA(1) (41 MJ/m^3). For higher CAC content [PAcγ-CD-Dod-HEA-CAC(1,3): 110 MJ/m^3 and PAcγ-CD-Dod-HEA-CAC(1,5): 152 MJ/m^3], the fracture energy increased drastically (Figure 4-9a). In addition, the CAC also increased the Young's modulus (Figure 4-9b). PAcγ-CD-Dod-HEA(1) showed Young's modulus 1.3 MPa, when CAC reinforced with supramolecular polymer the Young's modulus increased [PAcγ-CD-Dod-HEA-CAC(1,1): 4.6 MPa, PAcγ-CD-Dod-HEA-CAC(1,3): 8.1 MPa, and PAcγ-CD-Dod-HEA-CAC(1,5): 14.5 MPa]. These results confirmed that reinforcement of CAC increased the mechanical properties of supramolecular polymeric materials.

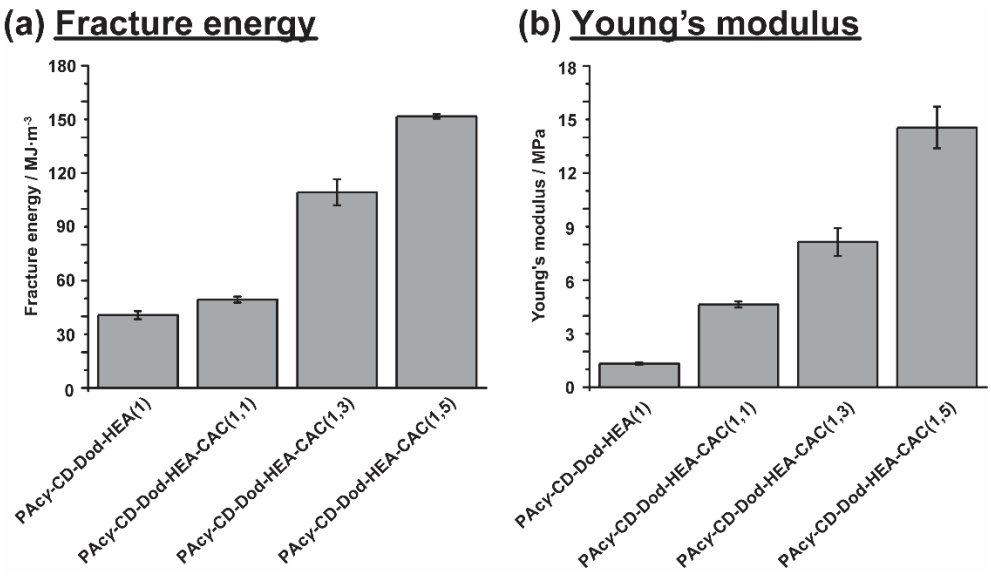

Figure 4-9. Mechanical properties of PAcγ-CD-Dod-HEA(1) and PAcγ-CD-Dod-HEA-CAC(1,*x*): (**a**) fracture energy and (**b**) Young's modulus. Notation 1 indicates the mol% of host-guest interactions between PAcγ-CD and Dod, respectively and *x* indicates the wt% of CAC.

The mechanical properties increased because of inter molecular hydrogen bond between CAC with the supramolecular polymer. Then, to prove this theory CAC reinforced supramolecular polymeric materials with several reference samples were prepared with omitting the hydroxyl group and the result showed heterogeneous or even phase-separated materials (Figure 4-10).

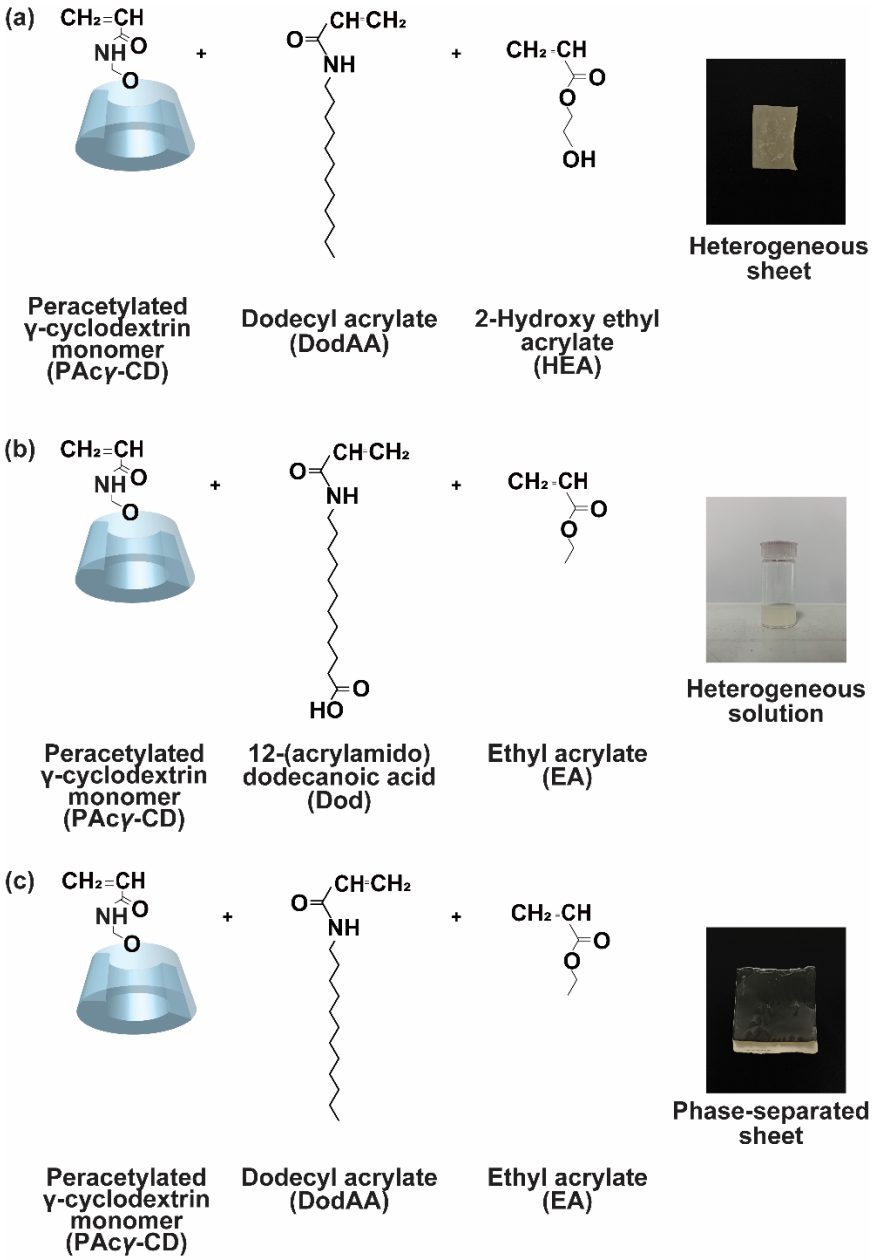

Figure 4-10. Hydrogen bond importance check by changing the guest or side chain polymer: (**a**) PAc*γ*-CD-DodAA-HEA-CAC(1,5), (**b**) PAc*γ*-CD-Dod-EA-CAC(1,5), (**c**) PAc*γ*-CD-DodAA-EA-CAC(1,5). Guest substitute: dodecyl acrylate (DodAA) and side chain polymer substitute: ethyl acrylate (EA).

4.3.4. Self-healing properties

Reversible bond in host-guest interactions always popular for their capability as self-healing material. Herein, self-healing properties were showed through measurement of fracture energy after recovery. Figure 4-11a shows the procedure of self-healing experiments. The initial tensile test was measured for PAc*γ*-CD-Dod-HEA(1) and PAc*γ*-CD-Dod-HEA-CAC(1,*x*) with 1 mm/s tensile velocity and fracture energy ($F_{initial}$) was calculated. After fracturing another samples of PAcγCD-Dod-HEA(1) and PAcγCD-Dod-HEA-CAC(1,*x*), samples rejoined for 12 hours in room temperature (RT) or 70ºC. Then recovered samples were measured again with tensile test and fracture energy was calculated again ($F_{recovery}$). Self-healing ratio was calculated as:

$$\text{Recovery ratio} = \frac{F_{recovery}}{F_{initial}} \times 100\%$$

Figure 4-11b shows the recovery ratio for the self-healing experiments of PAc*γ*-CD-Dod-HEA(1) and PAc*γ*-CD-Dod-HEA-CAC(1,*x*). Recovery ratio in RT of PAc*γ*-CD-Dod-HEA-CAC(1,*x*) [PAc*γ*-CD-Dod-HEA-CAC(1,1): 20%, PAc*γ*-CD-Dod-HEA-CAC(1,3): 32%, and **(c)** PAc*γ*-CD-Dod-HEA-CAC(1,5): 36%] are higher than PAc*γ*-CD-Dod-HEA(1): 14%. These results showed that the self-healing mechanism not only from reversible host-guest interactions but also inter molecular hydrogen bond. While the sample put in 70ºC, the recovery ratio showed more than doubled value with PAc*γ*-CD-Dod-HEA-CAC(1,*x*) [PAc*γ*-CD-Dod-HEA-CAC(1,1): 56%, PAc*γ*-CD-Dod-HEA-CAC(1,3): 57%, and **(c)** PAc*γ*-CD-Dod-HEA-CAC(1,5): 86%] and PAc*γ*-CD-Dod-HEA(1): 35% with PAc*γ*-CD-Dod-HEA-CAC(1,*x*) recovery ratio still higher than PAc*γ*-CD-Dod-HEA(1). These results indicate that higher temperature affected molecular mobility in polymer which supported faster self-healing mechanism.

Figure 4-11c shows the mechanism of self-healing. When PAc*γ*-CD-Dod-HEA-CAC(1,*x*) was cut, the hydrogen bond from Dod in host-guest interactions dissociated then followed by host-guest interactions dissociation. Since the host-guest dissociated, several hydrogen bonds also dissociated. During reattachment, first the host-guest interactions re-joined again then followed by hydrogen bonds as support.

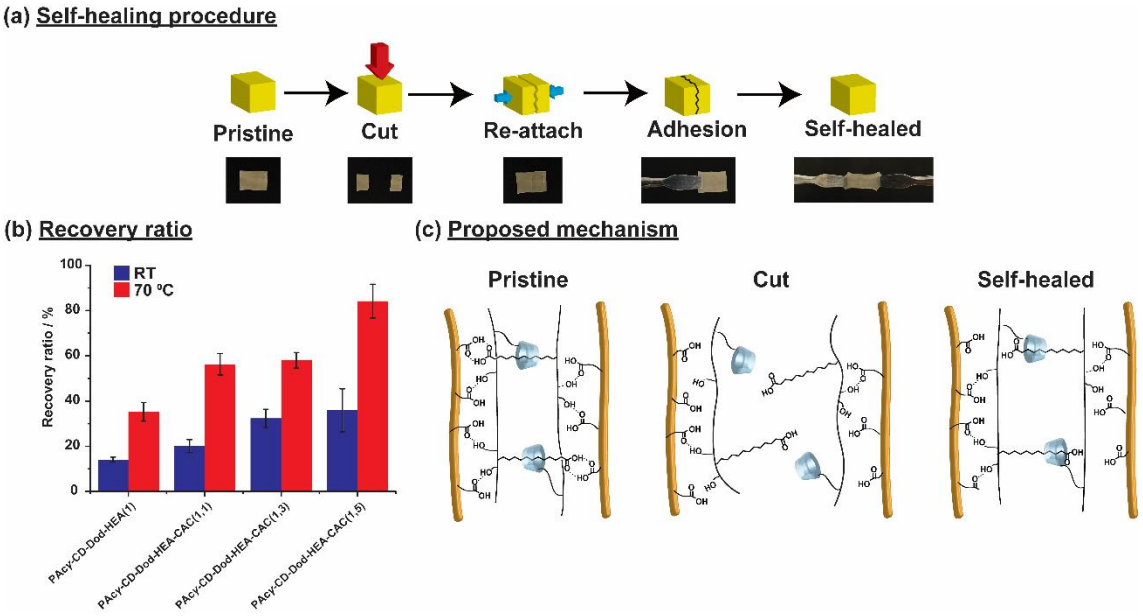

Figure 4-11. (**a**) Self-healing procedure and (**b**) recovery ratio of PAc*γ*-CD-Dod-HEA(1) and PAc*γ*-CD-Dod-HEA-CAC(1,*x*). (c) Self-healing mechanism of PAc*γ*-CD-Dod-HEA-CAC(1,*x*). Notation 1 indicates the mol% of host-guest interactions between PAc*γ*-C and Dod, respectively and *x* indicates the wt% of CAC.

4.4. Conclusions

CNFs reinforced supramolecular polymeric materials were successfully prepared from the radical copolymerization of host-guest inclusion complex mixture containing PAc*γ*-CD and Dod with CAC mixture. PAc*γ*-CD-Dod-HEA-CAC(1,*x*) showed higher those of the usual fiber reinforced materials, indicating the importance of host-guest interactions as flexible cross-linking points. The fracture energy and Young's modulus of PAc*γ*-CD-Dod-HEA-CAC(1,*x*) were higher than PAc*γ*-CD-Dod-HEA(1). PAc*γ*-CD-Dod-HEA-CAC(1,*x*) also showed higher self-healing recovery ratio than PAc*γ*-CD-Dod-HEA(1) after 12 hours at room temperature and 70 ºC. In conclusion, host-guest interactions and inter molecular hydrogen bond are important part to prepare CAC reinforced supramolecular polymeric materials.

References

1. Ritchie, R. O., *Nat. Mater.* **2011,** *10*, 817.
2. Hofmann, D. C.; Suh, J.-Y.; Wiest, A.; Duan, G.; Lind, M.-L.; Demetriou, M. D.; Johnson, W. L., *Nature* **2008,** *451*, 1085.
3. Lu, K.; Lu, L.; Suresh, S., *Science* **2009,** *324*, 349-352.
4. Zhu, T.; Li, J., *Progress in Materials Science* **2010,** *55*, 710-757.
5. Rodriguez, N. M., *J. Mater. Res.* **1993,** *8*, 3233-3250.
6. Tibbetts, G. G.; Lake, M. L.; Strong, K. L.; Rice, B. P., *Composites Science and Technology* **2007,** *67*, 1709-1718.
7. Al-Saleh, M. H.; Sundararaj, U., *Carbon* **2009,** *47*, 2-22.
8. Coleman, J. N.; Khan, U.; Blau, W. J.; Gun'ko, Y. K., *Carbon* **2006,** *44*, 1624-1652.
9. Coleman, J. N.; Khan, U.; Gun'ko, Y. K., *Adv. Mater.* **2006,** *18*, 689-706.
10. Byrne, M. T.; Gun'ko, Y. K., *Adv. Mater.* **2010,** *22*, 1672-1688.
11. Ramanathan, T.; Abdala, A. A.; Stankovich, S.; Dikin, D. A.; Herrera-Alonso, M.; Piner, R. D.; Adamson, D. H.; Schniepp, H. C.; Chen, X.; Ruoff, R. S.; Nguyen, S. T.; Aksay, I. A.; Prud'Homme, R. K.; Brinson, L. C., *Nat. Nanotechnol.* **2008,** *3*, 327.
12. Liang, J.; Huang, Y.; Zhang, L.; Wang, Y.; Ma, Y.; Guo, T.; Chen, Y., *Adv. Funct. Mater.* **2009,** *19*, 2297-2302.
13. Zhu, H.; Zhu, S.; Jia, Z.; Parvinian, S.; Li, Y.; Vaaland, O.; Hu, L.; Li, T., *Proc. Natl. Acad. Sci. U. S. A.* **2015,** *112*, 8971.
14. Klemm, D.; Heublein, B.; Fink, H.-P.; Bohn, A., *Angew. Chem. Int. Ed.* **2005,** *44*, 3358-3393.
15. Klemm, D.; Kramer, F.; Moritz, S.; Lindström, T.; Ankerfors, M.; Gray, D.; Dorris, A., **2011,** *50*, 5438-5466.
16. Chinga-Carrasco, G., *Nanoscale Research Letters* **2011,** *6*, 417.
17. Moon, R. J.; Martini, A.; Nairn, J.; Simonsen, J.; Youngblood, J., *Chem. Soc. Rev.* **2011,** *40*, 3941-3994.
18. Abdul Khalil, H. P. S.; Davoudpour, Y.; Islam, M. N.; Mustapha, A.; Sudesh, K.; Dungani, R.; Jawaid, M., *Carbohydr. Polym.* **2014,** *99*, 649-665.
19. Alexandrescu, L.; Syverud, K.; Gatti, A.; Chinga-Carrasco, G. J. C., **2013,** *20*, 1765-1775.
20. Tanpichai, S.; Quero, F.; Nogi, M.; Yano, H.; Young, R. J.; Lindström, T.; Sampson, W. W.; Eichhorn, S. J., *Biomacromolecules* **2012,** *13*, 1340-1349.
21. Saito, T.; Kuramae, R.; Wohlert, J.; Berglund, L. A.; Isogai, A., *Biomacromolecules* **2013,** *14*, 248-253.
22. Azizi Samir, M. A. S.; Alloin, F.; Dufresne, A., *Biomacromolecules* **2005,** *6*, 612-626.
23. Eichhorn, S. J.; Dufresne, A.; Aranguren, M.; Marcovich, N. E.; Capadona, J. R.; Rowan, S. J.; Weder, C.; Thielemans, W.; Roman, M.; Renneckar, S.; Gindl, W.; Veigel, S.; Keckes, J.; Yano, H.; Abe, K.; Nogi, M.; Nakagaito, A. N.; Mangalam, A.; Simonsen, J.; Benight, A. S.; Bismarck, A.; Berglund, L. A.; Peijs, T., *J. Mater. Sci.* **2010,** *45*, 1-33.
24. Siró, I.; Plackett, D., *Cellulose* **2010,** *17*, 459-494.
25. Fujisawa, S.; Saito, T.; Kimura, S.; Iwata, T.; Isogai, A., *Biomacromolecules* **2013,** *14*, 1541-1546.
26. Duri, S.; Tran, C. D., *Langmuir* **2013,** *29*, 5037-5049.
27. Coulibaly, S.; Roulin, A.; Balog, S.; Biyani, M. V.; Foster, E. J.; Rowan, S. J.; Fiore, G. L.; Weder, C., *Macromolecules* **2014,** *47*, 152-160.
28. Lin, N.; Dufresne, A., *Biomacromolecules* **2013,** *14*, 871-880.
29. McKee, J. R.; Appel, E. A.; Seitsonen, J.; Kontturi, E.; Scherman, O. A.; Ikkala, O., *Adv. Funct. Mater.* **2014,** *24*, 2706-2713.
30. White, S. R.; Sottos, N. R.; Geubelle, P. H.; Moore, J. S.; Kessler, M. R.; Sriram, S. R.; Brown, E. N.; Viswanathan, S., *Nature* **2001,** *409*, 794-797.

31. White, S. R.; Moore, J. S.; Sottos, N. R.; Krull, B. P.; Santa Cruz, W. A.; Gergely, R. C. R., *Science* **2014,** *344*, 620-623.
32. Binder, W. H., *Self-Healing Polymers: From Principles to Applications*. Wiley-VCH Verlag GmbH & Co. KGaA: Weinheim, 2013.
33. Yang, Y.; Urban, M. W., *Adv. Mater. Interfaces* **2018,** *5*, 1800384.
34. Roy, N.; Bruchmann, B.; Lehn, J.-M., *Chem. Soc. Rev.* **2015,** *44*, 3786-3807.
35. Burattini, S.; Greenland, B. W.; Chappell, D.; Colquhoun, H. M.; Hayes, W., *Chem. Soc. Rev.* **2010,** *39*, 1973-1985.
36. Cordier, P.; Tournilhac, F.; Soulié-Ziakovic, C.; Leibler, L., *Nature* **2008,** *451*, 977.
37. Brunsveld, L.; Folmer, B. J. B.; Meijer, E. W.; Sijbesma, R. P., *Chem. Rev.* **2001,** *101*, 4071-4098.
38. Harada, A., *Supramolecular Polymer Chemistry*. Wiley-VCH Verlag & Co. KGaA: Weinheim, 2012.
39. Lehn, J. M., *Supramolecular Chemistry: Concepts and Perspectives*. Wiley-VCH Verlag & Co. KGaA: Weinheim, 1995.
40. Takashima, Y.; Harada, A., *J. Inclusion Phenom. Macrocyclic Chem.* **2017,** *87*, 313-330.
41. Takashima, Y.; Sawa, Y.; Iwaso, K.; Nakahata, M.; Yamaguchi, H.; Harada, A., *Macromolecules* **2017,** *50*, 3254-3261.

Summary of this thesis

In this thesis, ionic liquid was utilized in supramolecular materials cross-linked by host-guest interactions. Host-guest interactions was formed between CD as host molecules and guest molecules in acrylate monomers.

In *Chapter 2*, the author developed supramolecular polymeric ionic liquid gel (IG) based on host-guest interaction and the importance of host-guest interactions for its ionic conductivity properties. Supramolecular polymeric ionic liquid gel was prepared from immersion of bulk copolymerization of the host-guest complex between peracetylated *γ*-CD monomer and 2-ethyl-2-adamantane monomer with acrylate (ethyl acrylate or butyl acrylate) monomer in 1-ethyl-3-methylimidazolium bis(trifluoromethylsulfonyl)imide (EMIm TFSI) ionic liquid. The ionic conductivity and self-diffusion coefficient of supramolecular polymeric IGs were higher than chemically cross-linked IGs and comparable with EMIm TFSI as native ionic liquid. The author concluded that host-guest interaction is an important part to increase ionic conductivity for supramolecular polymeric IGs. In the near future, this supramolecular polymeric IG based on host-guest interaction expectable to be use as electrochemical materials

In *Chapter 3*, the author investigated the mechanical properties of supramolecular elastomer swollen in ionic liquid (IE). Preparation of materials similar to *chapter 2* instead more acrylate variations was used (methyl acrylate, ethyl acrylate, butyl acrylate, and methyl methacrylate). Supramolecular IE showed lower Young's moduli compared to the chemically cross-linked IE because of the flexible cross-linking points. Usually, low Young's modulus materials are generally soft and brittle however the fracture energy of the supramolecular IE is higher than that of the chemically cross-linked IE. Supramolecular IE also show full recovery results after 12 hours at room temperature and at 80 °C which cannot be achieved by chemically cross-linked IE.

In *Chapter 4*, the author prepared self-healable cellulose nanofiber (CNF) supramolecular polymeric materials. Citric acid modified cellulose nanofiber (CAC) was first dissolved in 1-butyl-3-methylimidazolium chloride (BMIm Cl). Dissolved CAC then mixed with host-guest inclusion complex mixture between peracetylated *γ*-CD monomer and 12-(acrylamido) dodecanoic acid monomer in the presence of 2-

hydroxyethyl acrylate. The solution mixture then radical copolymerized to obtain polymer sheet. Then, polymer sheet was washed (with ethanol and water) and dried to obtain CAC reinforced supramolecular polymeric materials. The fracture energy, Young's modulus, and self-healing ratio of CAC reinforced polymeric supramolecular materials were higher than supramolecular materials without fiber addition. These mechanical properties are due to host-guest interactions and intra molecular hydrogen bond in the CAC reinforced supramolecular polymeric materials.

List of publications

Original papers

1. Sinawang, G.; Kobayashi, Y.; Zheng Y. T.; Takashima, Y.; Harada, A.; Yamaguchi, H. "Preparation of Supramolecular Ionic Liquid Gels Based on Host–Guest Interactions and Their Swelling and Ionic Conductive Properties" *Macromolecules* **2019**, *52*, 2932-2938.
2. Sinawang, G.; Kobayashi, Y.; Osaki, M.; Takashima, Y.; Harada, A.; Yamaguchi, H. "Mechanical and self-recovery properties of supramolecular ionic liquid elastomers based on host-guest interaction and correlation with ionic liquid content", *RSC Advances* **2019**, *9*, 22295-22301.
3. Sinawang, G.; Asoh, T.-A.; Takashima, Y.; Harada, A.; Yamaguchi, H.; Uyama, H. "Self-healable cellulose nanofiber reinforced supramolecular polymeric materials based on host-guest interactions" to be submitted.

Other papers

1. Sinawang, G.; Wang, J. L.; Wu, B.; Wang, X. G.; He, Y. N. "Photoswitchable aggregation-induced emission polymer containing dithienylethene and tetraphenylethene moieties" *RSC Advances* **2016**, *6*, 12647-12651.
2. Sinawang, G.; Wu, B.; Wang, J. L.; Li, S.; He, Y. N. "Polystyrene Based Visible Light Responsive Polymer with Donor–Acceptor Stenhouse Adduct Pendants" *Macromol. Chem. Phys.* **2016**, *217*, 2409-2414.
3. Wang, J. L.; Wu, B.; Li, S.; Sinawang, G.; Wang, X. G.; He, Y. N. "Synthesis and Characterization of Photoprocessible Lignin Based Azo Polymer" *ACS Sustainable Chem. Eng.* **2016**, *4*, 4036-4042.
4. Sinawang, G.; Takashima, Y.; Yamaguchi, H.; Harada, A. "Supramolecular self-healing materials from non-covalent cross-linking host-guest interactions" to be submitted. (Review Article).